



RESEARCH MEMORANDUM

CHARACTERISTICS THROUGHOUT THE SUBSONIC SPEED RANGE OF
A PLANE WING AND OF A CAMBERED AND TWISTED WING,
BOTH HAVING 45° OF SWEEPBACK

By Ben H. Johnson, Jr., and Harry H. Shibata

Ames Aeronautical Laboratory
Moffett Field, Calif.

NATIONAL ADVISORY COMMITTEE
FOR AERONAUTICS

WASHINGTON
July 12, 1951

NATIONAL ADVISORY COMMITTEE FOR AERONAUTICS

RESEARCH MEMORANDUMCHARACTERISTICS THROUGHOUT THE SUBSONIC SPEED RANGE OF
A PLANE WING AND OF A CAMBERED AND TWISTED WING,
BOTH HAVING 45° OF SWEEPBACK

By Ben H. Johnson, Jr., and Harry H. Shibata

SUMMARY

A wind-tunnel investigation has been made of two semispan wing models having 45° of sweepback, an aspect ratio of 5, and a taper ratio of 0.565. One wing had no camber or twist and the other wing was cambered for a design lift coefficient of 0.4 and twisted to relieve the loading at the tip which accompanies sweepback. The airfoil sections normal to the quarter-chord line were the NACA 64A010 for the plane wing and the NACA 64A810 for the cambered and twisted wing. The cambered and twisted wing had 8.7° of washout between the root and the tip. The tests were made at Mach numbers from 0.25 to 0.94. At each Mach number the Reynolds number was varied over as wide a range as possible within the limitations of wind-tunnel power and wind-tunnel pressure. At Mach numbers above 0.70, the maximum Reynolds number was 2,000,000; at a Mach number of 0.25, the maximum Reynolds number was 10,000,000. The effects of a fuselage, of boundary-layer fences, and of surface roughness were also investigated.

At a Reynolds number of 10,000,000 and a Mach number of 0.25, the combined camber and twist were effective in delaying extensive separation on the wing to a higher lift coefficient. At the lower Reynolds numbers, the effectiveness of camber and twist in delaying extensive separation was seriously reduced. The aerodynamic characteristics of both wings were seriously influenced by dynamic-scale effects.

At Mach numbers greater than 0.70, wind-tunnel power limitations prevented testing at Reynolds numbers greater than 2,000,000. Because of the large dynamic-scale effects previously noted, direct application of these data to the design of airplanes which operate at substantially higher Reynolds numbers is not recommended. Based on the data obtained at a Reynolds number of 2,000,000, the combined camber and twist improve

the drag characteristics of the wing at lift coefficients above 0.3 up to a Mach number of 0.85. At the higher Mach numbers, the improvements in drag due to camber and twist were seriously reduced as would be expected for a wing with such highly cambered sections. At a Reynolds number of 2,000,000, the pitching-moment characteristics of the wing were impaired by the use of camber and twist, especially at Mach numbers of 0.90 and above.

The addition of a chordwise fence at the midsemispan to the upper surface of the cambered and twisted wing resulted in marked improvement of the pitching-moment characteristics of the wing, especially at Mach numbers of 0.90 and above. No similar improvement was noted when fences were applied to the plane wing.

INTRODUCTION

Theoretical studies and a number of experimental investigations have indicated that camber and twist may improve the characteristics of swept wings. This improvement results from more uniform distribution of load, both spanwise and chordwise, which alleviates the flow separation and the attendant stability and drag deterioration at moderate and high lift coefficients. That such improvement is obtainable through the use of camber and twist has been demonstrated by the low-speed investigation reported in references 1 and 2. To extend the study of the effects of camber and twist, an investigation has been made in the Ames 12-foot pressure wind tunnel at Mach numbers up to 0.94 of two 45° swept-back wings similar to those reported in references 1 and 2. One of the wings had no twist and the wing profile was symmetrical. The other wing was cambered for a design wing-lift coefficient of 0.4 and twisted to relieve the loading at the tip which accompanies sweepback.

COEFFICIENTS AND SYMBOLS

The following coefficients and symbols are used in this report:

- a speed of sound, feet per second
- b wing span measured perpendicular to the plane of symmetry, feet
- c local chord measured parallel to plane of symmetry, feet
- \bar{c} local chord measured perpendicular to the quarter-chord line, feet
- \bar{c} wing mean aerodynamic chord $\left(\frac{\int_0^{b/2} c^2 dy}{\int_0^{b/2} c dy} \right)$, feet

C_D	drag coefficient $\left(\frac{\text{drag}}{qS}\right)$
C_L	lift coefficient $\left(\frac{\text{lift}}{qS}\right)$
c_l	section lift coefficient
C_m	pitching-moment coefficient about the lateral axis through the quarter-chord point of the wing mean aerodynamic chord $\left(\frac{\text{pitching moment}}{qS\bar{c}}\right)$
C_{m_0}	pitching-moment coefficient at zero lift
$\frac{L}{D}$	lift-drag ratio
l	length of body, feet
M	Mach number $\left(\frac{V}{a}\right)$
q	dynamic pressure $\left(\frac{1}{2} \rho V^2\right)$, pounds per square foot
R	Reynolds number $\left(\frac{\rho V \bar{c}}{\mu}\right)$
r	radius of body, feet
r_0	maximum radius of body, feet
S	area of semispan wing, square feet
t	maximum thickness of wing section, feet
V	free-stream velocity, feet per second
x	longitudinal distance, feet
y	lateral distance, feet
α	angle of attack of the chord line at wing root, degrees
α_t	angle of twist with reference to root chord (positive for wash-in), degrees
μ	coefficient of viscosity of air, slugs per foot-second

- ρ mass density of air, slugs per cubic foot
- λ taper ratio $\left(\frac{\text{tip chord}}{\text{root chord}} \right)$

MODEL AND APPARATUS

The wing models used in this investigation were similar in plan form and represented wings having an aspect ratio of 5, a taper ratio of 0.565, and a sweepback angle of the quarter-chord line of 45° . A dimensional sketch of the wings is shown in figure 1. The wing profiles normal to the quarter-chord line were the NACA 64A010 for the wing model hereinafter referred to as the plane wing, and the NACA 64A810 with a modified $a=0.8$ mean line (reference 3) for the wing model hereinafter referred to as the cambered and twisted wing. The angle of twist of the cambered and twisted wing varied from 0° at the root to -8.7° (wash-out) at the tip as shown in figure 2. This twist distribution was a straight-line-element type wherein all constant-percent points of the local chords lie in straight lines along the span. As a result of maintaining the local chords of the root and tip constant while the wing was twisted, the projected area of the cambered and twisted wing was approximately 0.4 percent less than that of the plane wing. In the reduction of all force and moment data to aerodynamic coefficients, this difference in wing areas was neglected and the area and the mean aerodynamic chord of the plane wing was used. The wings were constructed of solid aluminum alloy.

The body used in combination with both wing models had a fineness ratio of 12.5. The equation defining the coordinates of the body is given in figure 1. The plane wing was mounted with its root chord coincident with the longitudinal axis of the body. The cambered and twisted wing was also centrally mounted but with -1.3° incidence of the root chord relative to the longitudinal axis of the body.

The tests were conducted in the Ames 12-foot pressure wind tunnel, which is a closed-throat variable-density wind tunnel with a low turbulence level closely approximating that of free air.

As shown in figure 3, the models were mounted with the wing plane perpendicular to the floor which served as a reflection plane. The gap between the body and the tunnel floor was maintained between $1/32$ and $1/16$ inch. No attempt was made to remove the tunnel-floor boundary layer which, at the location of the model, had a displacement thickness of approximately 0.50 inch. The boundary-layer displacement thickness over the body in the region of the wing was approximately 0.15 inch.

The fences were constructed of 1/16-inch steel with 1/2-inch flanges for attachment to the wing. Pertinent dimensions of the fences are given in figure 1.

TEST CONDITIONS

Lift, drag, and pitching-moment data were obtained for both wing models with and without the body. At a Reynolds number of 2,000,000, the models were tested at Mach numbers from 0.25 to 0.94. At higher Reynolds numbers, the maximum Mach number was limited by wind-tunnel power to the following: 0.70 at a Reynolds number of 3,000,000, 0.60 at a Reynolds number of 4,000,000, 0.40 at a Reynolds number of 6,000,000, and 0.25 at a Reynolds number of 10,000,000.

To investigate the effectiveness of fences in improving the longitudinal stability characteristics of the model, the wings were tested with fences of two different heights located at 50 and 70 percent of the wing semispan. These tests were conducted at a Reynolds number of 2,000,000 through a range of Mach numbers from 0.25 to 0.94 and at a Mach number of 0.25 through a range of Reynolds numbers from 2,000,000 to 10,000,000.

To study the influence of surface roughness, the plane wing was tested at a Reynolds number of 2,000,000 and a Mach number of 0.25 with roughness on both the upper and lower surfaces extending forward from 15 percent of the chord to 0, 2, 5, and 10 percent of the chord. Additional tests were conducted at a Reynolds number of 2,000,000 and Mach numbers of 0.94, 0.90, and 0.80 with roughness applied to both the upper and lower surfaces from 5 percent to 15 percent of the chord. The surface roughness was number 60 grain carborundum. Tests were also conducted using number 120 and number 180 grain carborundum, but data for these grain sizes are not presented as they indicated no difference from the data using the number 60 grain size.

CORRECTIONS TO DATA

The data have been corrected for the effects of tunnel-wall interference, including the effects of constriction due to the tunnel walls, and approximately for model-support tare forces. The method of reference 4 was used in computing the corrections for tunnel-wall interference due to induced effects occurring as a result of lift on the model. The following corrections were added:

$$\Delta\alpha = 0.254C_L$$

$$\Delta C_D = 0.0040C_L^2$$

$$\Delta C_m = 0$$

Corrections to the data for the constriction effects of the tunnel walls have been evaluated by the method of reference 5. The magnitudes of these corrections as applied to Mach number and dynamic pressure are illustrated by the following table:

Corrected Mach number	Uncorrected Mach number		$\frac{q_{\text{corrected}}}{q_{\text{uncorrected}}}$	
	Wing alone	Wing and body	Wing alone	Wing and body
0.940	0.936	0.930	1.005	1.010
.920	.916	.913	1.003	1.008
.900	.898	.895	1.003	1.006
.850	.849	.847	1.002	1.004
.800	.799	.798	1.001	1.003
.700	.700	.699	1.001	1.002
.600	.600	.599	1.001	1.002
.400	.400	.400	1.001	1.001
.250	.250	.250	1.000	1.001
.150	.150	.150	1.000	1.001

The measured choking Mach number for the wing-body combination was approximately 0.97.

Tare corrections due to the air forces exerted on the turntable were measured with the model removed from the tunnel. Possible interference effects between the model and the turntable were not evaluated. The tare-drag coefficients subtracted from the data, representing the drag coefficients of the exposed surface of the turntable expressed in terms of wing area, are presented in the following table:

Mach number	Reynolds number									
	2,000,000		3,000,000		4,000,000		6,000,000		10,000,000	
	Wing alone	Wing and body	Wing alone	Wing and body	Wing alone	Wing and body	Wing alone	Wing and body	Wing alone	Wing and body
0.15	---	---	---	---	0.0072	0.0061	---	---	---	---
.25	0.0078	0.0067	0.0076	0.0065	.0074	.0063	0.0072	0.0062	0.0070	0.0060
.40	.0083	.0071	.0081	.0069	.0079	.0067	.0077	.0066		
.60	.0090	.0077	.0088	.0075	.0086	.0073				
.70	.0094	.0080	.0092	.0078	.0090	.0076				
.80	.0100	.0086								
.85	.0104	.0089								
.90	.0108	.0092								
.92	.0110	.0094								
.94	.0112	.0096								

RESULTS AND DISCUSSION

Plane Wing

Effects of Mach number.— In figures 4 through 7, lift, drag, and pitching-moment data for the plane wing are presented for Mach numbers from 0.25 to 0.94 and a Reynolds number of 2,000,000, for Mach numbers from 0.25 to 0.70 and a Reynolds number of 3,000,000, and for Mach numbers from 0.15 to 0.60 and a Reynolds number of 4,000,000. The data in figure 4 indicate that, as Mach number increased, there was an increase in the lift-curve slope for lift coefficients less than 0.4 throughout the Mach number range at Reynolds numbers less than 4,000,000 and a decrease in the maximum lift for Mach numbers up to 0.90. In figure 6, the variation of drag coefficient with Mach number at a Reynolds number of 2,000,000 is compared with the variation of the section drag coefficient with Mach number obtained from reference (6) by applying

simple sweep theory to the section lift coefficients and the Mach number¹ of the section data. While no attempt has been made to correct the section drag data for the effect of either sweep or aspect ratio, such corrections would only affect the absolute magnitude of the drag coefficient and not its variation with Mach number. At lift coefficients of 0.30 and less, both the experimental and the predicted variation of drag coefficient with Mach number show no large effects of compressibility up to the maximum Mach number at which data were obtained.

The pitching-moment data in figure 7 show that, at lift coefficients less than 0.30, the variation of pitching-moment coefficient with lift coefficient was fairly linear except at the lower Mach numbers and Reynolds numbers. As the lift coefficient was increased in the range from 0.30 to 0.50, the aerodynamic center moved rearward. This rearward movement of the aerodynamic center suggests the development of a vortex type of flow similar to that reported in reference 7. At lift coefficients greater than 0.50, the aerodynamic center moved forward with increasing lift. At low lift coefficients, the aerodynamic center moved rearward with increasing Mach number, the total movement between Mach numbers of 0.25 and 0.94 being of the order of 3 percent of the mean aerodynamic chord. The data in figure 7 indicate a positive value of the pitching-moment coefficient at zero lift. Inspection of parts (a), (b), and (c) of figure 7 reveals that the value of this C_{m_0} generally decreased with an increase of either Mach number or Reynolds number. The exact reason for the existence of this pitching moment is not known, but, because of its dependence on the Reynolds number, it is believed to be associated with differences in the boundary layer on the upper and lower surfaces of the wing.

Effects of Reynolds number.— The lift, drag, and pitching-moment data for the plane wing are presented in figures 8 through 10 for a range of Reynolds numbers up to 10,000,000. The lift data in figure 8 indicate that the range of lift coefficients for which the lift-curve slope was essentially linear increased with increasing Reynolds number. As shown in figure 9, the rate of increase of drag with lift decreased with increasing Reynolds number, the greatest percentage change occurring between Reynolds numbers of 6,000,000 and 10,000,000. The pitching-moment data in figure 10 indicate that the range of lift coefficients for which the variation of pitching moment with lift was fairly linear increased with increasing Reynolds number. The lift coefficient at which dC_m/dC_L attained a large positive value increased from approximately 0.5 at a Reynolds number of 2,000,000 to approximately 0.7 at a Reynolds number of 10,000,000.

¹The application of theory to the section data was as follows:

$$C_L = c_l \cos^2 45^\circ, \quad M = \frac{M_{\text{section}}}{\cos 45^\circ}$$

Cambered and Twisted Wing

Effects of Mach number.— In figures 11 through 14, lift, drag, and pitching-moment data for the cambered and twisted wing are presented for Mach numbers from 0.25 to 0.94 and a Reynolds number of 2,000,000, for Mach numbers from 0.25 to 0.70 and a Reynolds number of 3,000,000, and for Mach numbers from 0.15 to 0.60 and a Reynolds number of 4,000,000. The data in figure 11 indicate that the variation of lift with angle of attack was nonlinear for most of the angle-of-attack range. At lift coefficients between about 0.30 and 0.80, the lift-curve slope decreased with increasing Mach number up to a Mach number of 0.85 and then increased with further increase in the Mach number. The maximum lift coefficient decreased with increasing Mach number up to a Mach number of 0.85. In figure 13, the variation of drag coefficient with Mach number for a Reynolds number of 2,000,000 is compared with the variation of the section drag coefficient with Mach number obtained by applying simple sweep theory to the section lift coefficient and the Mach number¹ and interpolating values of drag coefficient from the section data of reference 6. While no attempt has been made to offer a quantitative prediction of the wing drag, inspection of figure 13 shows that adverse effects of compressibility on the drag characteristics of the cambered and twisted wing were in qualitative agreement with the effects predicted from section data.

As can be seen from figure 14, the variation of pitching-moment coefficient with lift coefficient of the cambered and twisted wing was nonlinear over the entire range of lift coefficients. At lift coefficients less than about 0.1, the shape of the pitching-moment curves suggests that flow separation was occurring on the lower surface of the wing. A similar effect has been noted in the section data reported in reference 8. At the higher lift coefficients, upper-surface separation is indicated. As a result of these separation effects, the stability characteristics of the cambered and twisted wing were undesirable at all lift coefficients. The positive lift coefficient at which the pitching-moment-curve slope first became positive increased with increasing Mach number up to a Mach number of 0.85. At Mach numbers above 0.85, this lift coefficient decreased with increasing Mach number. The preceding discussion of figure 14 is based on the data obtained at Reynolds numbers up to 4,000,000. The effect of increasing the Reynolds number will be discussed in the following paragraph.

Effects of Reynolds number.— The lift, drag, and pitching-moment characteristics of the cambered and twisted wing are presented in figures 15 through 17 for a range of Reynolds numbers up to 10,000,000. Increasing the Reynolds number above 4,000,000 resulted in more nearly

¹See footnote, page 8.

linear variation of lift coefficient with angle of attack and caused a large reduction in the drag coefficient at the higher lift coefficients (figs. 15 and 16). Increasing the Reynolds number from 4,000,000 to 10,000,000 also had large effects on the pitching-moment characteristics of the cambered and twisted wing (fig. 17). These effects of increasing Reynolds number were an increase in the lift coefficient at which dC_m/dC_L became positive, an increase in the lift coefficient range for which dC_m/dC_L was approximately zero, an increase in the negative value of C_{m_0} , and a reduction in the lift coefficient at which lower surface separation occurred.

Wing-Body Combinations

Plane wing with the body.— Lift, drag, and pitching-moment data for the plane wing with the body are compared with data for the plane wing alone for representative combinations of Mach number and Reynolds number in figure 18. These data indicate that the addition of the body caused an increase in the drag at low lift coefficients, a slight increase in lift-curve slope, and a forward movement of the center of pressure at the higher lift coefficients at Mach numbers below 0.80. At Mach numbers above 0.80, addition of the body resulted in a more rearward center of pressure at the higher lift coefficients. However the maximum change of pitching-moment coefficient due to the addition of the body was only 0.02.

Cambered and twisted wing with the body.— In figure 19, the lift, drag, and pitching-moment characteristics of the cambered and twisted wing with the body and of the cambered and twisted wing alone are compared for representative combinations of Mach number and Reynolds number. These data indicate that the addition of the body caused a slight increase in the lift-curve slope, a slight increase in the drag at low lift coefficients, and a slight rearward movement of the center of pressure at low lift coefficients. At lift coefficients below the stall, the maximum change of pitching-moment coefficient due to the addition of the body was less than 0.025.

Effect of Camber and Twist

In figure 20 the lift, drag, and pitching-moment characteristics of the plane wing with the body are compared with those of the cambered and twisted wing with the body at representative combinations of Mach number and Reynolds number. These data indicate that camber and twist as applied to this model decreased the drag at the higher lift coefficients and increased the maximum lift. Due to the large effects of Reynolds number on the characteristics of these wings

and to the limit on Reynolds number attainable at Mach numbers greater than 0.40, it is impossible to evaluate adequately the effects of camber and twist at the higher Mach numbers. At a Reynolds number of 10,000,000 and a Mach number of 0.25, the drag data indicated that camber and twist were effective in delaying serious separation on the wing to a much higher lift coefficient. At a Reynolds number of 2,000,000 and a Mach number of 0.25, camber and twist reduced the drag coefficient of the wing at all lift coefficients greater than 0.2. Erratic changes in the position of the aerodynamic center with increasing lift were evident in the pitching-moment characteristics of both wings at Reynolds numbers of 4,000,000 and below. Based on the data obtained at a Reynolds number of 2,000,000, it may be seen that camber and twist were effective at all Mach numbers in increasing the lift coefficient at which the rapid drag rise occurred. At Mach numbers of 0.90 and above, camber and twist caused a moderate decrease in the drag at lift coefficients greater than 0.4 but a sizable increase in the drag at lift coefficients less than 0.3. The deleterious effects of the large amount of camber on the Mach number at which the drag rises abruptly may be predicted by application of simple sweep theory to two-dimensional data. The pitching-moment data at a Reynolds number of 2,000,000 indicate that camber and twist impaired the stability characteristics of the wing, especially at Mach numbers of 0.90 and above. A comparison of the low-speed characteristics (references 1 and 2) of a plane wing and of a cambered and twisted wing similar to the wings reported herein, has shown that, whereas separation on the outer portions of the plane wing occurred in the laminar boundary layer at the leading edge, separation on the outer portions of the cambered and twisted wing occurred in the turbulent boundary layer near the trailing edge. The deleterious effects of camber and twist on the stability characteristics of the wing at a Reynolds number of 2,000,000 may be partially attributed to the thickening of the boundary layer over the after parts of the outer wing sections due to spanwise drainage of the boundary-layer air. This spanwise drainage would be expected to have a much larger effect on the turbulent-type separation near the trailing edge of the outer wing sections of the cambered and twisted wing than on the laminar-type separation near the leading edge of the outer wing sections of the plane wing.

Effect of Fences

References 9 through 11 indicate that improvements in the stability of a swept-back wing may be gained through the use of chordwise fences. To study the effects of such a device on the aerodynamic characteristics of the two wings of this investigation, vane-type triangular fences extending forward from the trailing edge to 0.478c were tested. The trailing-edge type of fence was selected primarily to afford control of the boundary layer near the trailing edge of the wing.

The outward flow of this boundary layer was believed to be the cause of the early separation noted on the cambered and twisted wing at low Reynolds numbers. For purposes of comparison, identical fences were tested on the plane wing. The pertinent dimensions of the fences and their location on the wing plan form are shown in figure 1.

Plane wing.— Lift, drag, and pitching-moment data for the plane wing and body combination with high fences (maximum height twice the wing thickness) at 50 percent of the wing semispan and also with high fences at 50 and 70 percent of the wing semispan are presented in figure 21. These data are for a Mach number of 0.25 and Reynolds numbers of 10,000,000 and 4,000,000, and for a Reynolds number of 2,000,000 and Mach numbers from 0.25 to 0.94. At lift coefficients less than 0.4 or 0.5, addition of the fences had little effect on the aerodynamic characteristics of the wing except for an irregular rearward movement of the center of pressure at a Reynolds number of 2,000,000 and a Mach number of 0.25. At slightly higher lift coefficients, the fences caused the wing pitching moment to become more negative. At the lift coefficient at which the lift, drag, and pitching-moment data indicated the onset of extensive separation on the plane wing, addition of the fences caused an abrupt reduction in the lift-curve slope, an increase in the drag, and a forward movement of the center of pressure. The fact that the fences did not increase the lift coefficient at which the wing-body combination became longitudinally unstable is believed to be due to the fact that separation on the plane wing occurred initially at the leading edge of the outer sections (references 1 and 2). Control of the trailing-edge boundary layer has little effect on the local lift coefficient at which this type of separation occurs. The reduction in the wing lift-curve slope following separation of the flow on the outer portions of the wing may be attributed to the reduction of the boundary-layer control on the root section of the wing resulting from the effectiveness of the fences in minimizing the spanwise boundary-layer drainage. Had the fence on the plane wing been of the leading-edge type, it is probable that it would have had a more beneficial effect on the aerodynamic characteristics of the wing (reference 12).

Cambered and twisted wing.— In figure 22, lift, drag, and pitching-moment data for the cambered and twisted wing and body combination with high fences at 50 percent and at both 50 and 70 percent of the wing semispan are presented. Data are also presented in figure 22 for the cambered and twisted wing with a high fence at 70 percent of the wing semispan. Data for the cambered and twisted wing-body combination with low fences (maximum height equal to the wing thickness) at 50 percent and at both 50 and 70 percent of the wing semispan are presented in figure 23 for Mach numbers from 0.25 to 0.94 and a Reynolds number of 2,000,000. At a Mach number of 0.25 and a Reynolds number of 10,000,000, addition of the high fences caused an increase in the lift-curve slope at lift

coefficients between 0.7 and 1.0 and a decrease in drag and pitching-moment coefficient for the same range of lift coefficients (fig. 22a)). At this Reynolds number and Mach number, the pitching-moment-curve slope of the cambered and twisted wing with fences at 50 and 70 percent of the wing semispan was approximately zero for lift coefficients from 0.1 to 0.9. At the stall, the pitching-moment coefficient became positive for all cases, indicating static longitudinal instability. At a Mach number of 0.25 and Reynolds numbers of 4,000,000 and 2,000,000, the effect of fences was similar to that observed at a Reynolds number of 10,000,000. It is of interest to compare the pitching-moment characteristics of the wing without fences at a Reynolds number of 10,000,000 with the characteristics of the wing with a fence at the mid-semispan at a Reynolds number of 4,000,000. It is observed that qualitatively the data are in good agreement in lift coefficients between about 0.5 and 0.9. At lift coefficients near the stall, the effect of increasing the Reynolds number differed from the effect of the fence, and in the lower lift range, as would be expected, the upper-surface fence was entirely ineffective in controlling the lower-surface separation. A similar comparison can be made between the data obtained without fences at a Reynolds number of 4,000,000 and that obtained with a fence at a Reynolds number of 2,000,000. This qualitative agreement suggests two things with regard to the effect of fences on a swept-back wing which is cambered and twisted in such a manner that initial separation occurs in the turbulent boundary layer at the trailing edge. First, that data obtained at Reynolds numbers considerably lower than flight Reynolds numbers may be more nearly representative of full-scale conditions if fences are applied to the wing; and second, that some high Reynolds number probably exists at which little improvement in the wing characteristics will result from the addition of fences.

At a Reynolds number of 2,000,000 and at Mach numbers from 0.60 to 0.85, the effects of fences were similar to those noted at a Mach number of 0.25. At Mach numbers of 0.90, 0.92, and 0.94, the effects of fences were extremely large and favorable at lift coefficients greater than about 0.40 (figs. 22 (g), (h), and (i)). At these Mach numbers, addition of the two fences completely eliminated the longitudinal instability occurring on the wing without fences at a lift coefficient of 0.40, increased the lift-curve slope at lift coefficients near 0.40, and decreased the drag at lift coefficients between 0.40 and the lift coefficient at which the stall occurred. With high fences installed at 50 and 70 percent of the wing semispan, longitudinal stability existed at lift coefficients from 0 to 0.75 at a Mach number of 0.90 and from 0 to 0.95 (the highest lift coefficient attained) at a Mach number of 0.94. At Mach numbers of 0.90 and 0.92, longitudinal instability accompanied the stall for all arrangements of fences.

Inspection of the data in figure 22 also shows that the fence at 70 percent of the wing semispan was not nearly as effective as the

fence at the mid-semispan and that little additional improvement resulted from addition of a fence at 70 percent of the wing semispan when the fence at 50 percent of the wing semispan was installed. In figure 24, the effects on the pitching-moment characteristics of the wing of fences having two different heights are compared. It can be seen that the low fences (maximum height equal to the wing thickness) were only slightly less effective than the high fences (maximum height equal to twice the wing thickness).

Effect of Surface Roughness

In an effort to increase the effective Reynolds number of the test data by artificially disturbing the flow in the laminar boundary layer, surface roughness was applied to the forward portions of the plane wing. Three different grades of roughness (numbers 60, 100, and 180 grit carborundum) were applied to both the upper and lower surfaces of the wing extending forward from 15 percent of the chord to the leading edge and, alternatively, to 2, 5, and 10 percent of the chord. The results of tests of the wing with number 60 grit carborundum at the various chordwise locations are presented in figure 25. The data obtained with numbers 100 grit and 180 grit carborundum showed no change due to this variation of grain size and therefore are not presented. Surface roughness caused an increase in the drag at low lift coefficients, but its effects on the lift and pitching moment were small.

Lift-Drag Ratio

The lift-drag ratios of the wings alone are presented in figures 26 and 27, and the lift-drag ratios of the wing-body combinations are presented in figures 26 and 28.

At all Reynolds numbers and at all Mach numbers less than 0.90, the maximum lift-drag ratio and the lift coefficient for maximum lift-drag ratio were greater for the cambered and twisted wing than for the plane wing. The effect of camber and twist on maximum lift-drag ratio decreased with increasing Reynolds number. Addition of the body to either of the wings reduced the maximum lift-drag ratio and increased the lift coefficient for maximum lift-drag ratio. Addition of the fences to the cambered and twisted wing-body combination reduced the maximum lift-drag ratio, but increased the lift-drag ratio at some of the higher lift coefficients. The reduction of the maximum lift-drag ratio resulting from addition of the fences might be minimized by more careful design of the fence installation.

CONCLUDING REMARKS

A wind-tunnel investigation of the aerodynamic characteristics of two 45° swept-back wings having an aspect ratio 5 and a taper ratio 0.565 has been made throughout the subsonic Mach number range. One wing had a symmetrical profile and possessed no twist. The second wing was cambered for a design lift coefficient of 0.4 and was twisted in such a manner as to relieve the loading of the tip which accompanies sweepback.

The investigation has indicated that at a Mach number of 0.25 and a Reynolds number of 10,000,000, camber and twist improved the aerodynamic characteristics of the wing at moderate and high lift coefficients. It was noted, however, that at lower Reynolds numbers the benefits derived from camber and twist were less marked and the aerodynamic characteristics of both wings were seriously influenced by dynamic-scale effects.

At high Mach numbers, data were obtained only at a Reynolds number of 2,000,000, and therefore the magnitude of the scale effects at high Mach numbers is unknown. At this low Reynolds number and at lift coefficients greater than 0.3, camber and twist improved the drag characteristics of the wing up to a Mach number of 0.85. At the higher Mach numbers, the improvement in the drag characteristics of the wing as a result of camber and twist was seriously reduced as would be expected for a wing with such a large amount of camber. At all Mach numbers and a Reynolds number of 2,000,000, camber and twist had deleterious effects upon the longitudinal stability characteristics of the wing.

Triangular upper-surface fences extending from the position of maximum thickness to the trailing edge of the cambered and twisted wing were effective in improving the static longitudinal stability characteristics of the wing, particularly at Mach numbers above 0.85. The same type of fences had little effect on the characteristics of the plane wing except for a sharp reduction in the lift-curve slope at the lift coefficient where the onset of separation was indicated by the pitching-moment data. The improvement in the characteristics of the cambered and twisted wing resulting from the addition of fences was of such a magnitude as to cancel the detrimental effects of camber and twist on the pitching-moment characteristics of the wing at Mach numbers above 0.85. Low-speed tests of wings of similar plan form and identical sections have shown that at a Reynolds number of 8,000,000 and a Mach number of 0.20, separation on the plane wing originated in the laminar boundary layer at the leading edge; while on the cambered and twisted wing, separation originated in the turbulent boundary layer at the trailing edge. The marked difference in the effectiveness of the fences on the two wings suggests that even at a Reynolds number of 2,000,000 and at Mach numbers as high as 0.94 the mechanism of separation on the two wings was entirely dissimilar. It was also noted that there was little to be gained by the addition of a fence outboard of

the mid-semispan of the wings or by employment of the high fence in preference to the low fence.

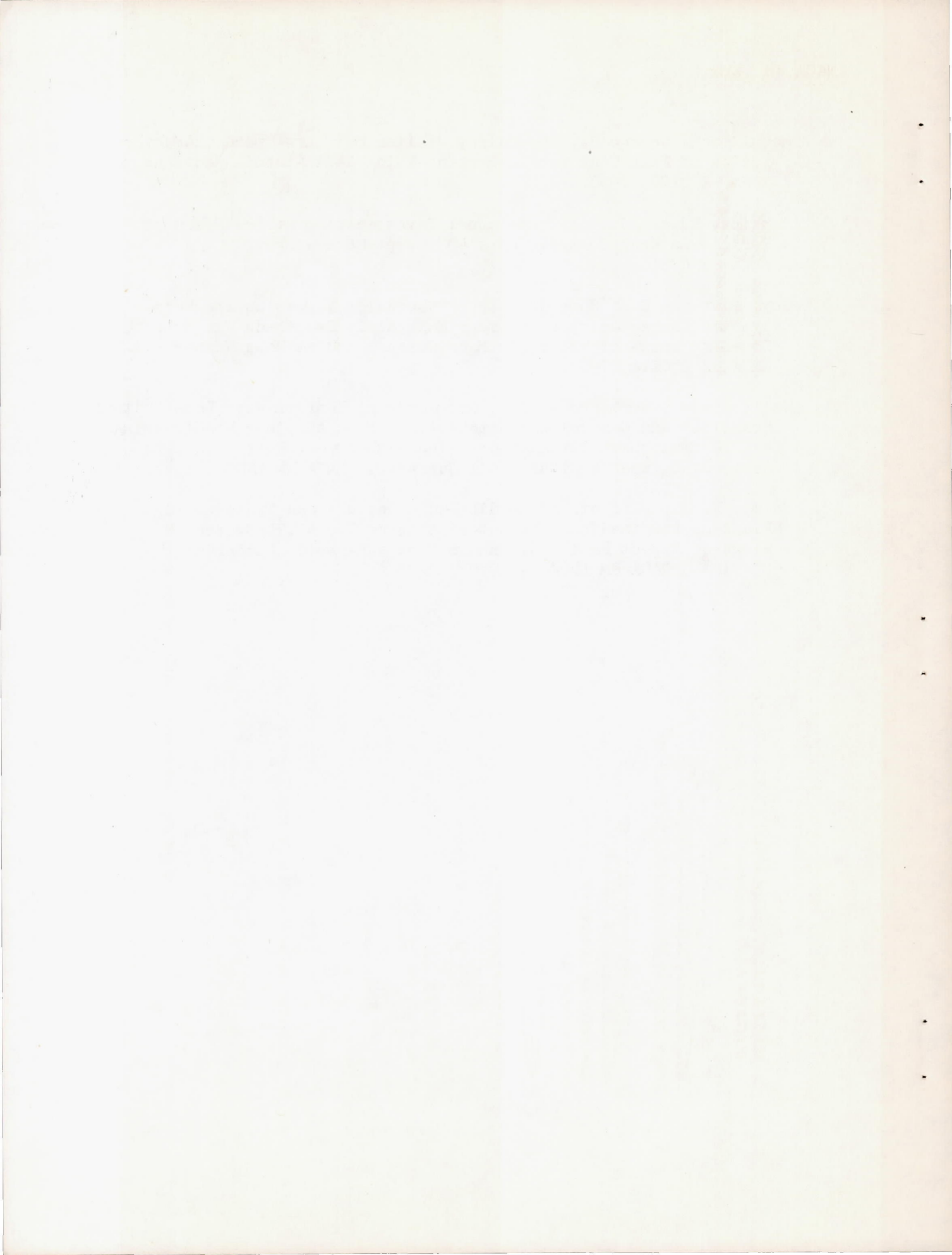
Application of surface roughness to the plane wing resulted in no indicated increase of the effective test Reynolds number. Addition of the fuselage caused little change in the characteristics of either wing, except a slight increase in the drag at low lift.

Ames Aeronautical Laboratory,
National Advisory Committee for Aeronautics,
Moffett Field, Calif.

REFERENCES

1. Hunton, Lynn W.: Effects of Twist and Camber on the Low-Speed Characteristics of a Large-Scale 45° Swept-Back Wing. NACA RM A50A10, 1950.
2. Hunton, Lynn W., and Dew, Joseph K.: The Effect of Camber and Twist on the Aerodynamic Loading and Stalling Characteristics of a Large-Scale 45° Swept-Back Wing. NACA RM A50J24, 1951.
3. Loftin, Lawrence K., Jr.: Theoretical and Experimental Data for a Number of NACA 6A-Series Airfoil Sections. NACA Rep. 903, 1948. (Formerly NACA RM L6J01, 1946; NACA TN 1368, 1947)
4. Sivells, James C., and Deters, Owen J.: Jet-Boundary and Plan-Form Corrections for Partial-Span Models with Reflection Plane, End Plate, or No End Plate in a Closed Circular Wind Tunnel. NACA Rep. 843, 1946. (Formerly NACA TN 1077, 1946)
5. Herriot, John G.: Blockage Corrections for Three-Dimensional-Flow Closed-Throat Wind Tunnels, With Consideration of the Effect of Compressibility. NACA Rep. 995, 1950. (Formerly NACA RM A7B28, 1947)
6. Summers, James L., and Treon, Stuart L.: The Effects of Amount and Type of Camber on the Variation with Mach Number of the Aerodynamic Characteristics of a 10-Percent-Thick NACA 64A-Series Airfoil Section. NACA TN 2096, 1950.
7. Salmi, Reino J., and Carros, Robert J.: Longitudinal Characteristics of Two 47.7° Sweptback Wings with Aspect Ratios of 5.1 and 6.0 at Reynolds Numbers Up to 10×10^6 . NACA RM L50A04, 1950.

8. McCullough, George B., and Haire, William M.: Low-Speed Characteristics of Four Cambered 10-Percent-Thick NACA Airfoil Sections. NACA TN 2177, 1950.
9. Hopkins, Edward J.: A Wind-Tunnel Investigation at Low Speed of Various Lateral Controls on a 45° Swept-Back Wing. NACA RM A7L16, 1948.
10. Guy, Lawrence D.: Some Effects of Chordwise Fences on the Aerodynamic Characteristics of Four Moderately Sweptback Wings in the Low-Lift Range at Transonic Mach Numbers and at Mach Number 1.9. NACA RM L5OE16, 1950.
11. Weil, Joseph, Comisarow, Paul, and Goodson, Kenneth W.: Longitudinal Stability and Control Characteristics of an Airplane Model Having a 42.8° Sweptback Circular-Arc Wing With Aspect Ratio 4.00, Taper Ratio 0.50, and Sweptback Tail Surfaces. NACA RM L7G28, 1947.
12. Salmi, R. J.: Effects of Leading-Edge Devices and Trailing-Edge Flaps on Longitudinal Characteristics of Two 47.7° Sweptback Wings of Aspect Ratios 5.1 and 6.0 at a Reynolds Number of 6×10^6 . NACA RM L5OF20, 1950.



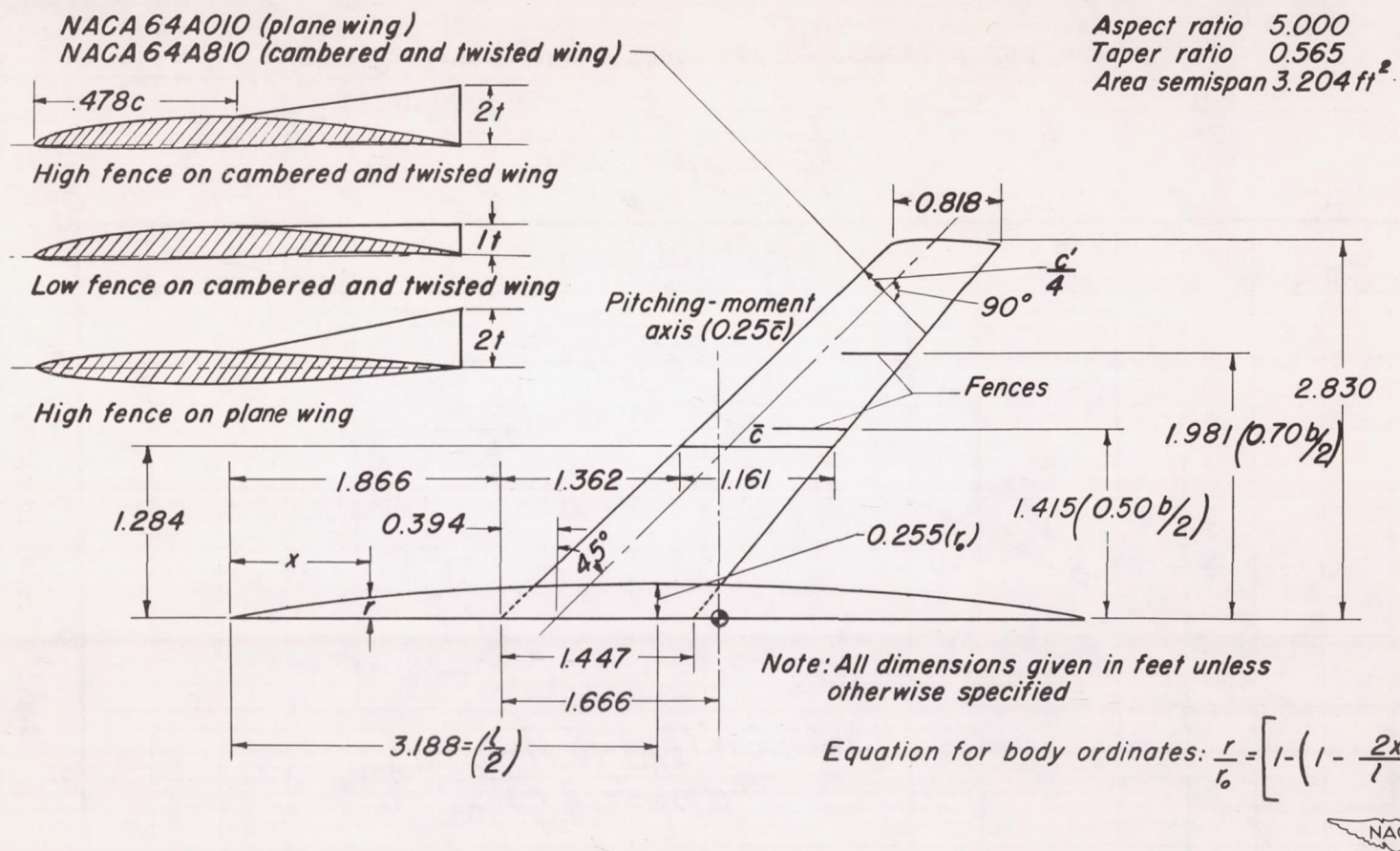


Figure 1.- Dimensional sketch of the wing-body model.

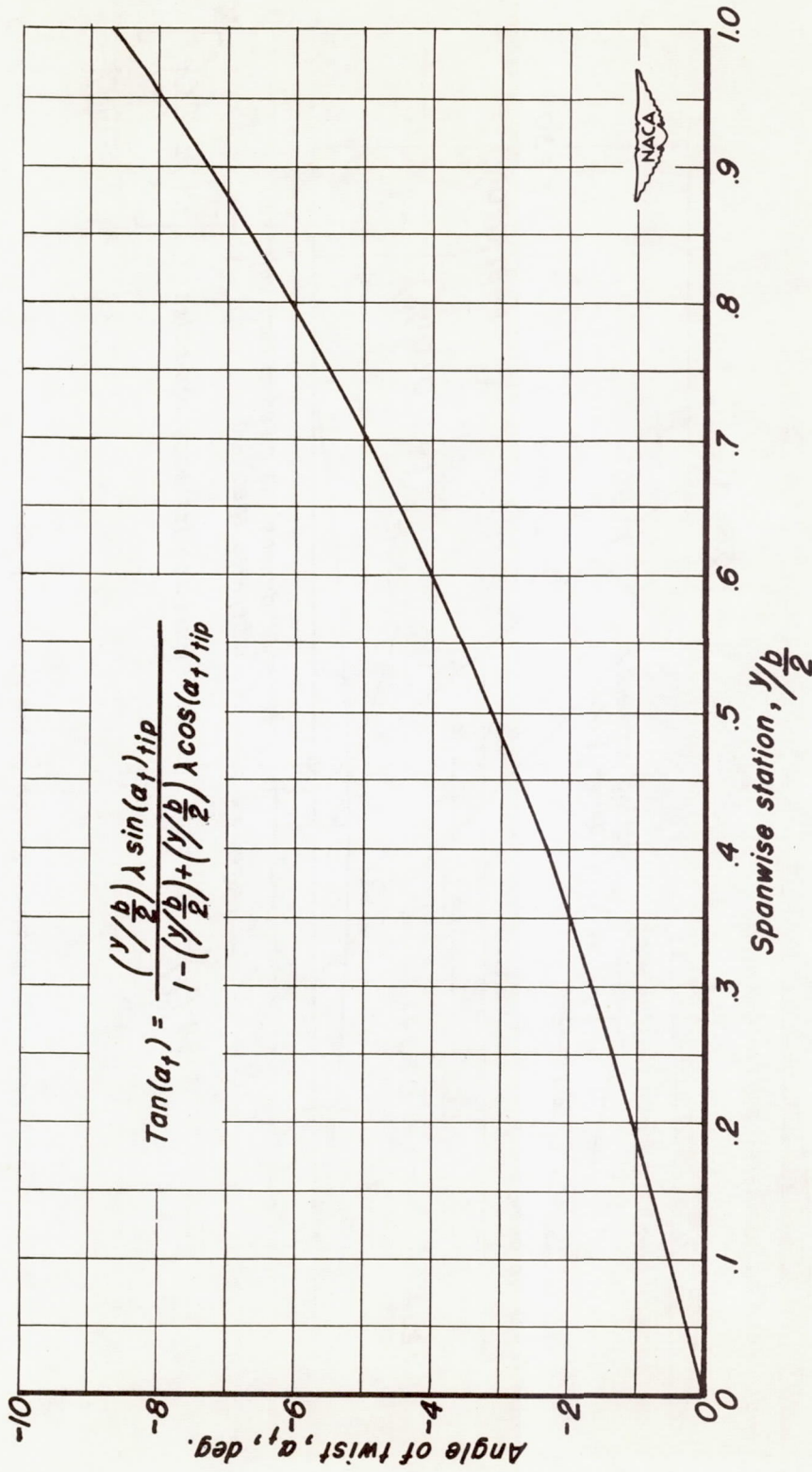
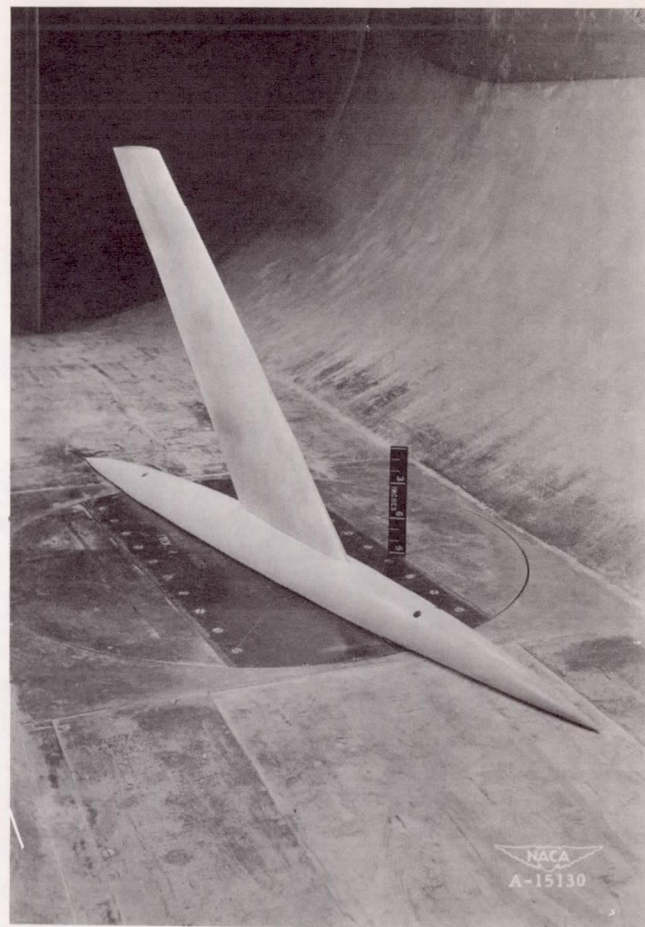


Figure 2.- The twist distribution of the cambered and twisted wing.

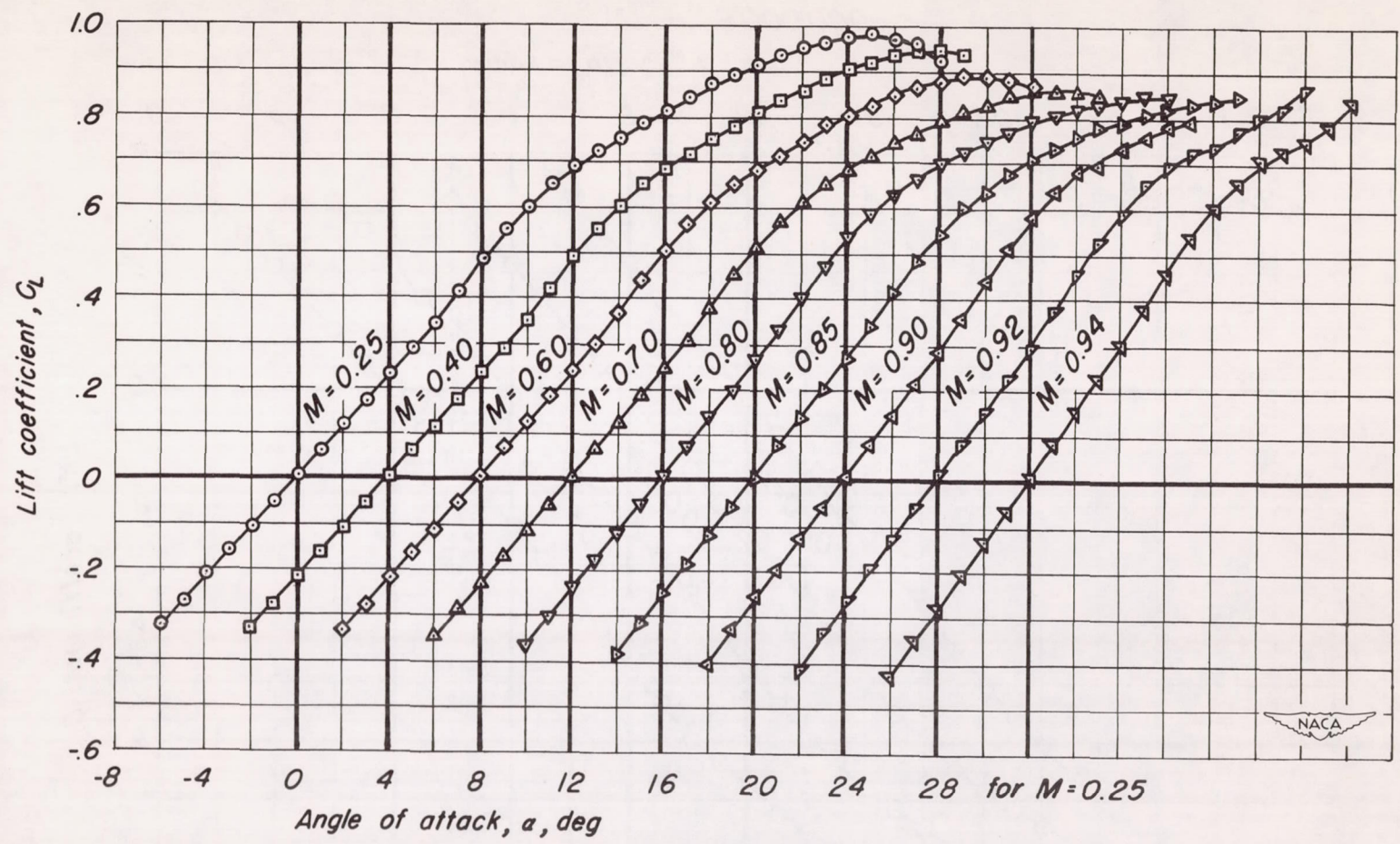


(a) Wing alone.



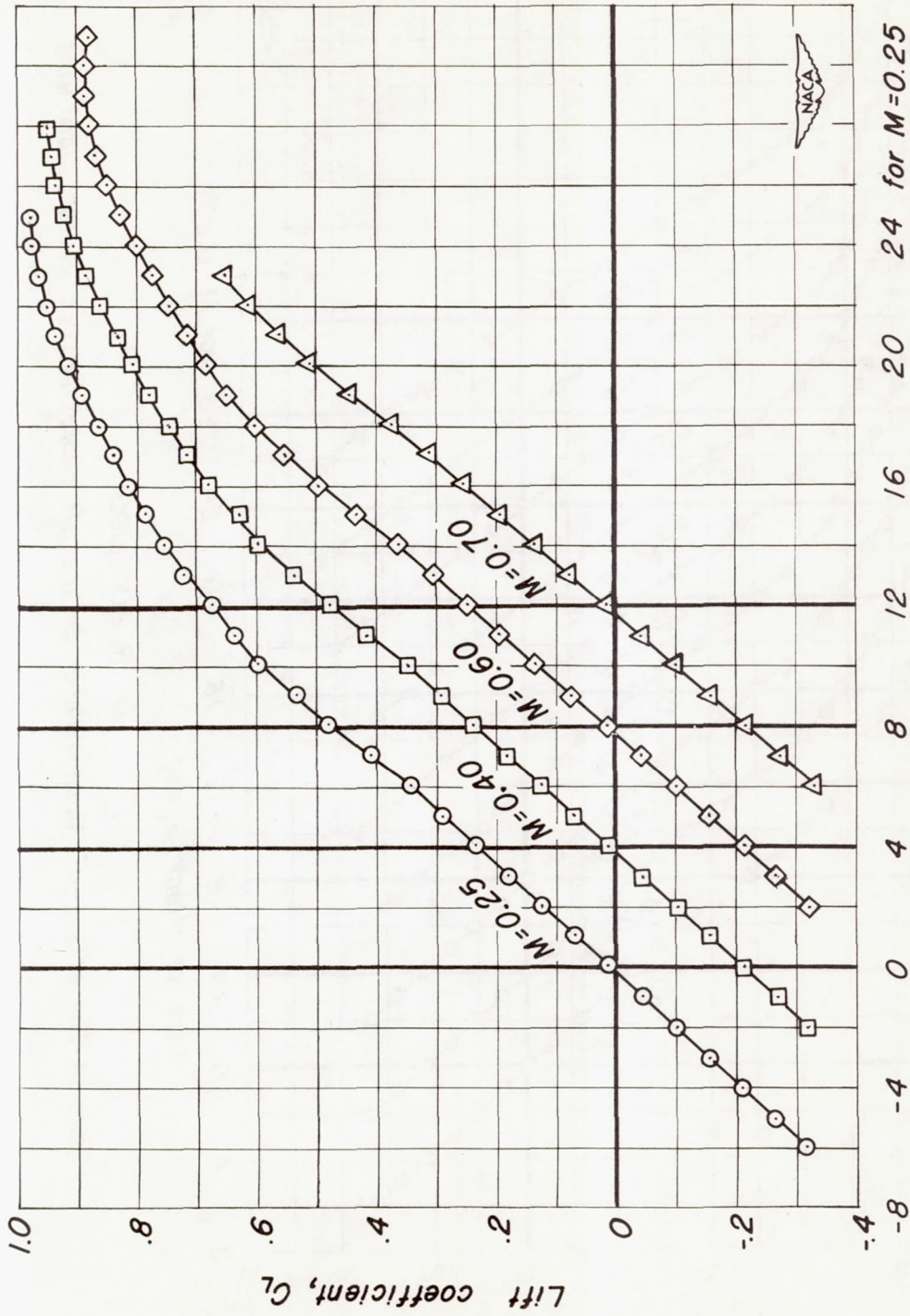
(b) Wing with body.

Figure 3.—The plane wing mounted in the Ames 12-foot pressure wind tunnel.



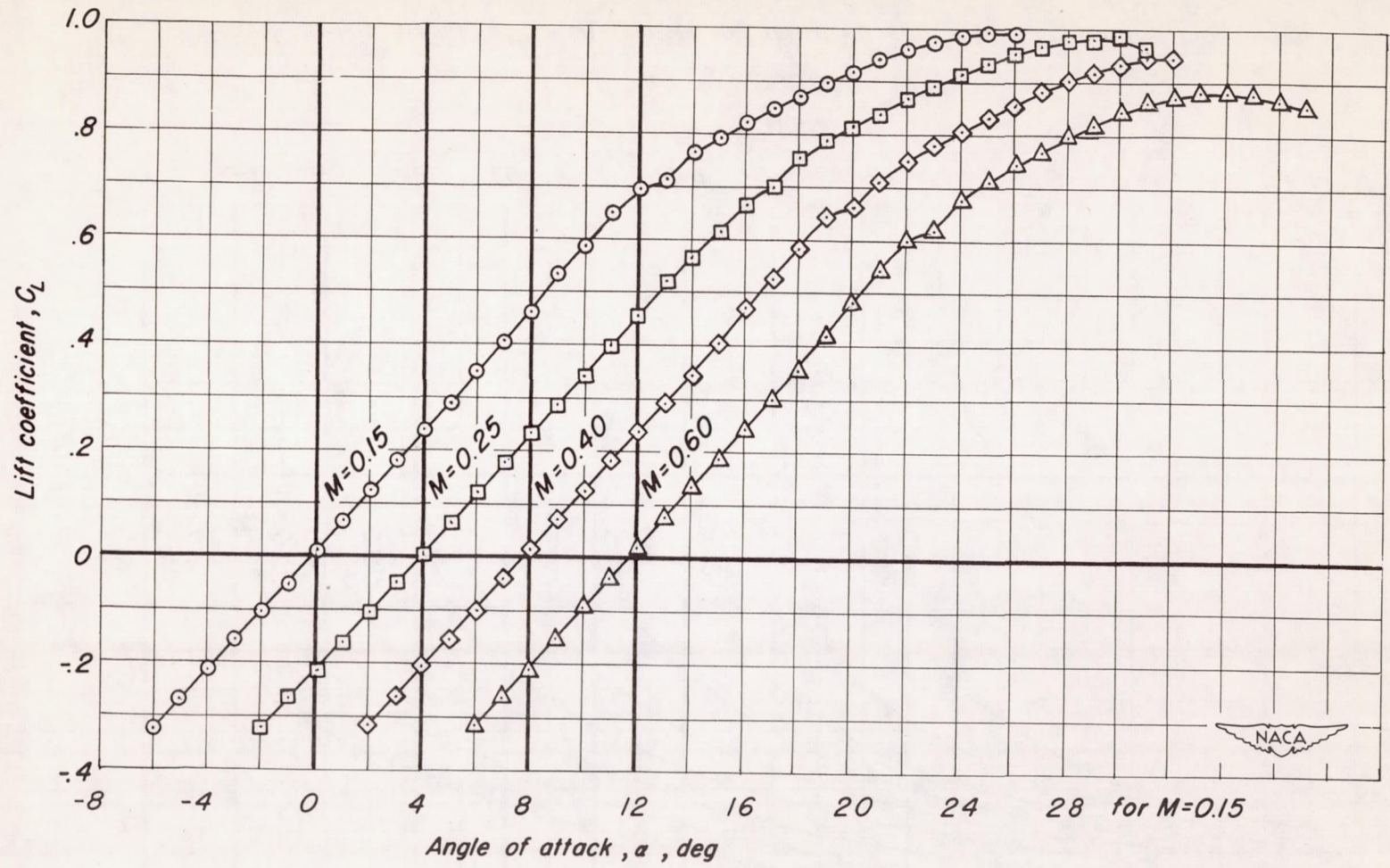
(a) $R, 2,000,000$

Figure 4-The effect of Mach number on the lift characteristics of the plane wing.



Angle of attack, α , deg

(b) R, 3,000,000
Figure 4.-Continued.



(c) $R, 4,000,000$
 Figure 4.- Concluded.

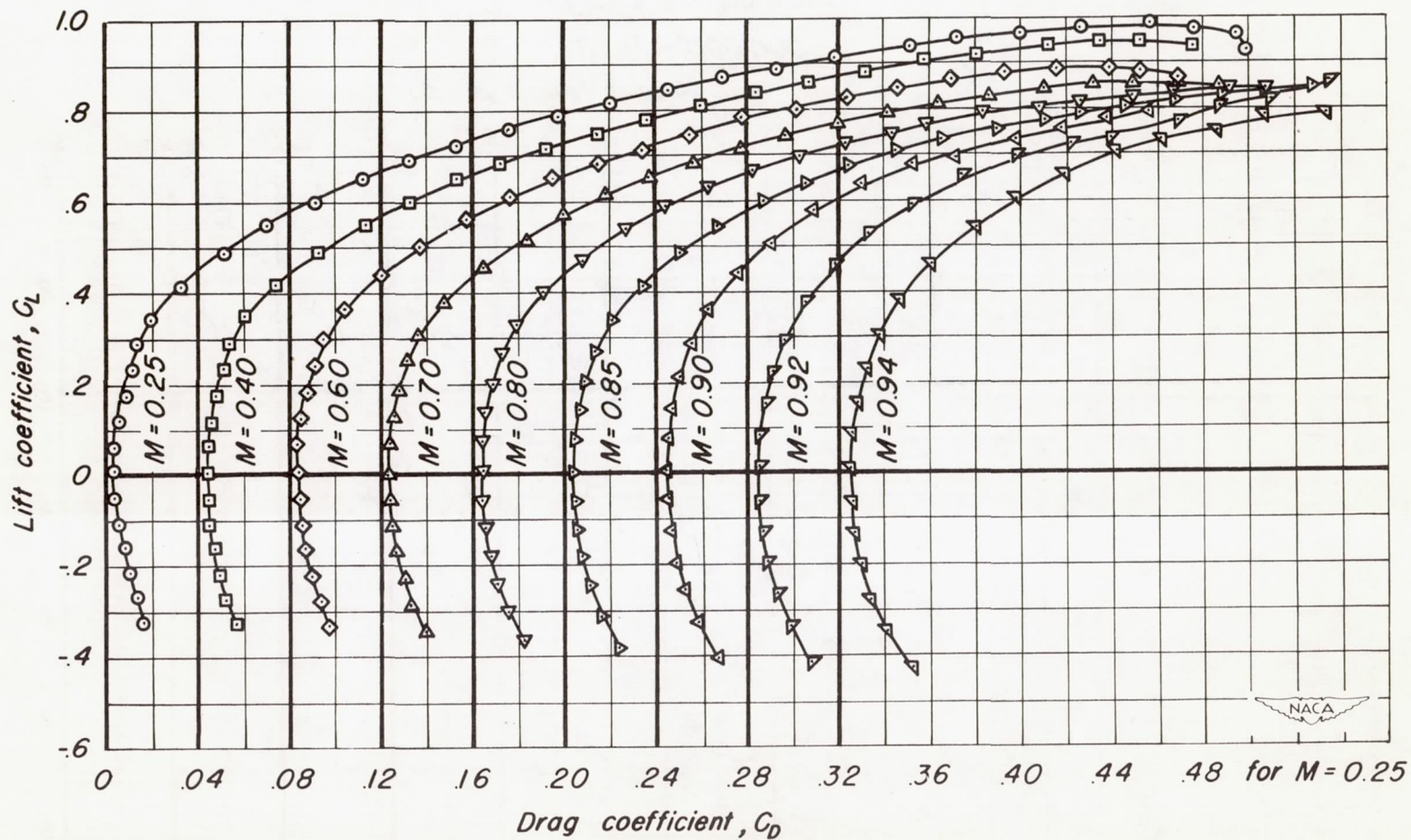
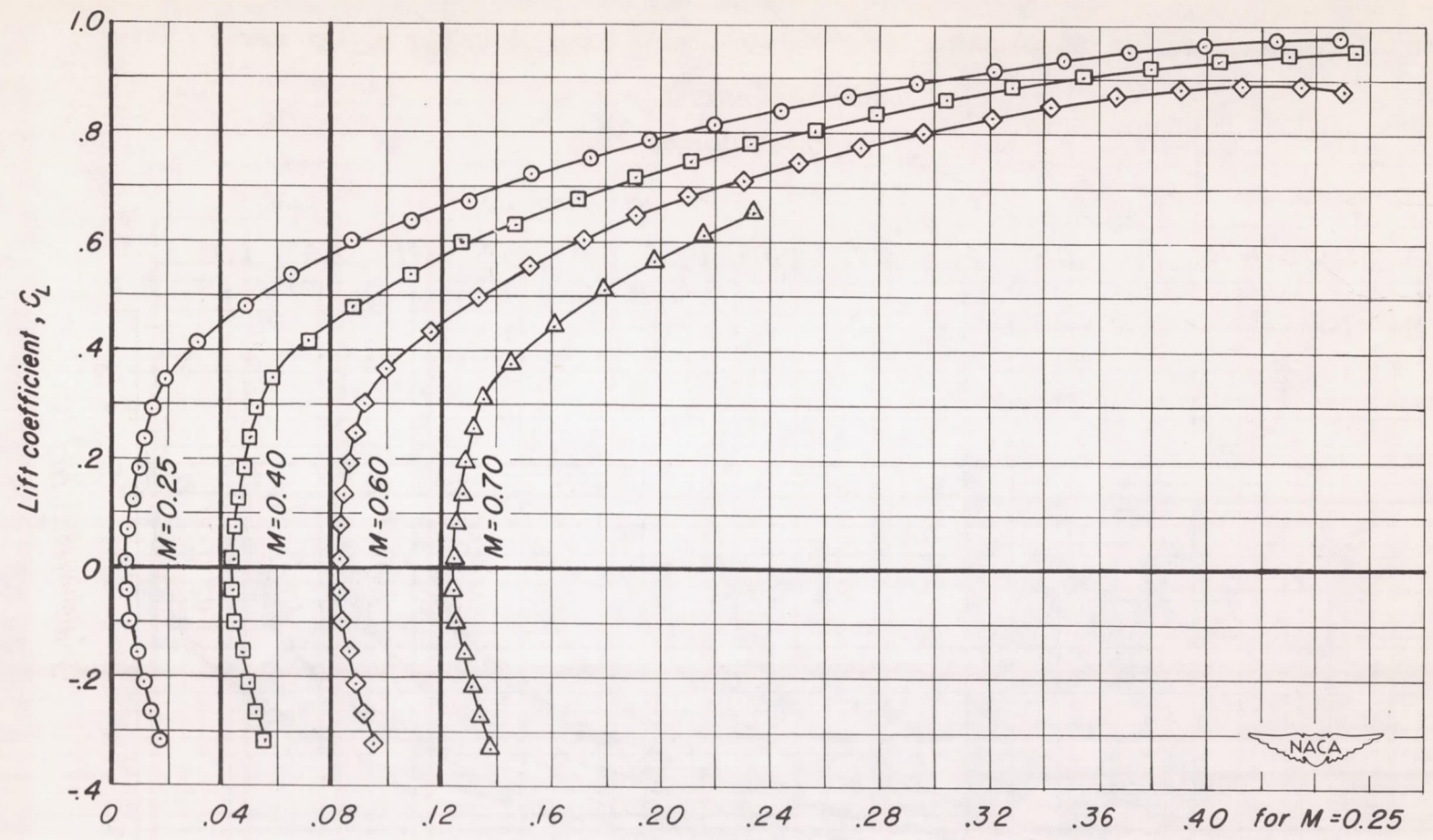
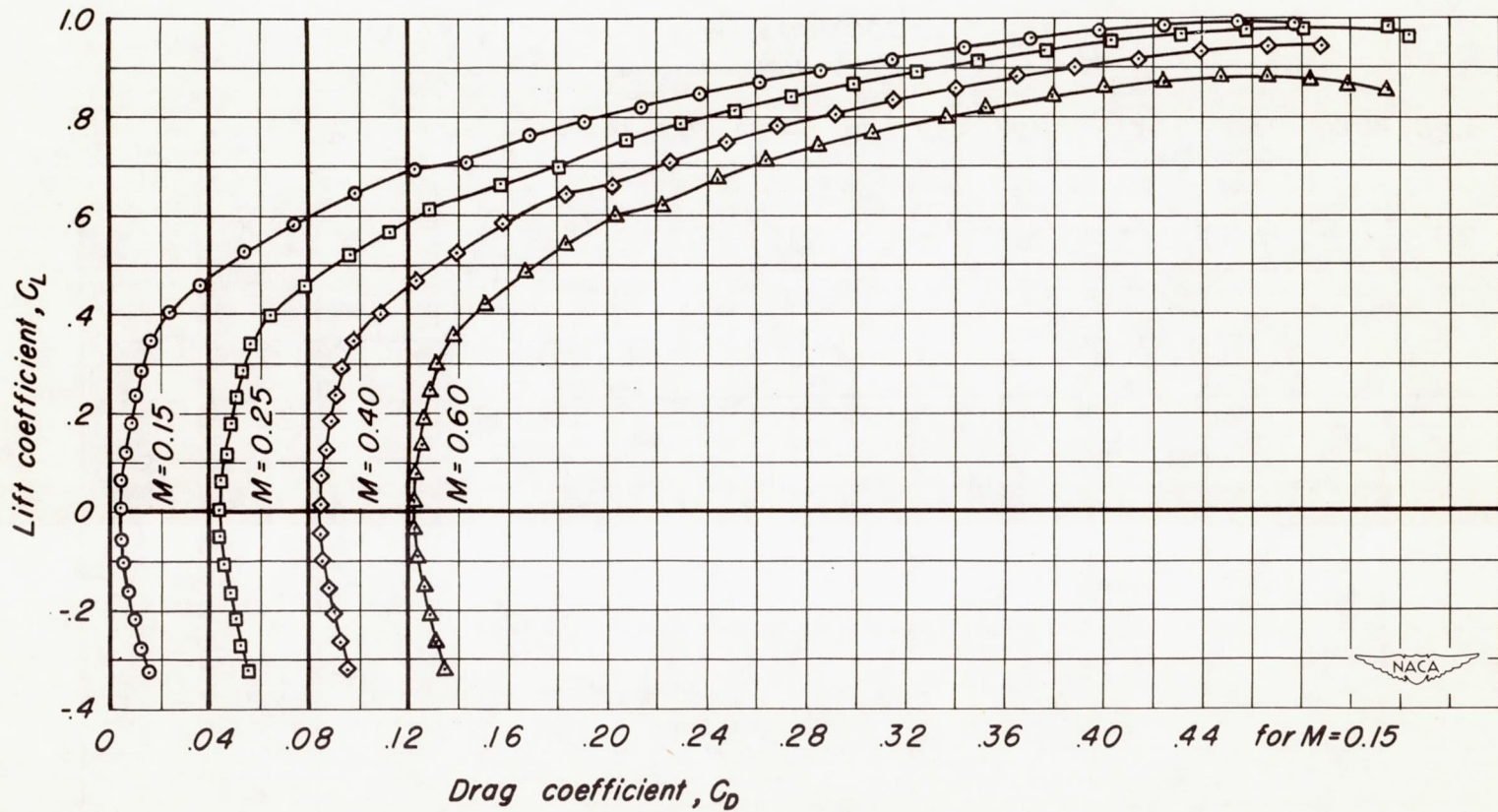
(a) $R, 2,000,000$

Figure 5.-The effect of Mach number on the drag characteristics of the plane wing.



Drag coefficient, C_D
(b) $R, 3,000,000$
Figure 5.—Continued.



(c) $R, 4,000,000$
 Figure 5.-Concluded.

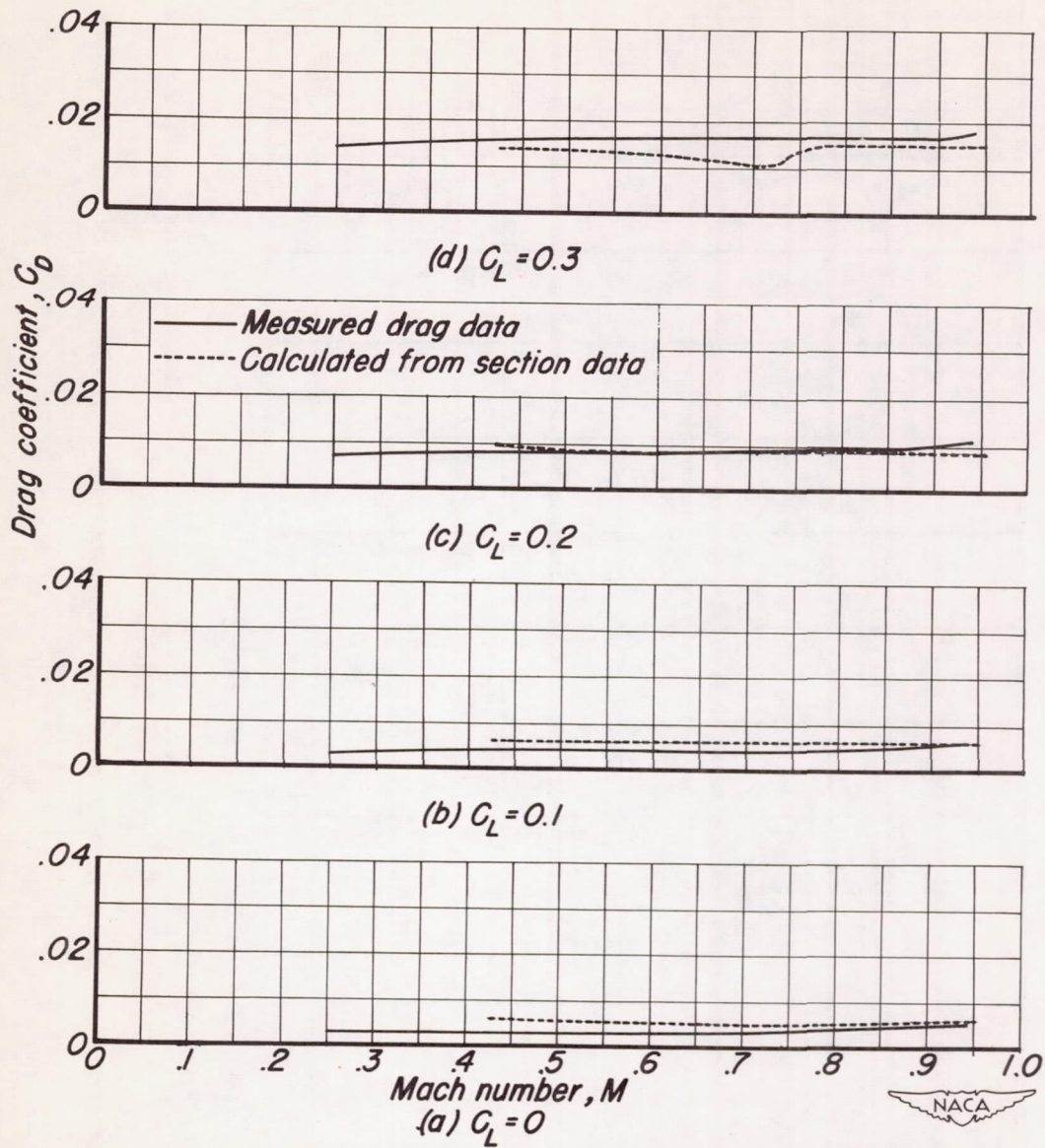
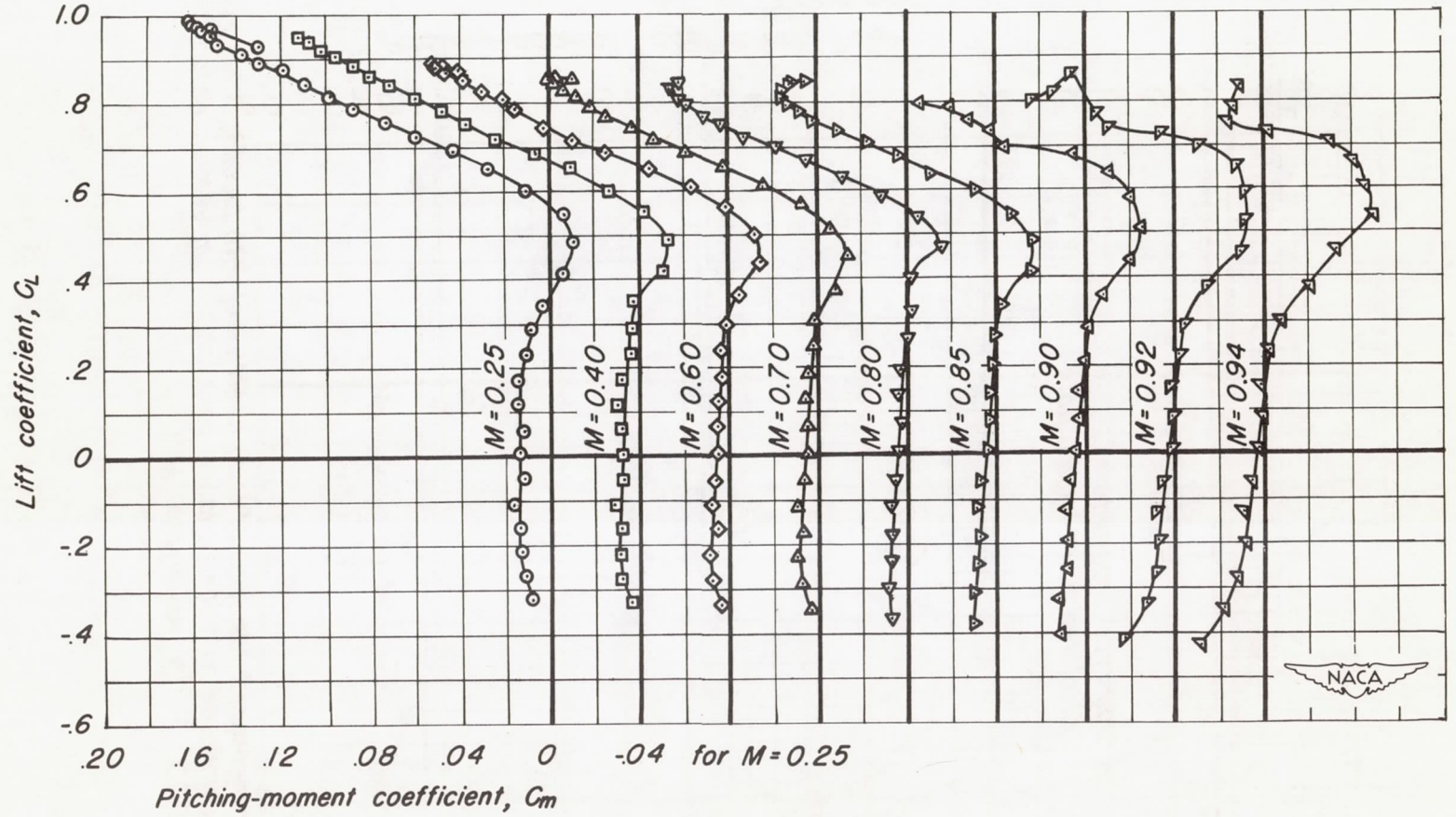
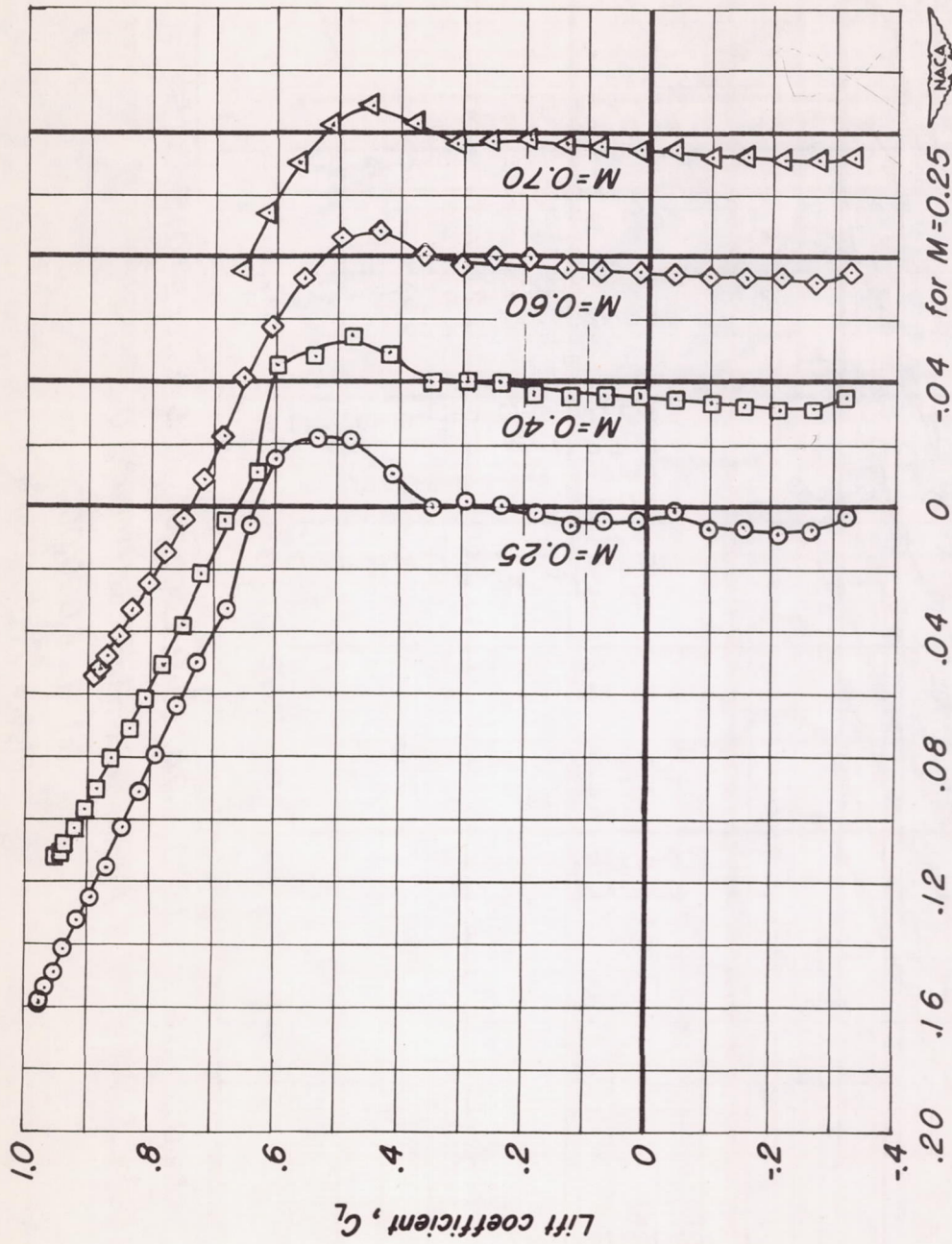


Figure 6.-The measured variation of drag coefficient with Mach number of the plane wing compared with the variation calculated from section data. $R, 2,000,000$.

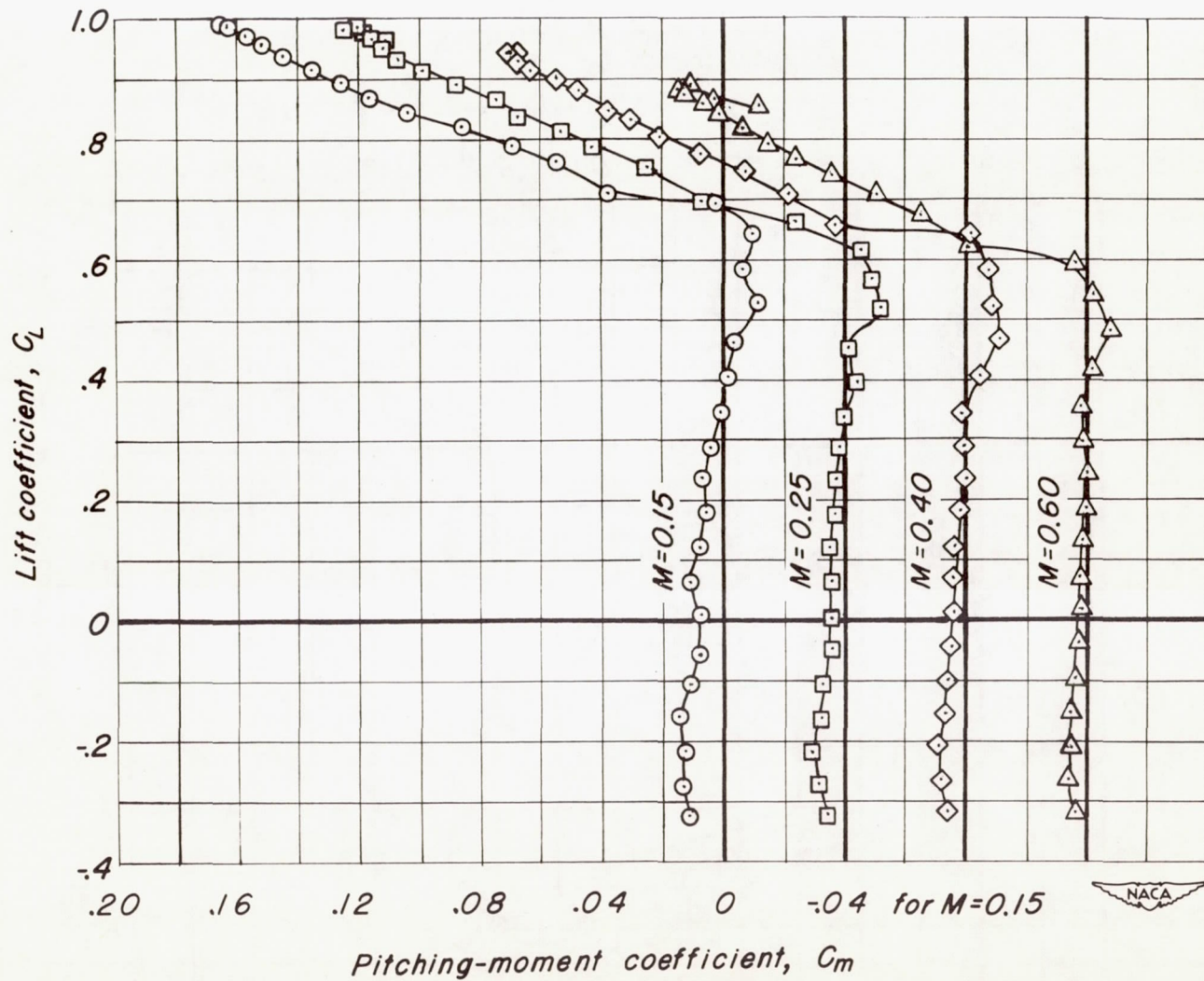


(a) R, 2,000,000

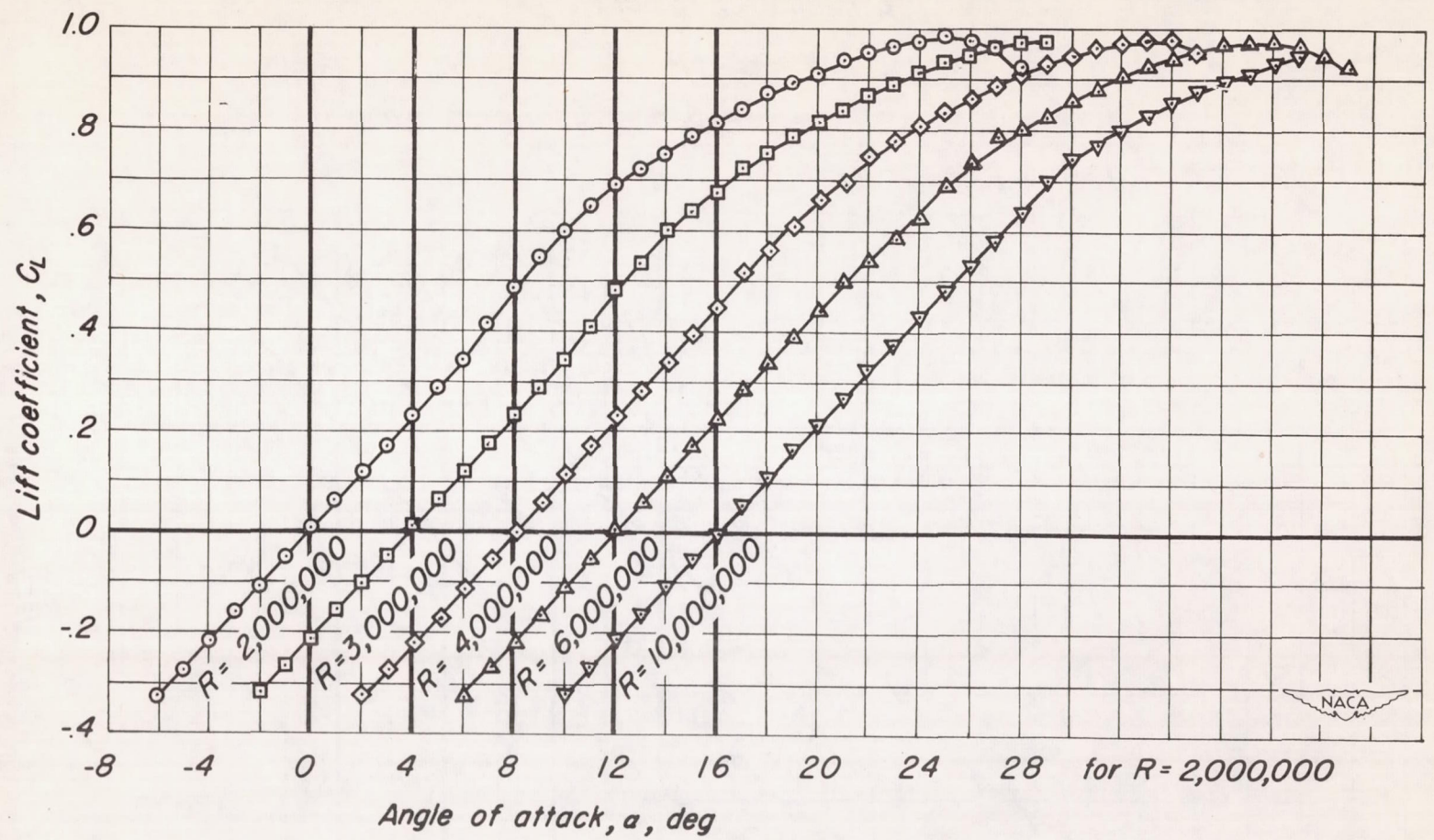
Figure 7:-The effect of Mach number on the pitching-moment characteristics of the plane wing.



Pitching-moment coefficient, C_m
(b) R, 3,000,000
Figure 7.-Continued.

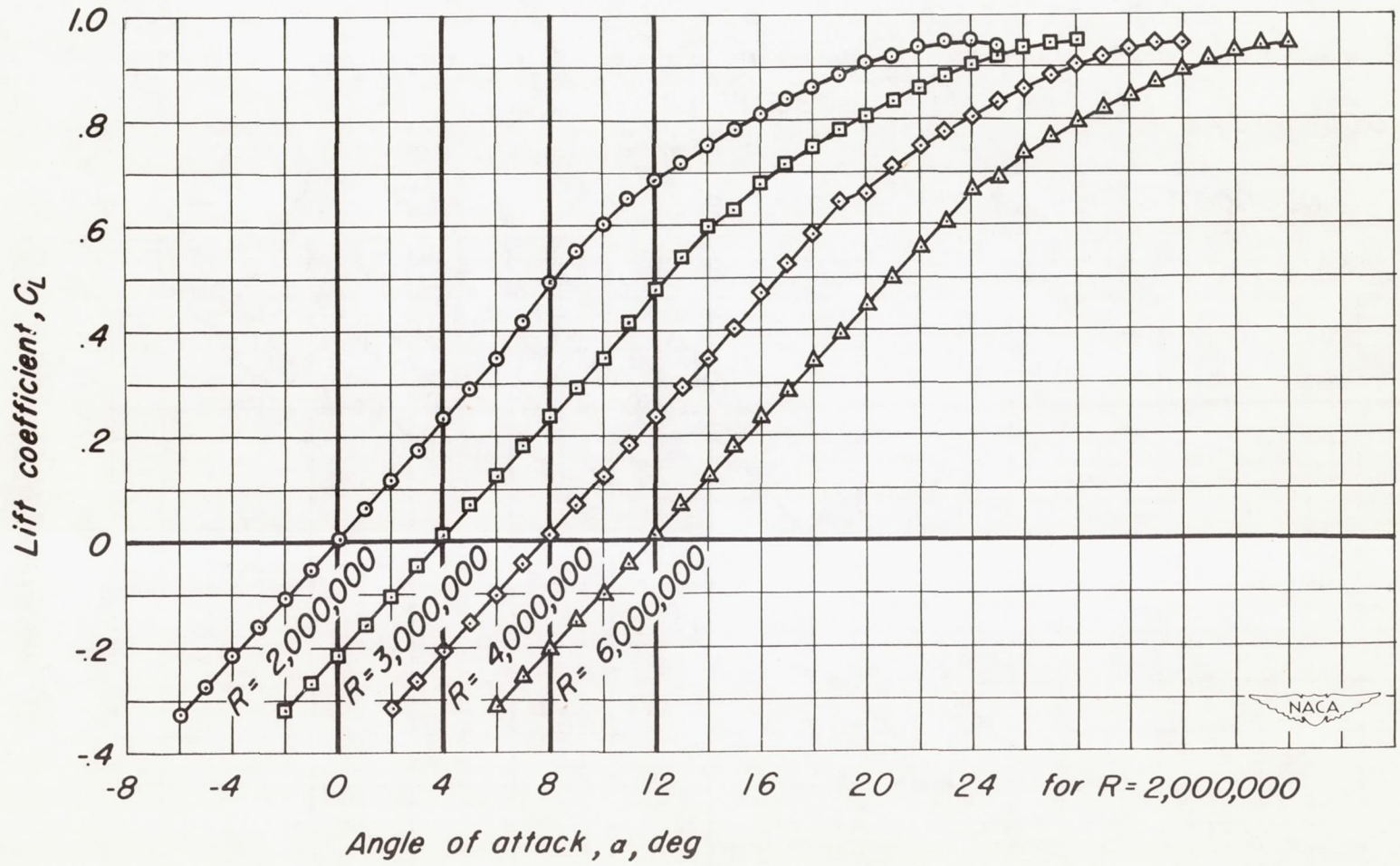


(c) R, 4,000,000
 Figure 7.- Concluded.



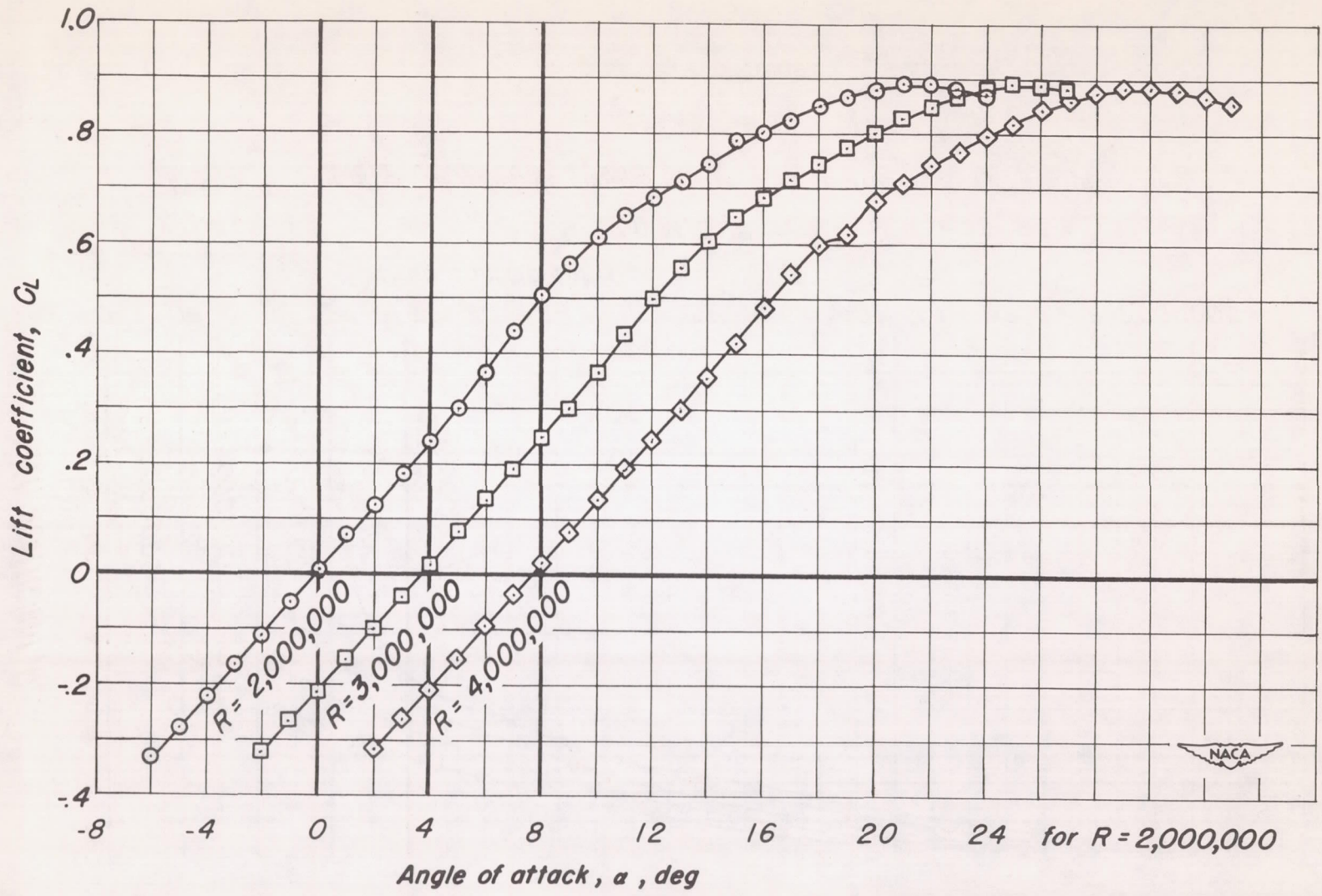
(a) $M, 0.25$

Figure 8.- The effect of Reynolds number on the lift characteristics of the plane wing.

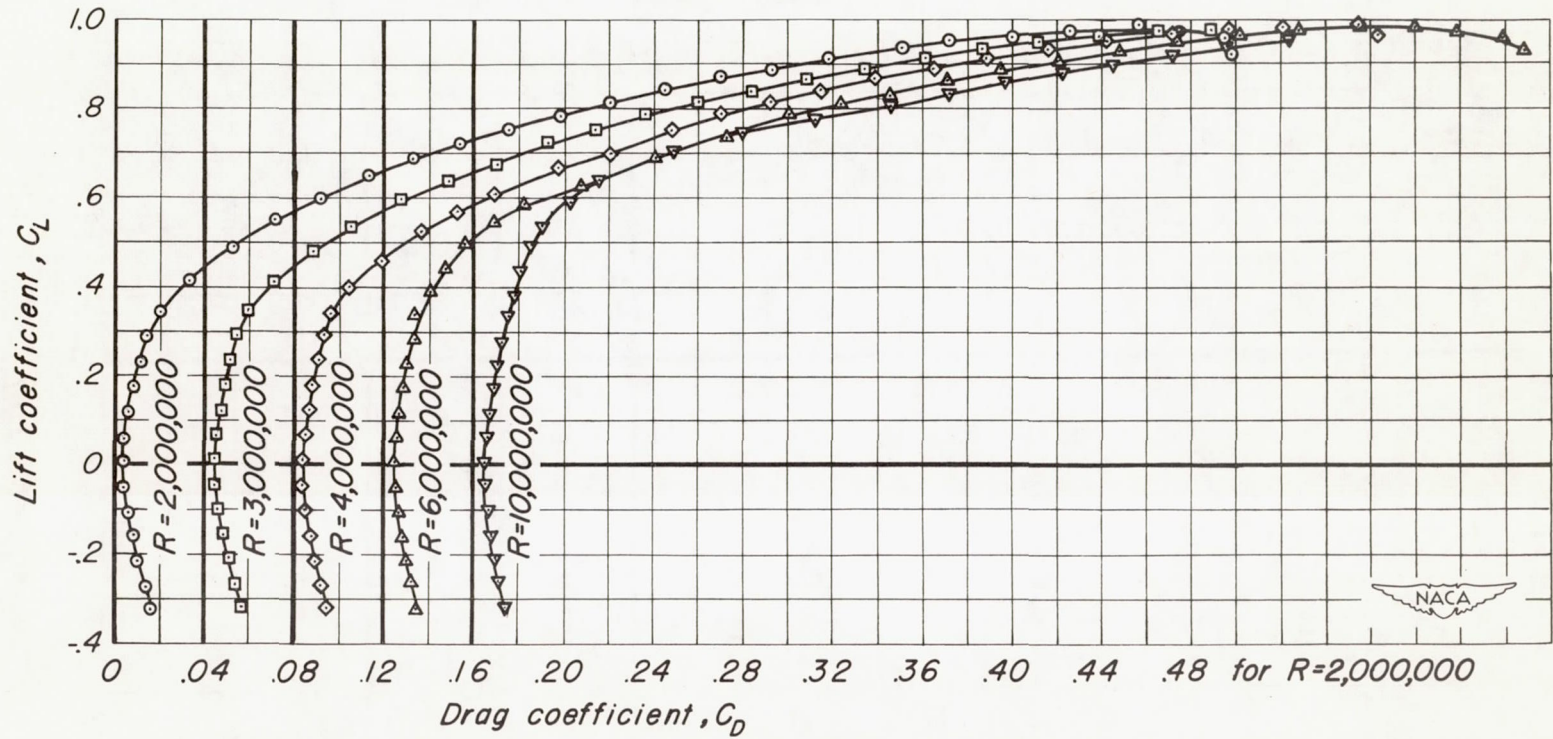


(b) $M, 0.40.$

Figure 8.-Continued.

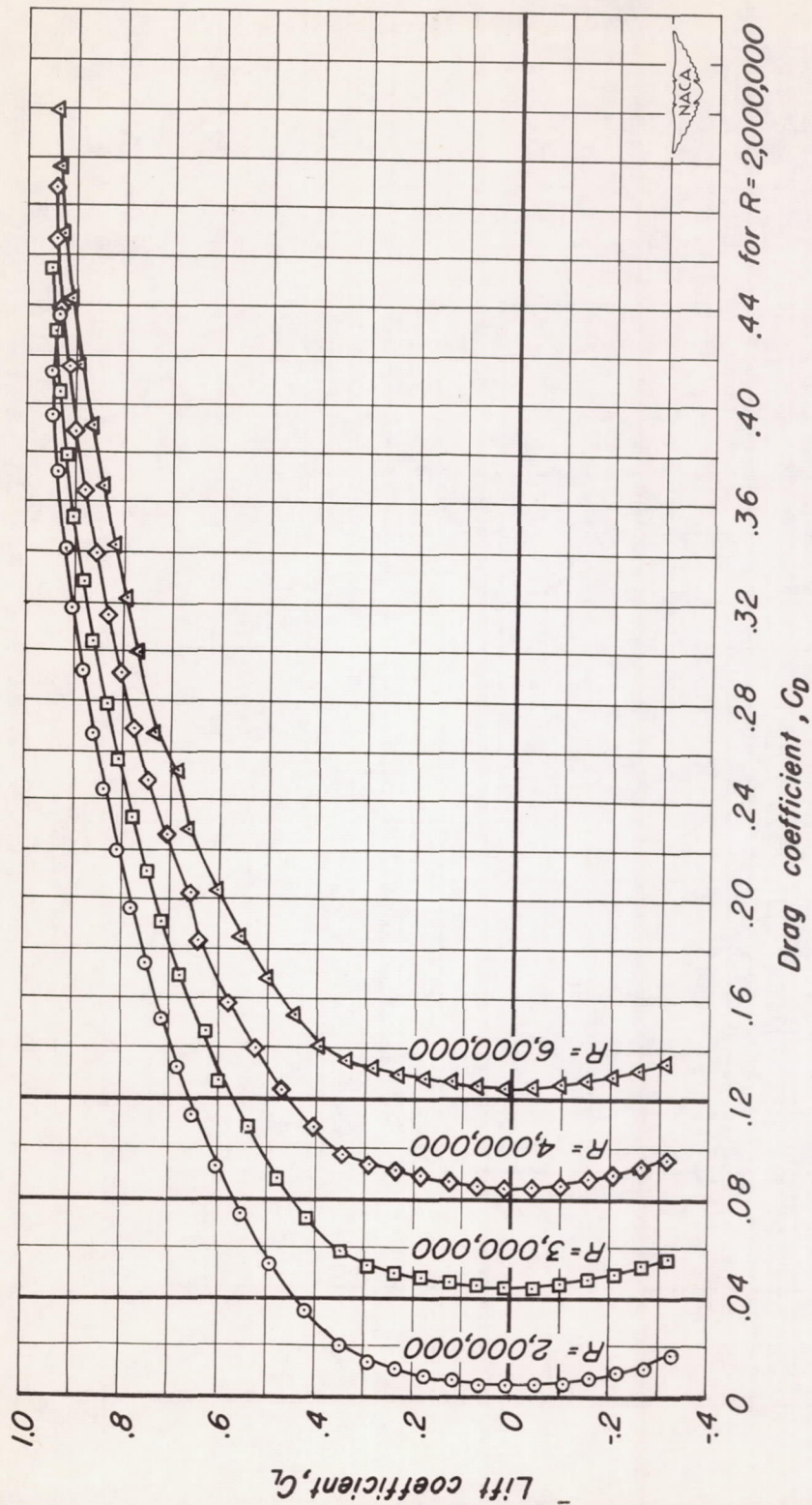


(c) $M, 0.60$
Figure 8.-Concluded.



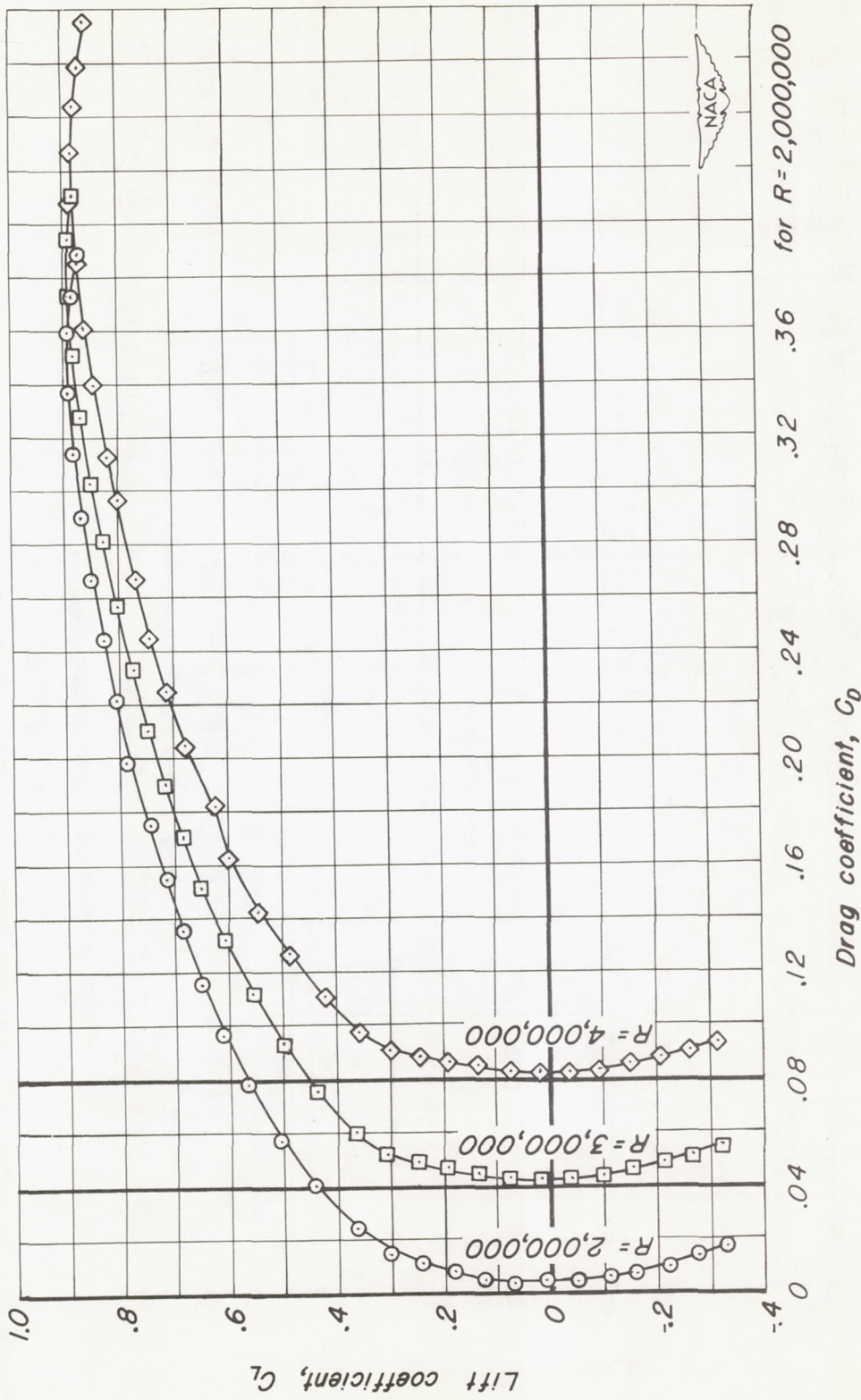
(a) $M, 0.25$

Figure 9.- The effect of Reynolds number on the drag characteristics of the plane wing.



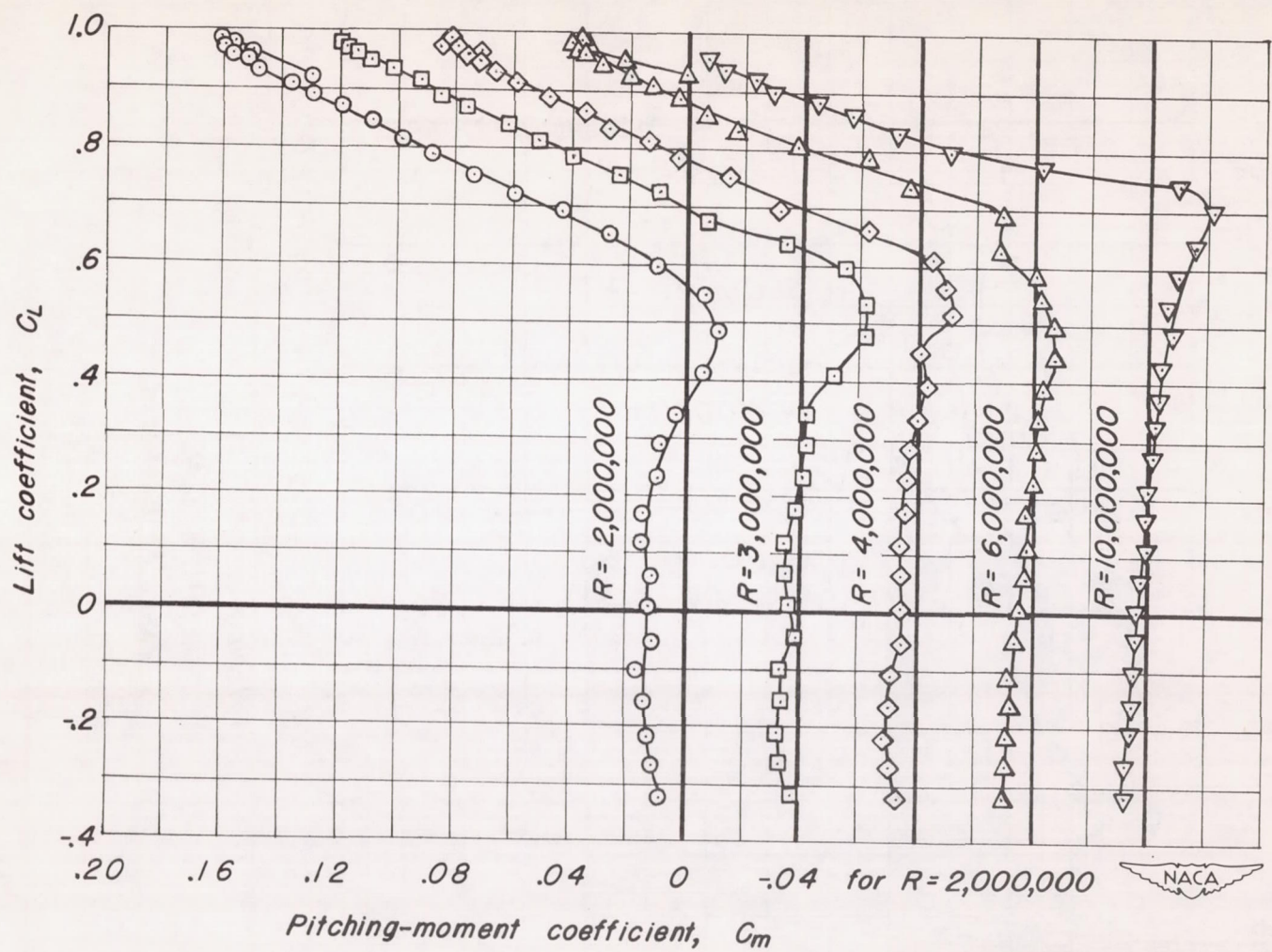
(b) $M, 0.40$

Figure 9.-Continued.



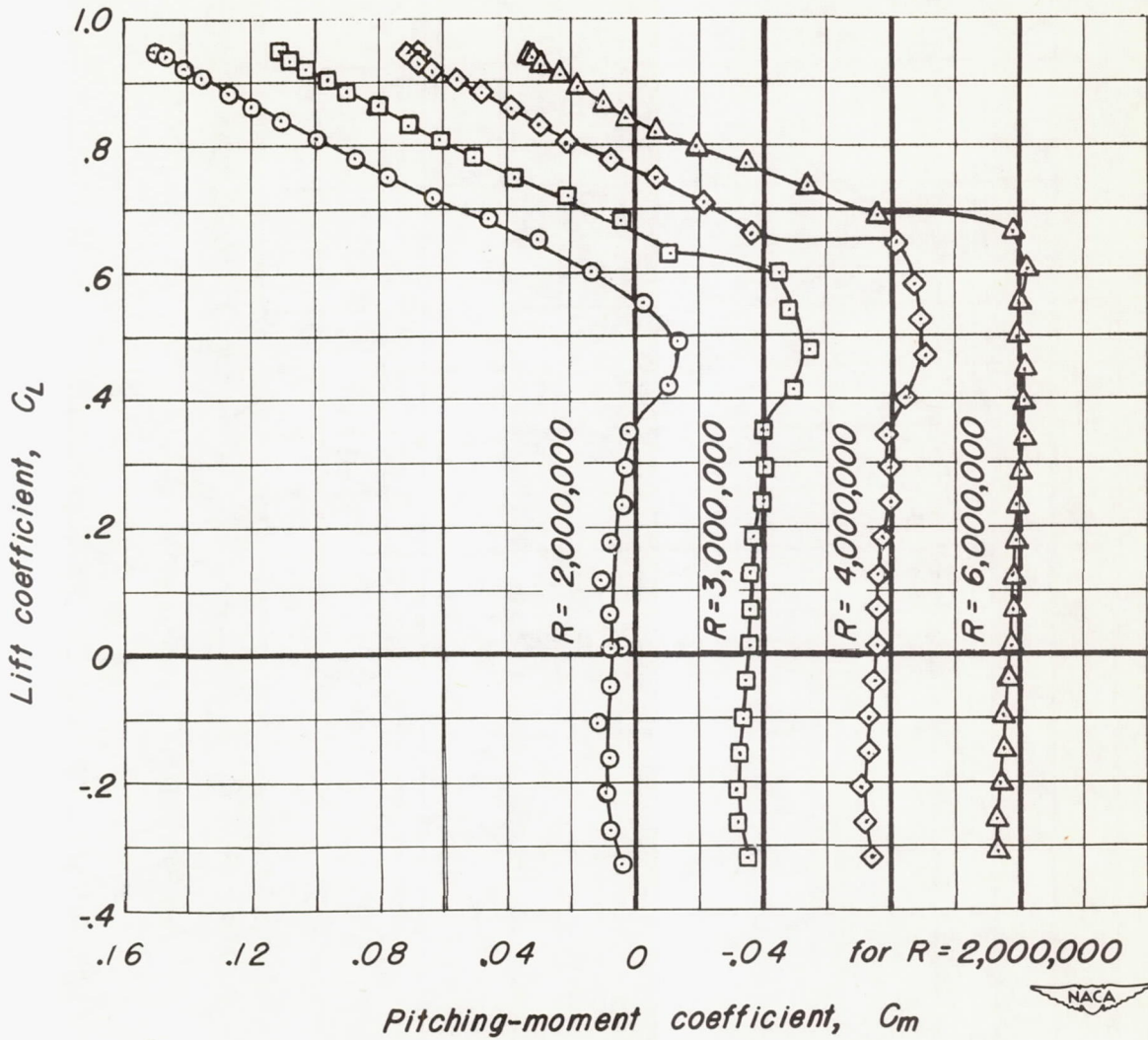
(c) $M, 0.60$

Figure 9. - Concluded.



(a) $M, 0.25$

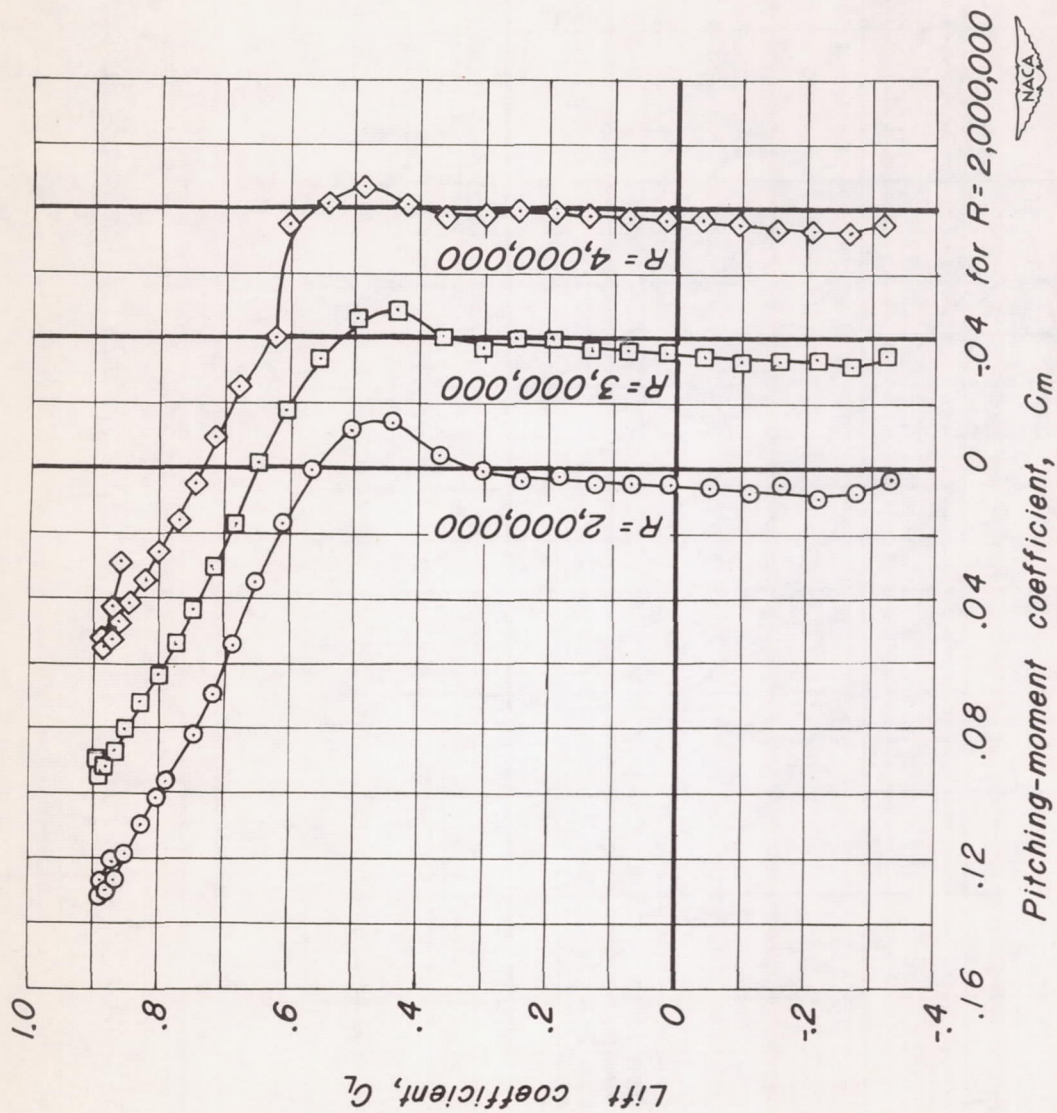
Figure 10.-The effect of Reynolds number on the pitching-moment characteristics of the plane wing.



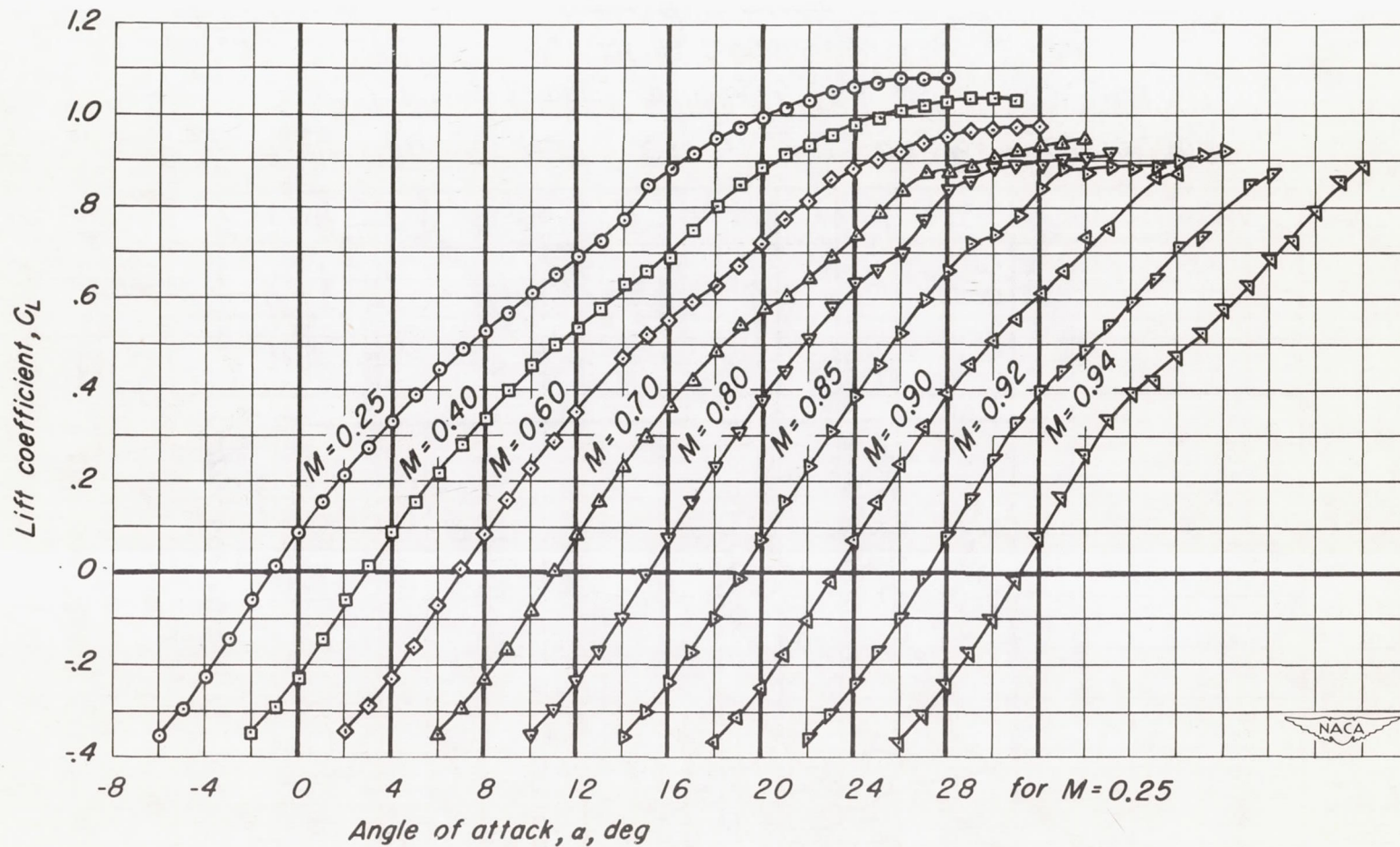
Pitching-moment coefficient, C_m

(b) $M, 0.40$

Figure 10.-Continued.

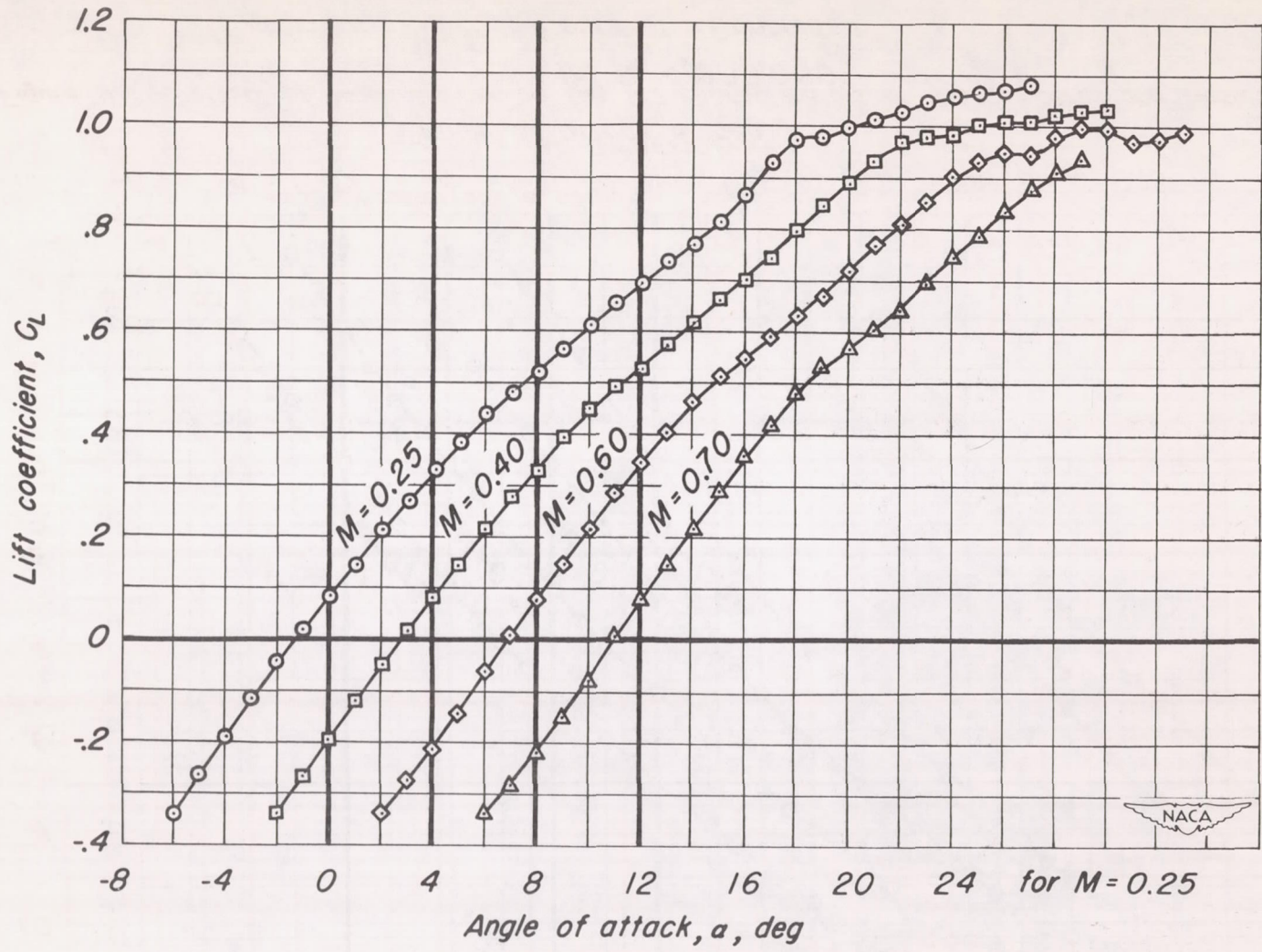


(c) $M, 0.60$
Figure 10.-Concluded.

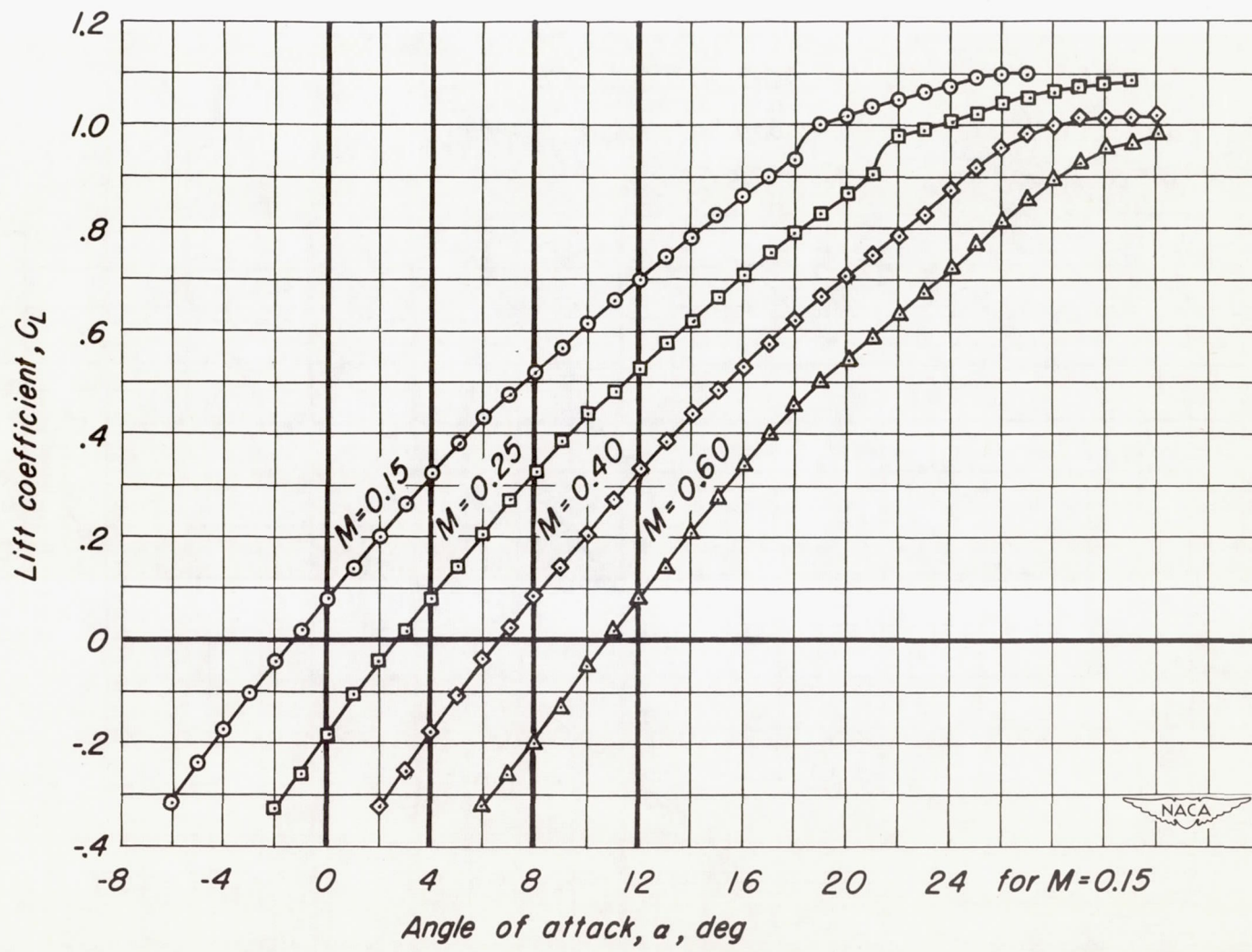


(a) $R, 2,000,000$

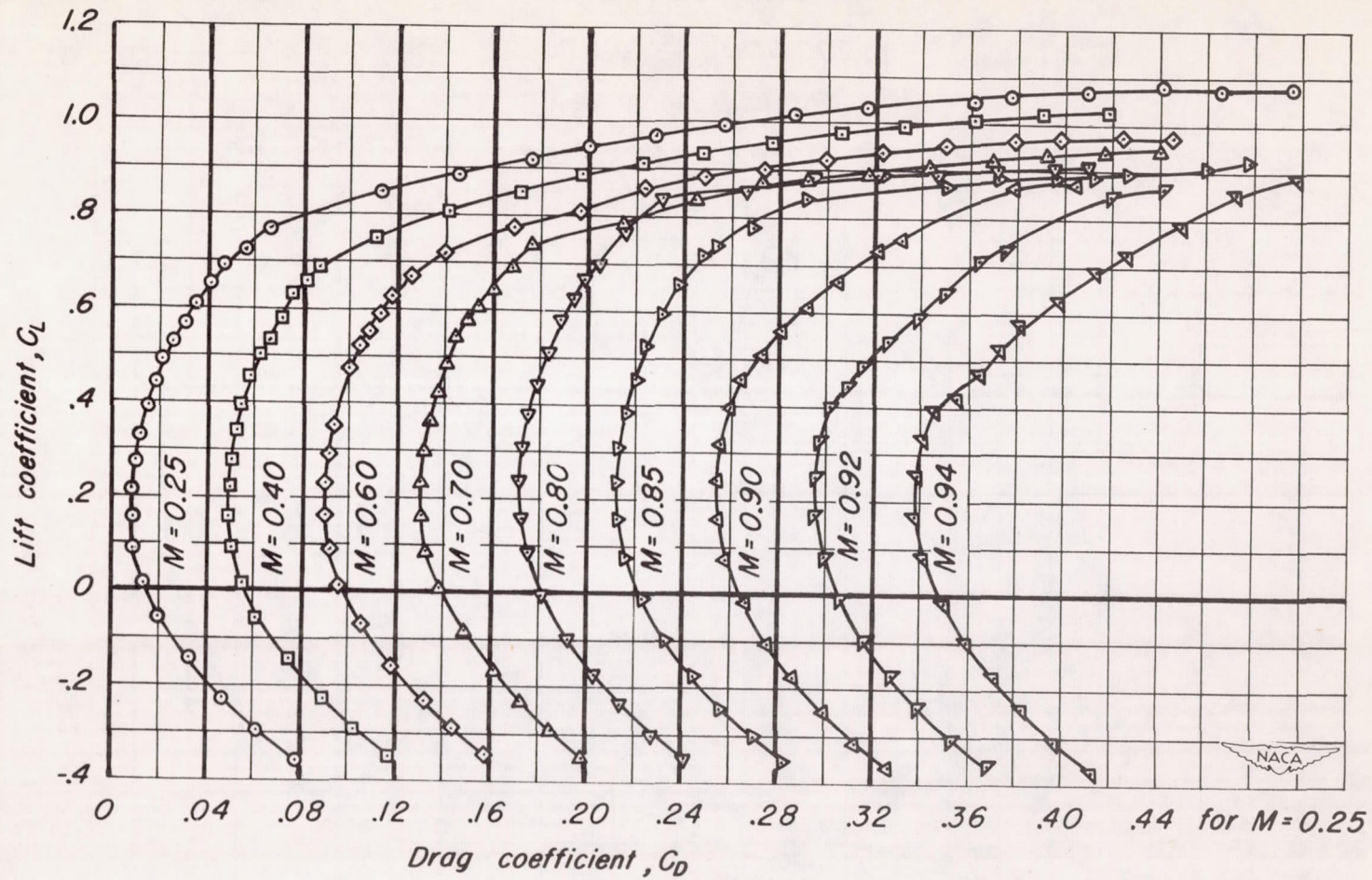
Figure 11.-The effect of Mach number on the lift characteristics of the cambered and twisted wing.



(b) R, 3,000,000
Figure II-Continued.

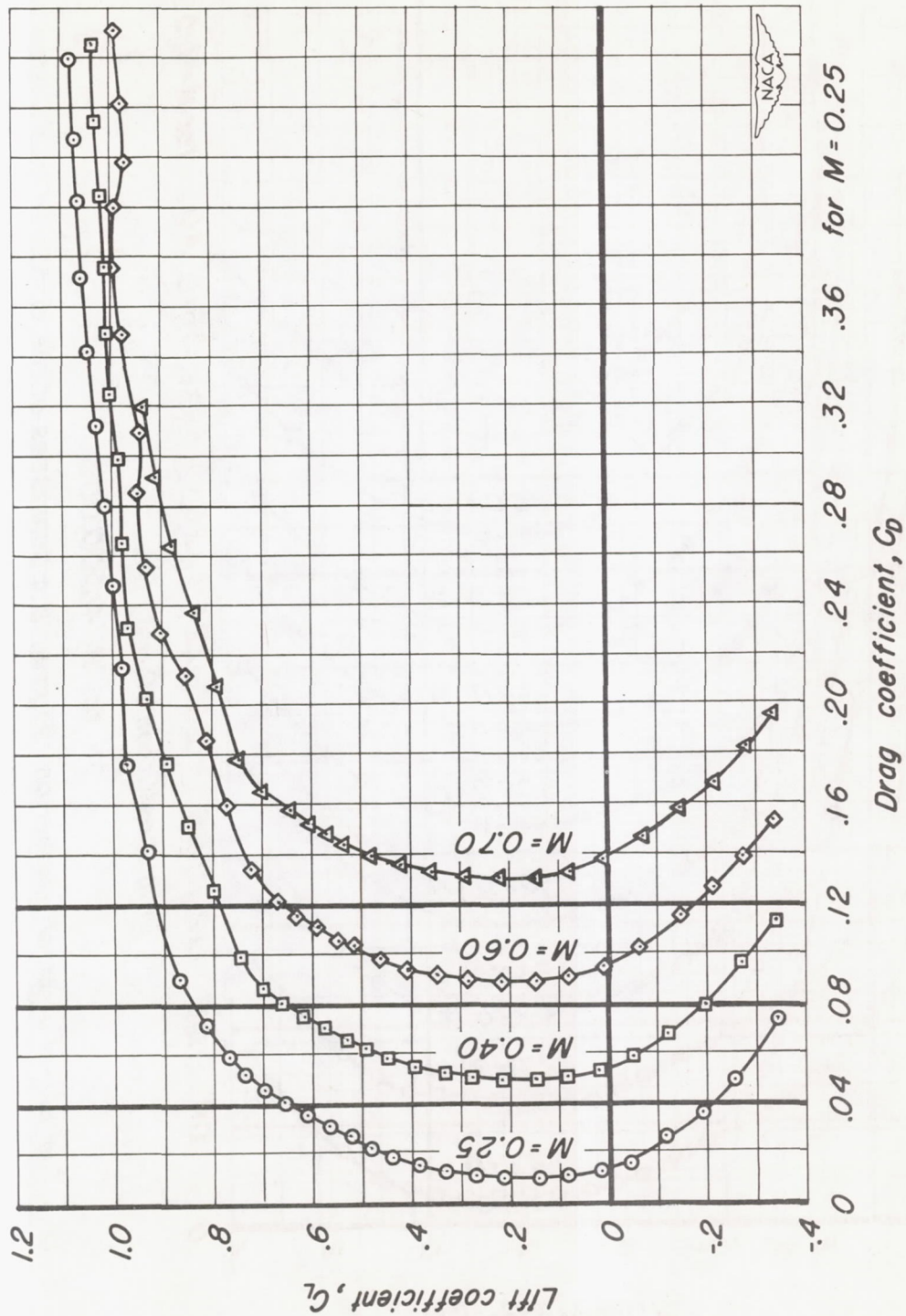


(c) $R, 4,000,000$
 Figure 11. - Concluded.



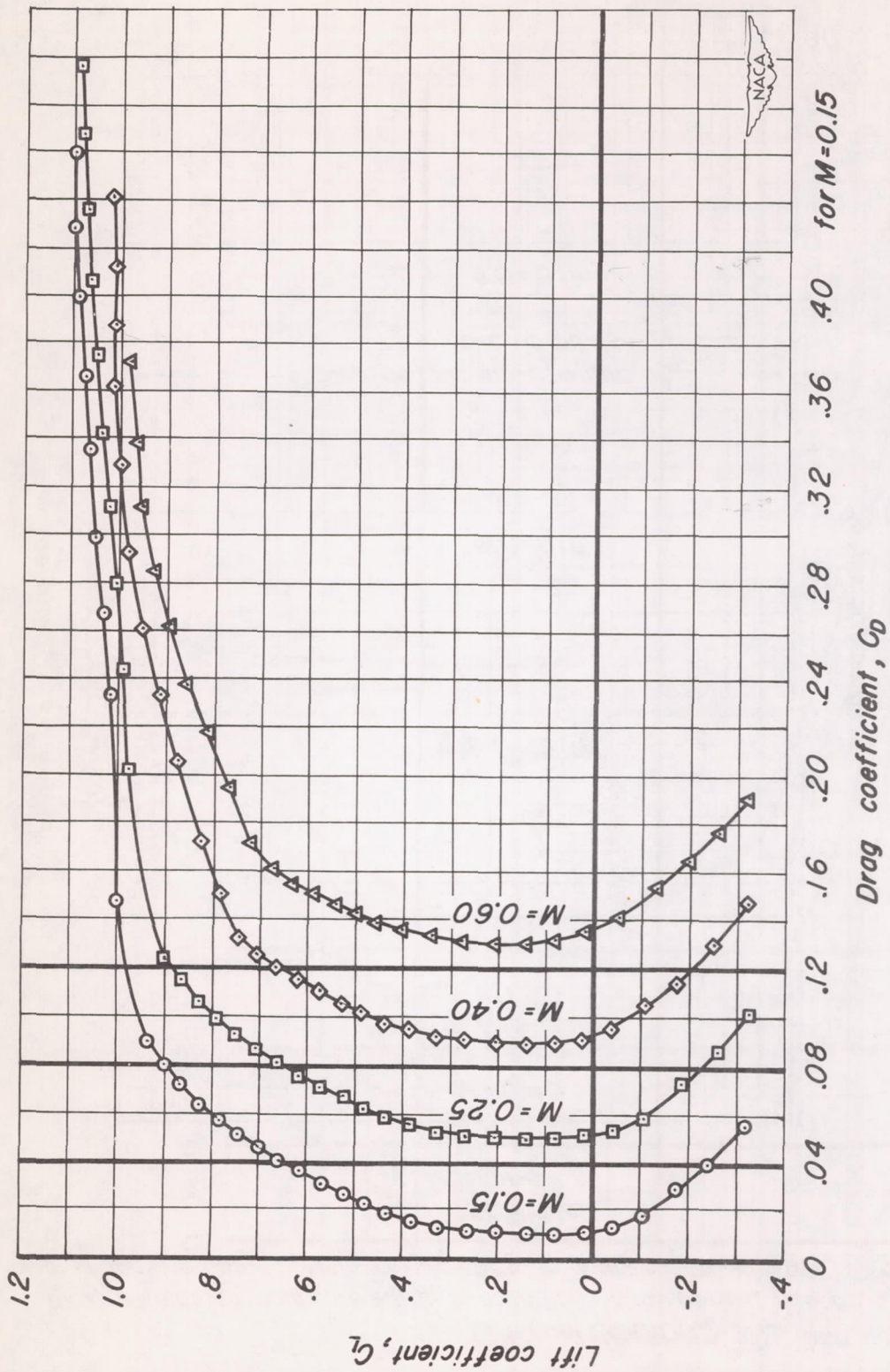
(a) $R, 2,000,000$

Figure 12.- The effect of Mach number on the drag characteristics of the cambered and twisted wing.



(b) R, 3,000,000

Figure 12.-Continued.



(c) R, 4,000,000
Figure 12. - Concluded.

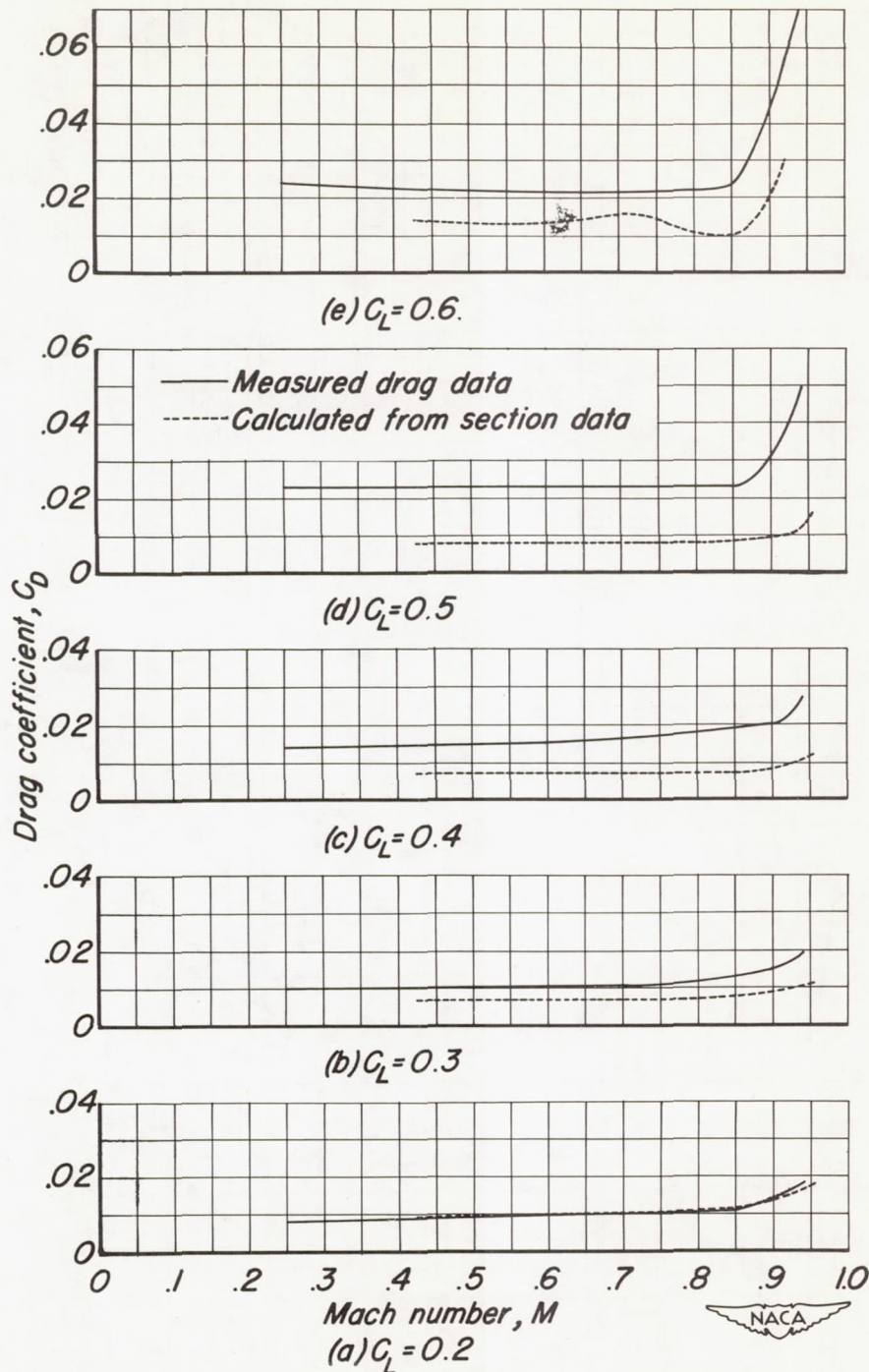
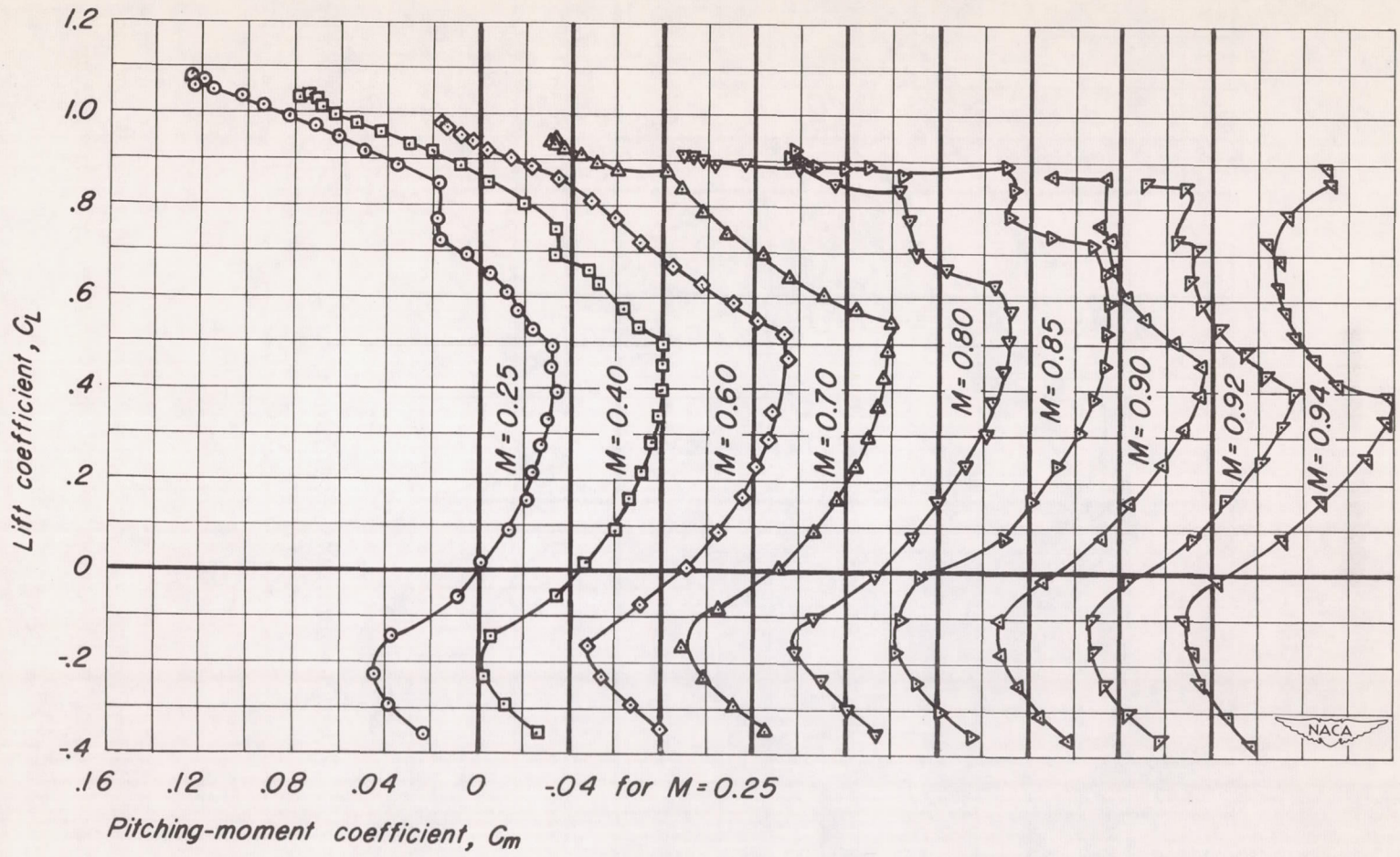


Figure 13.-The measured variation of drag coefficient with Mach number of the cambered and twisted wing compared with the variation calculated from section data. $R, 2,000,000$.



(a) $R, 2,000,000$

Figure 14.- The effect of Mach number on the pitching-moment characteristics of the cambered and twisted wing.

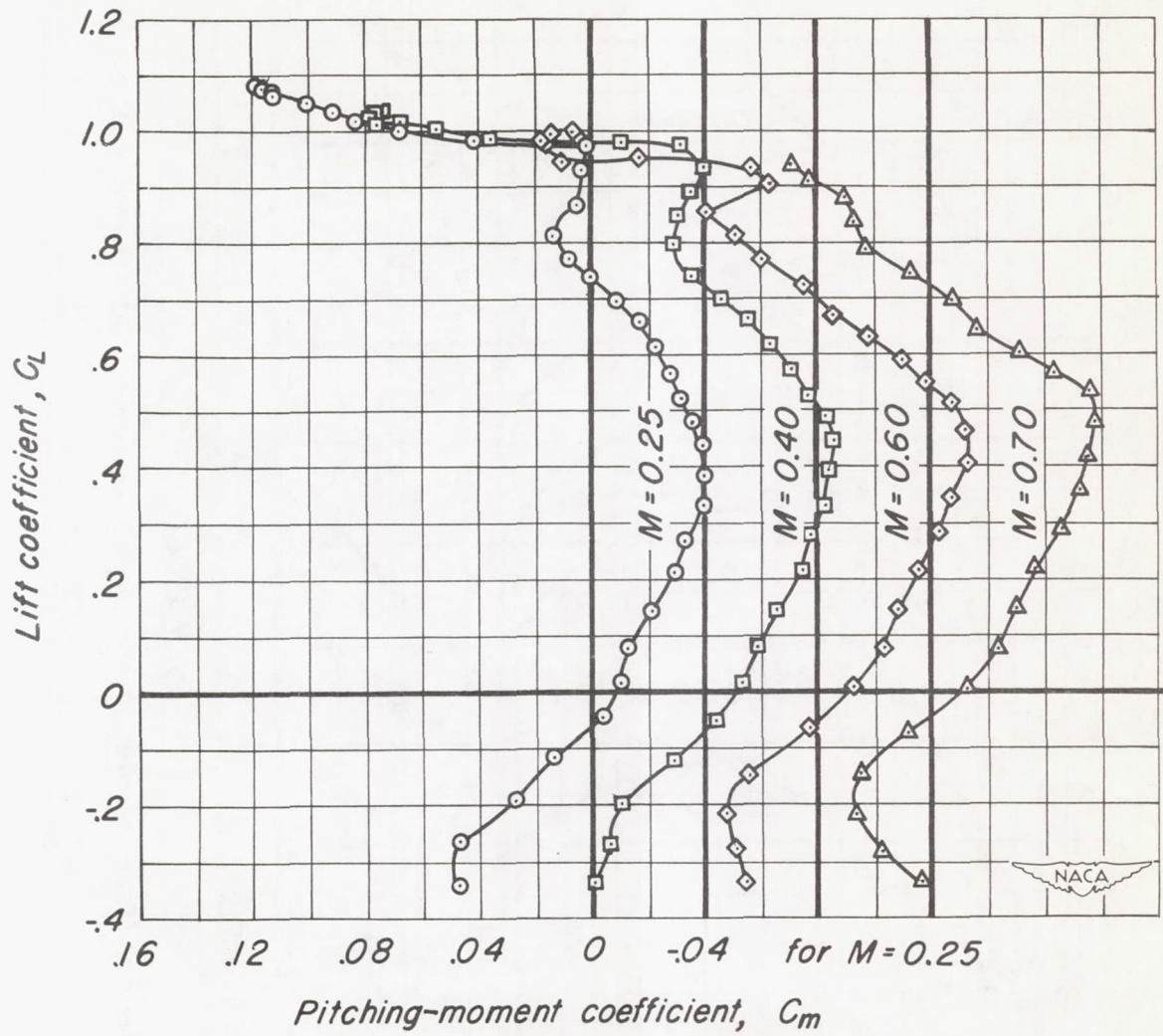
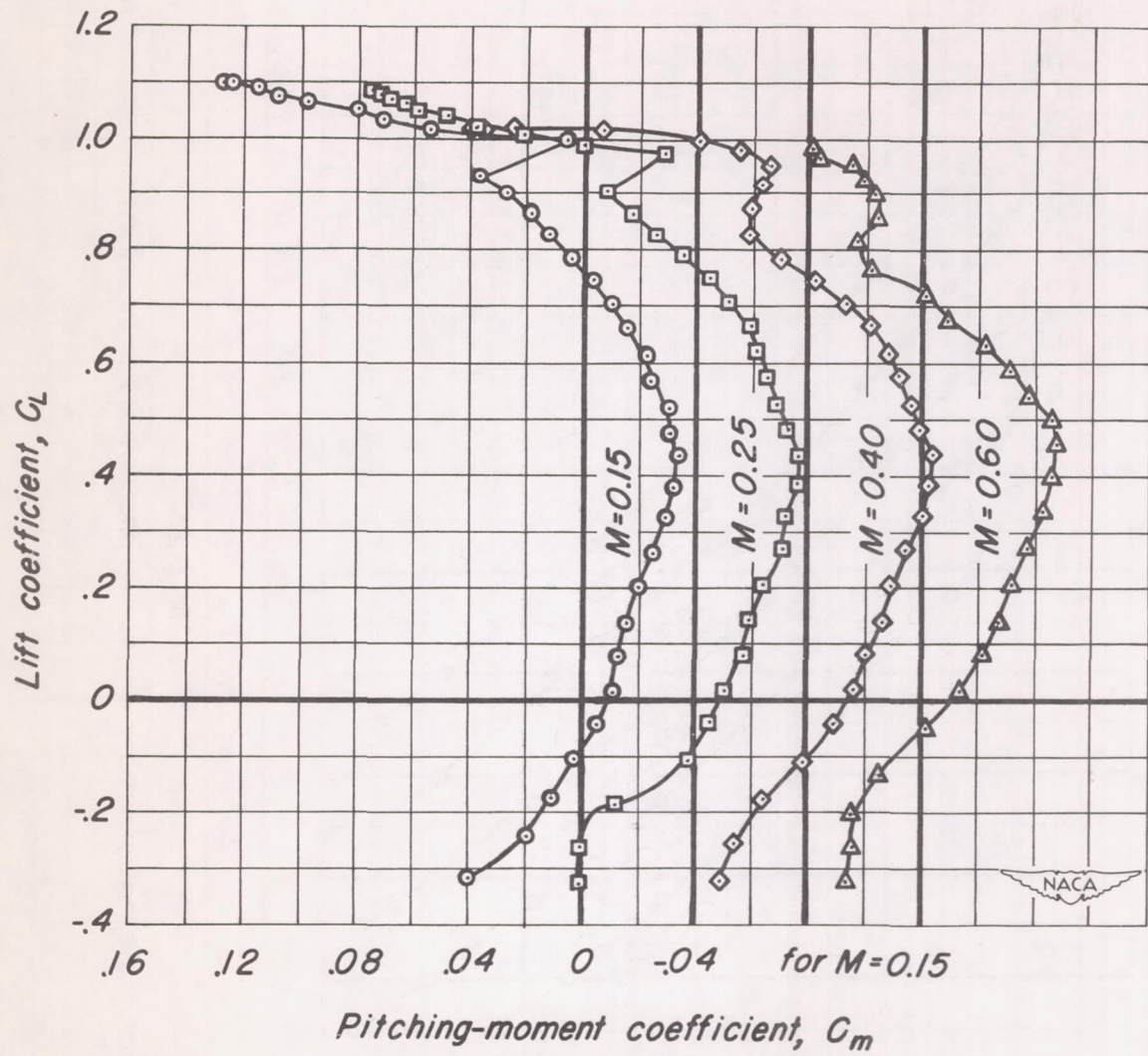


Figure 14.- Continued.



Pitching-moment coefficient, C_m

(c) $R, 4,000,000$

Figure 14.- Concluded.

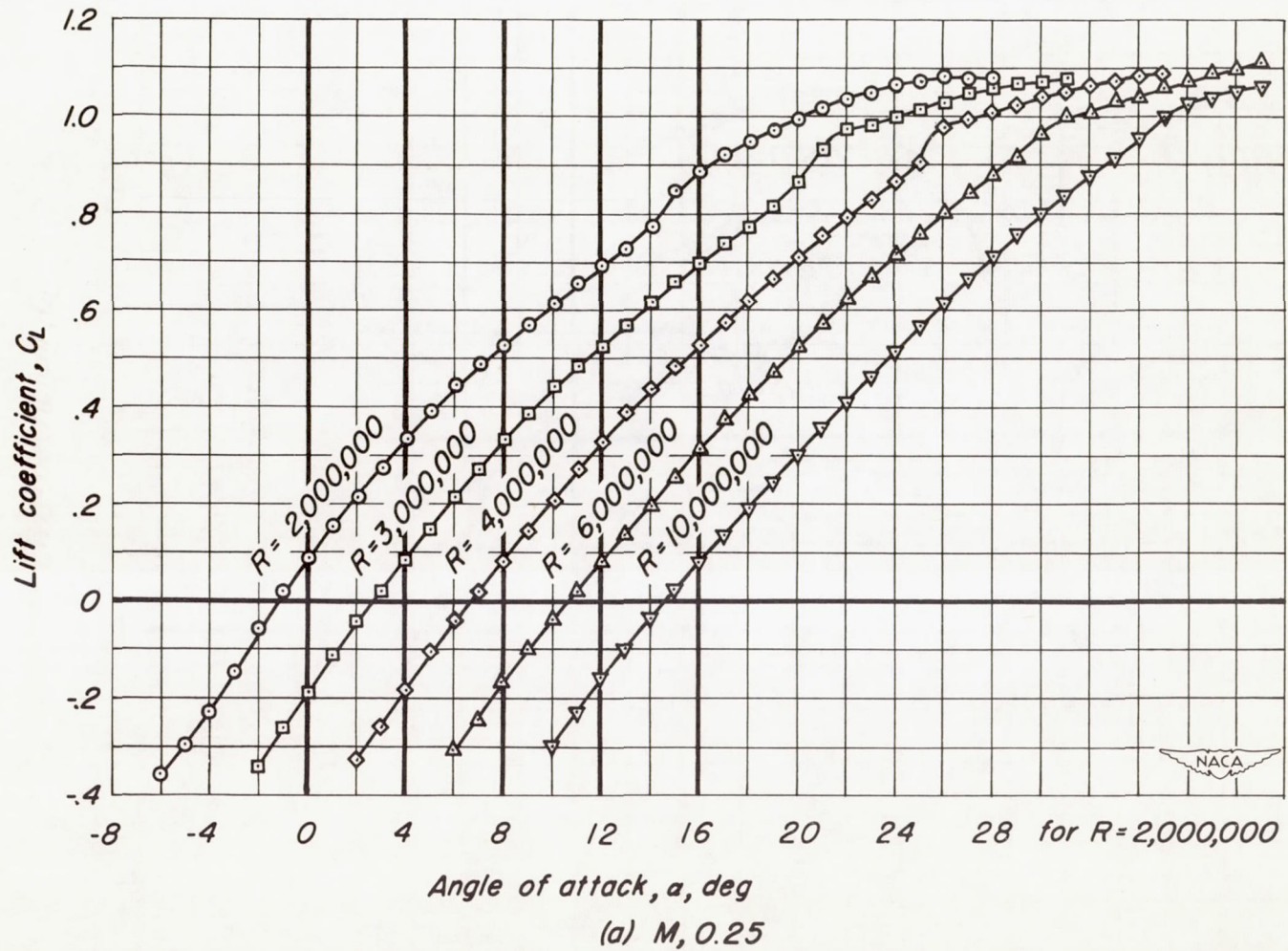
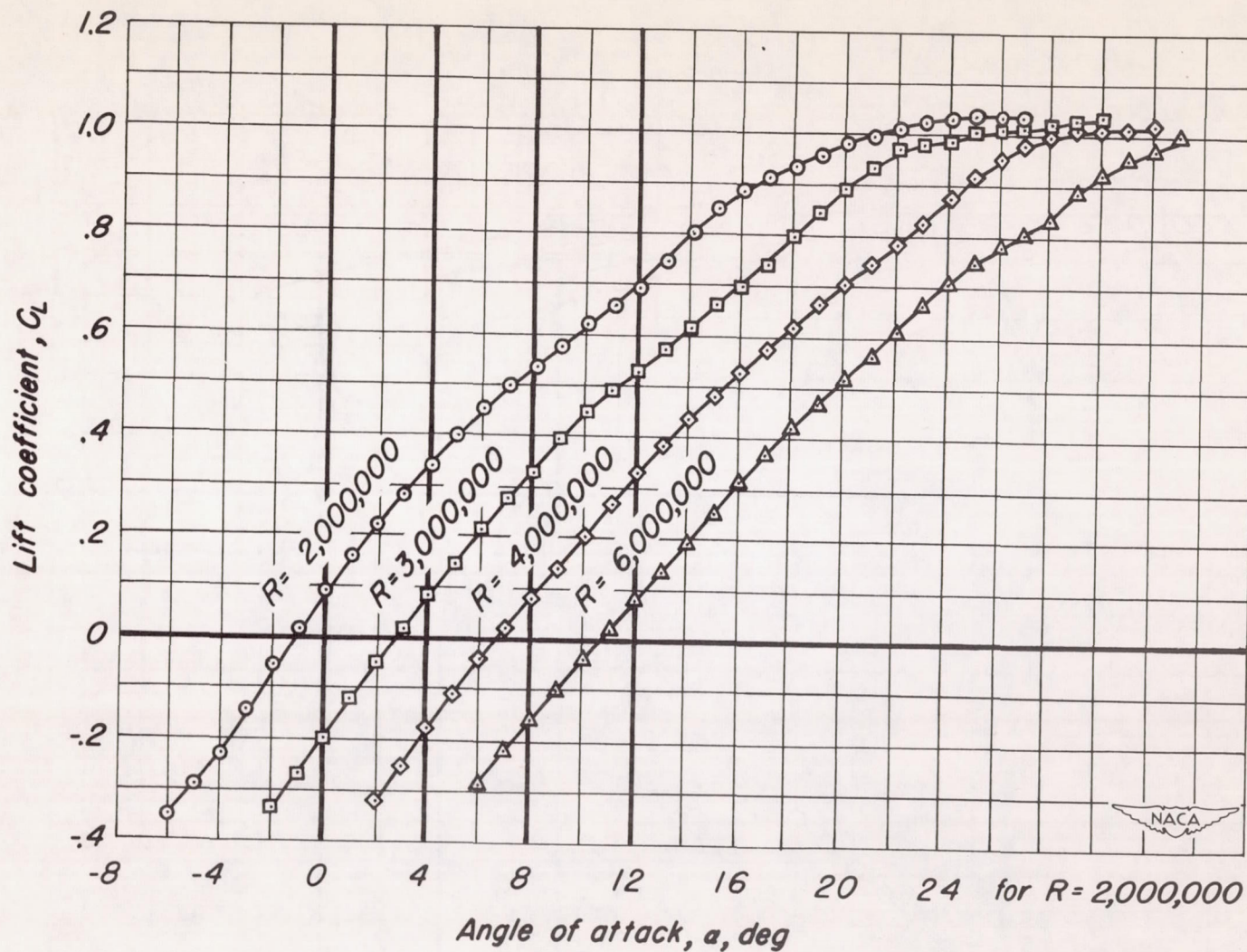
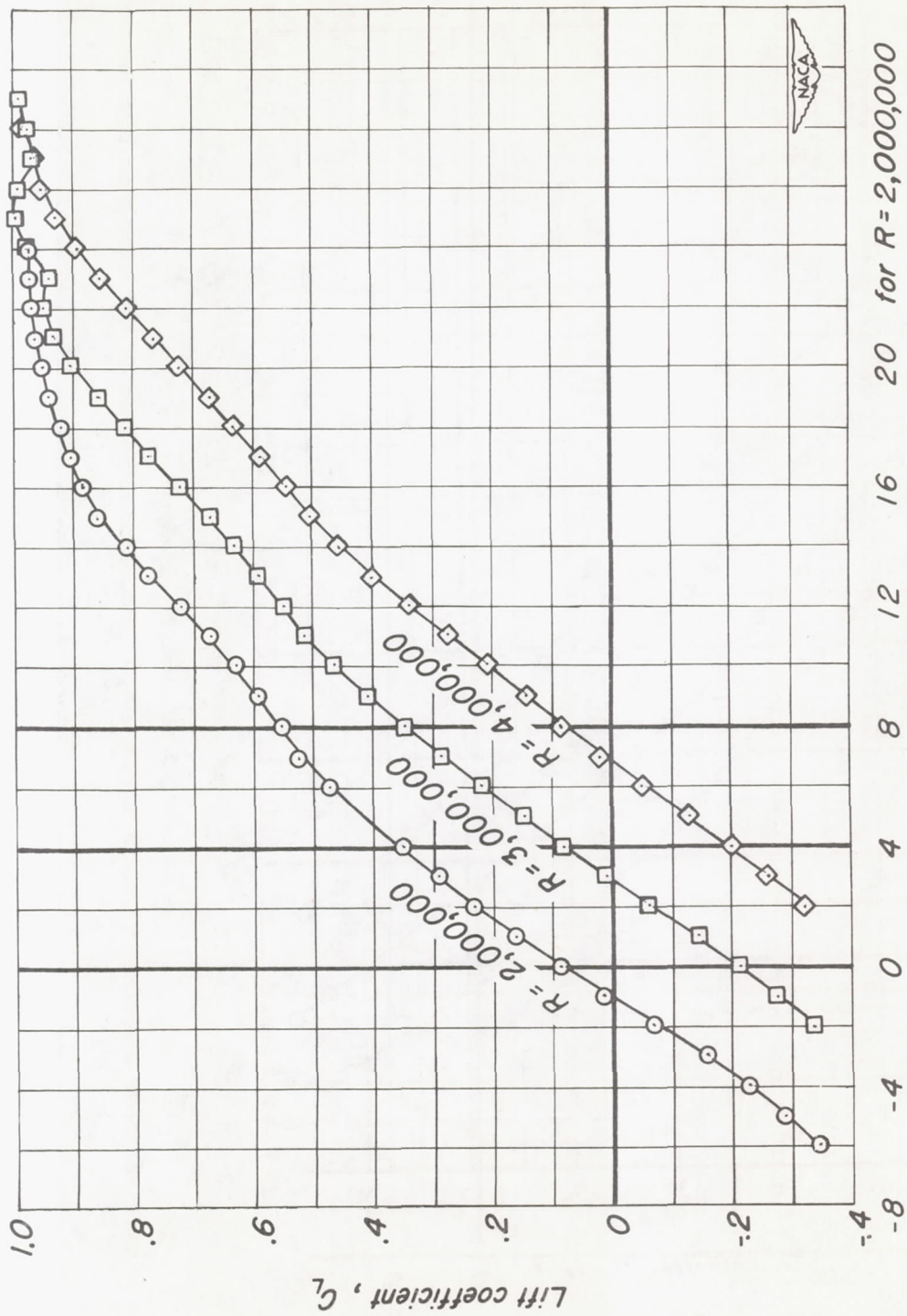


Figure 15.— The effect of Reynolds number on the lift characteristics of the cambered and twisted wing.

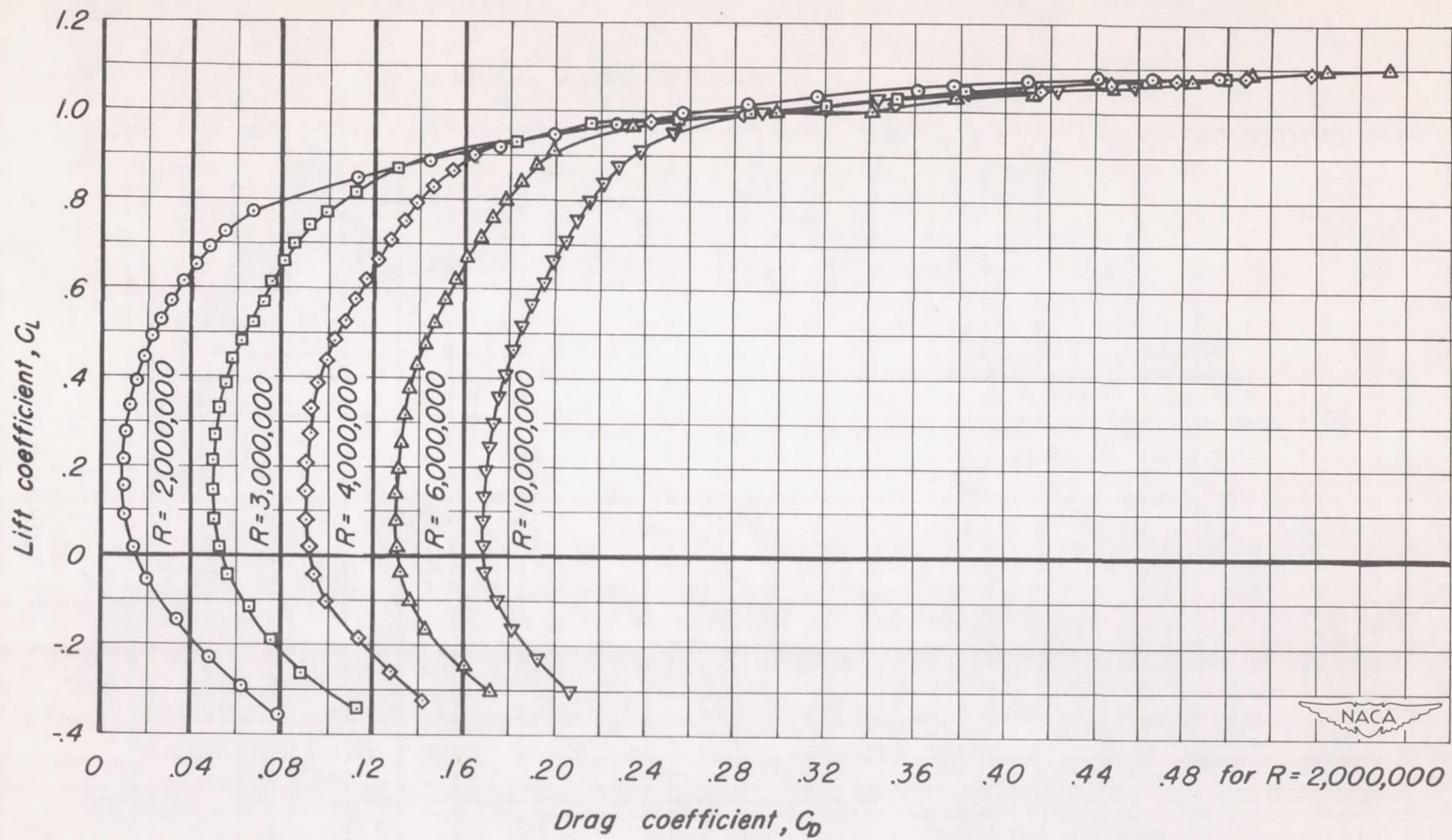


(b) $M, 0.40$

Figure 15.- Continued.

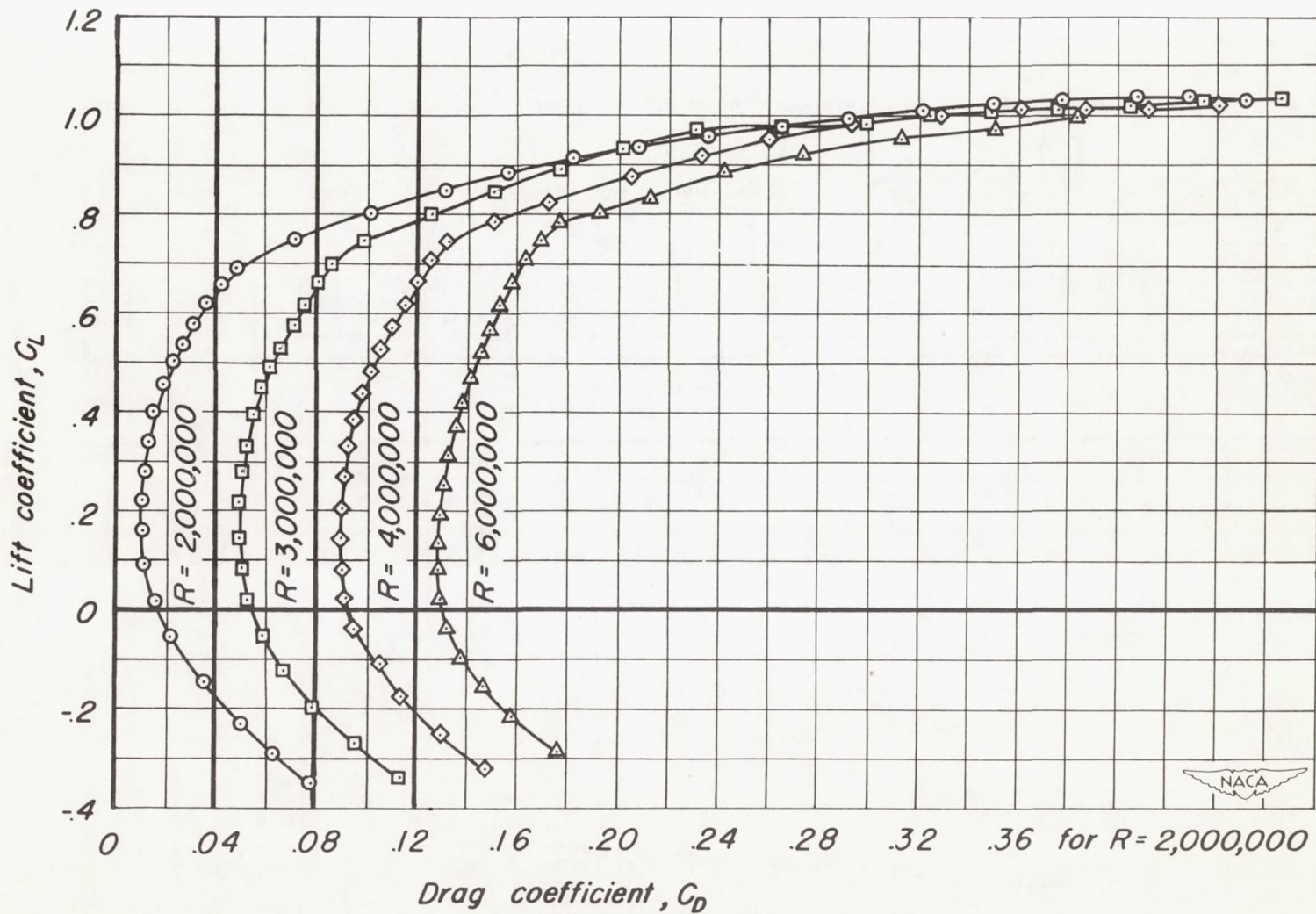


(c) $M, 0.60$
Figure 15.-Concluded.



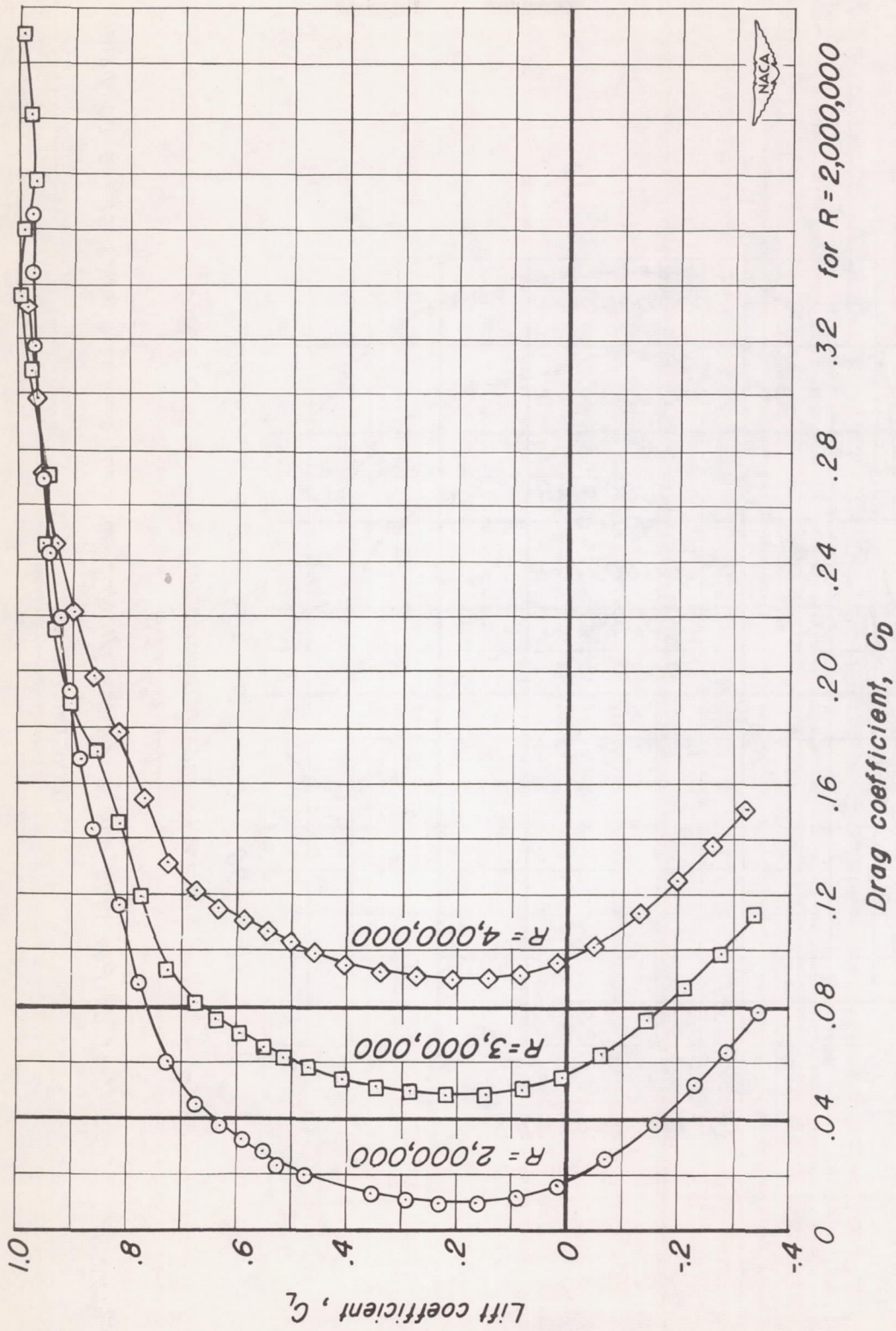
(a) $M, 0.25$

Figure 16.- The effect of Reynolds number on the drag characteristics of the cambered and twisted wing.



(b) $M, 0.40$

Figure 16. - Continued.



(c) $M, 0.60$
Figure 16.-Concluded.

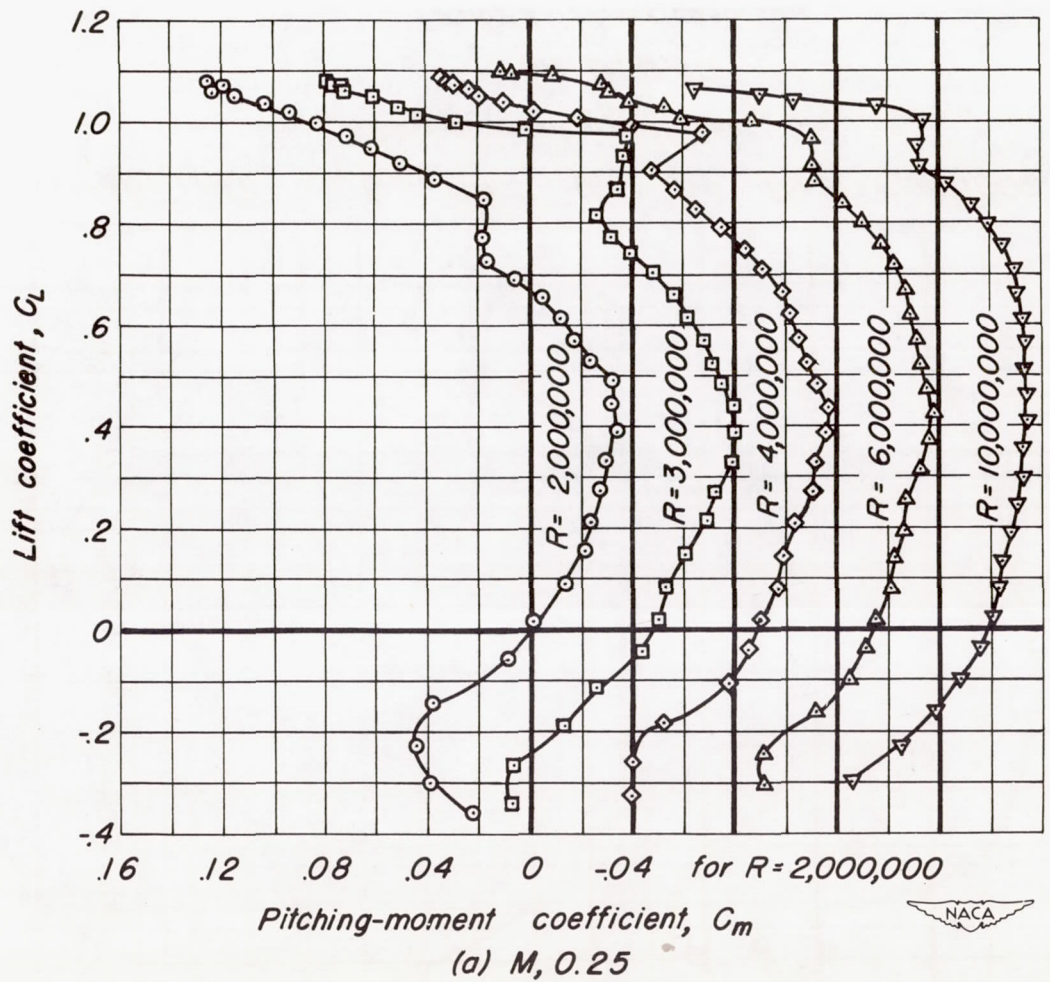
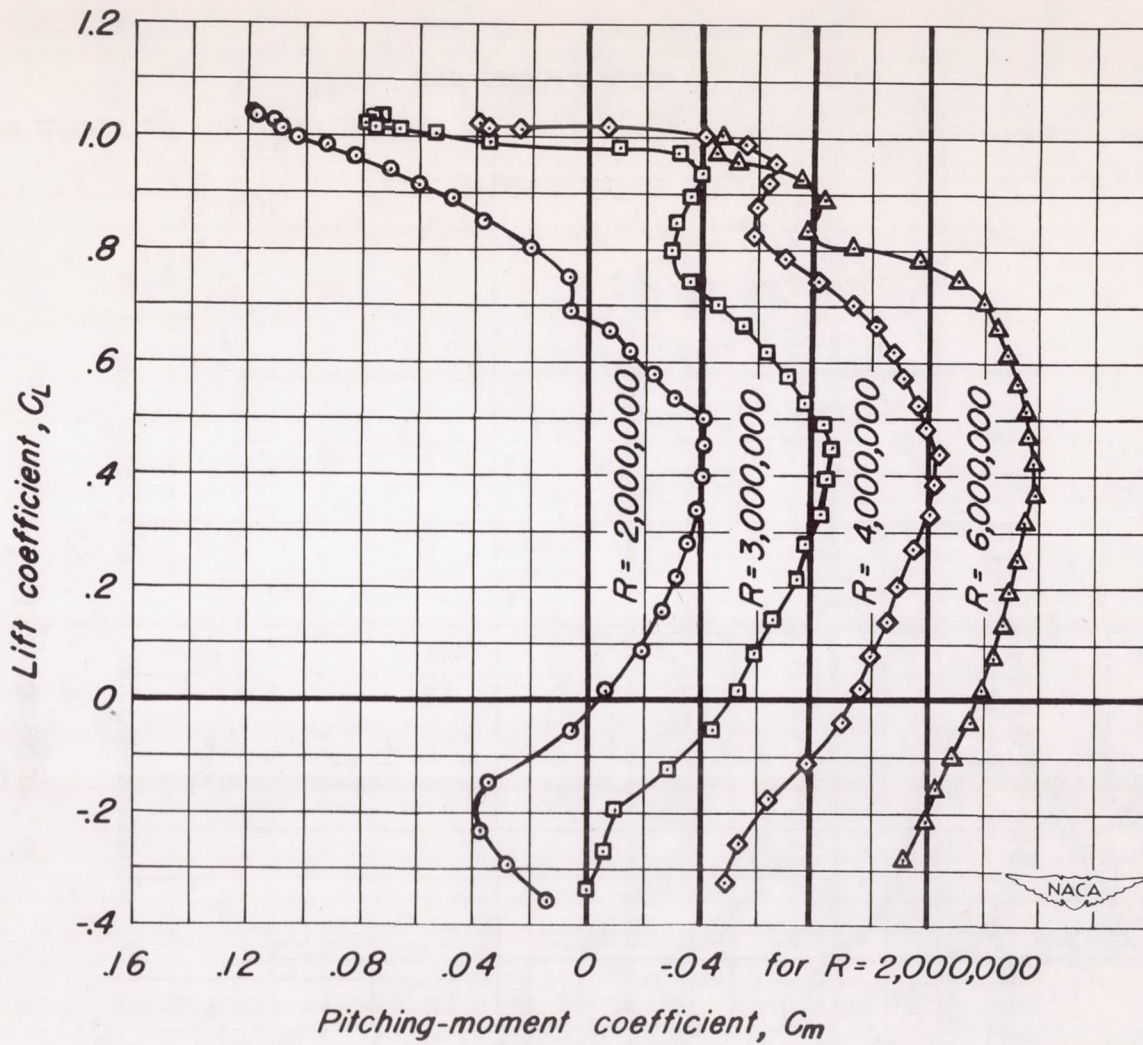
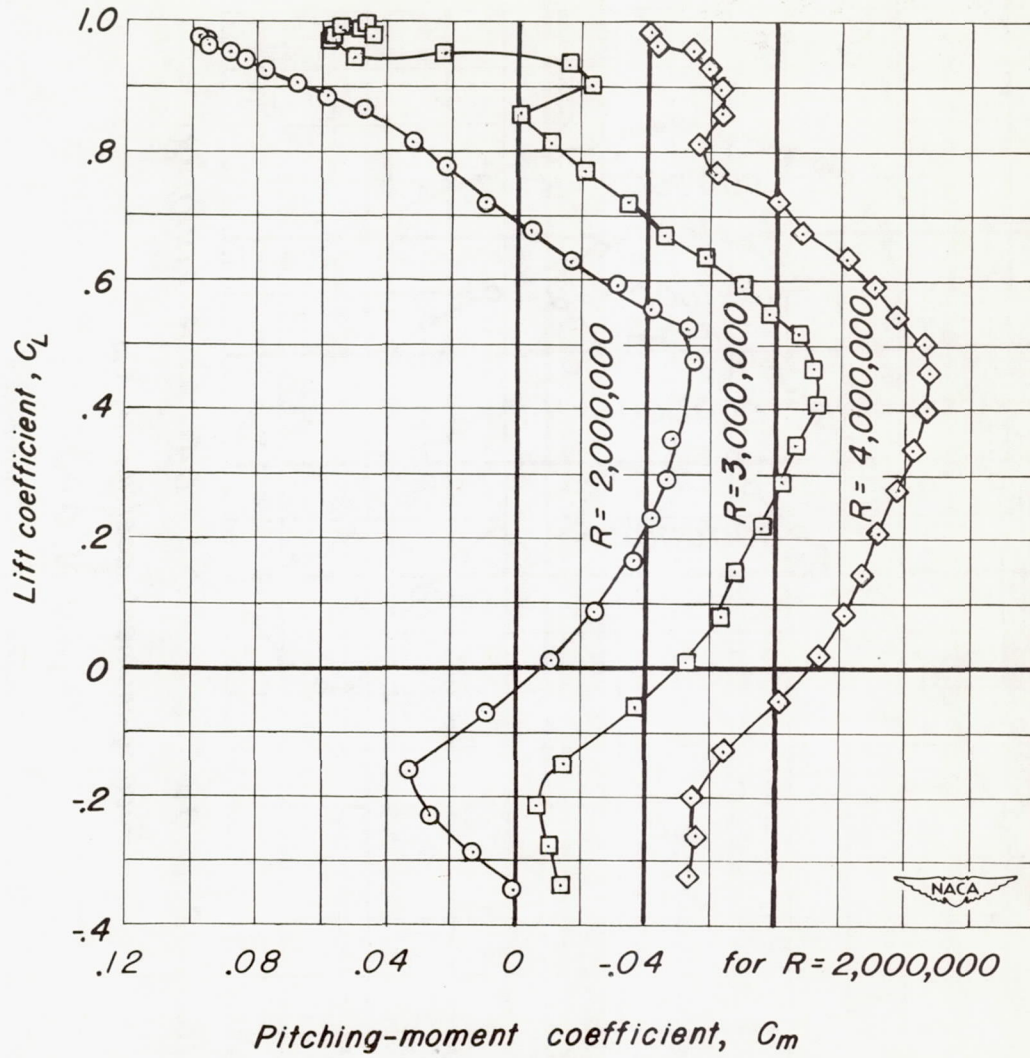


Figure 17.- The effect of Reynolds number on the pitching-moment characteristics of the cambered and twisted wing.

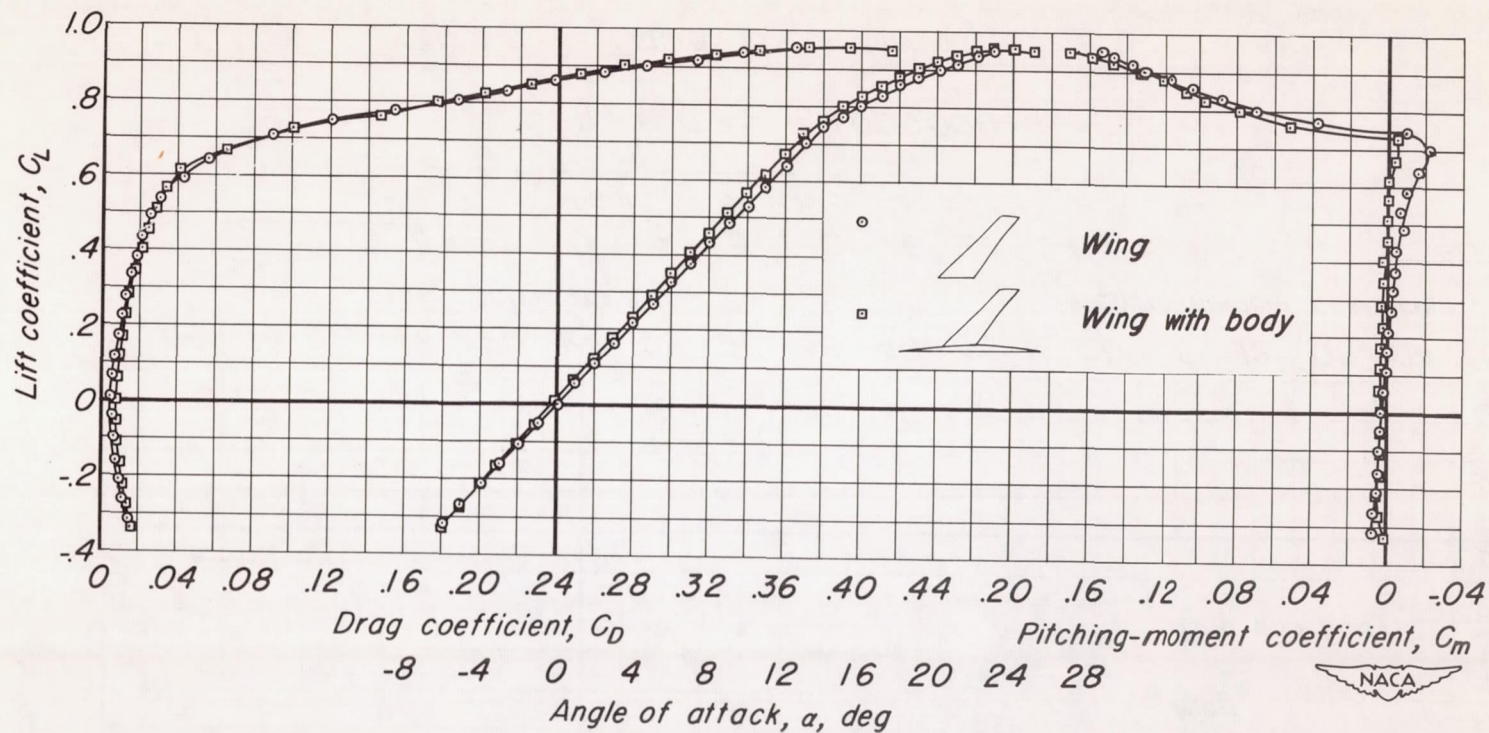


(b) $M, 0.40$

Figure 17.- Continued.

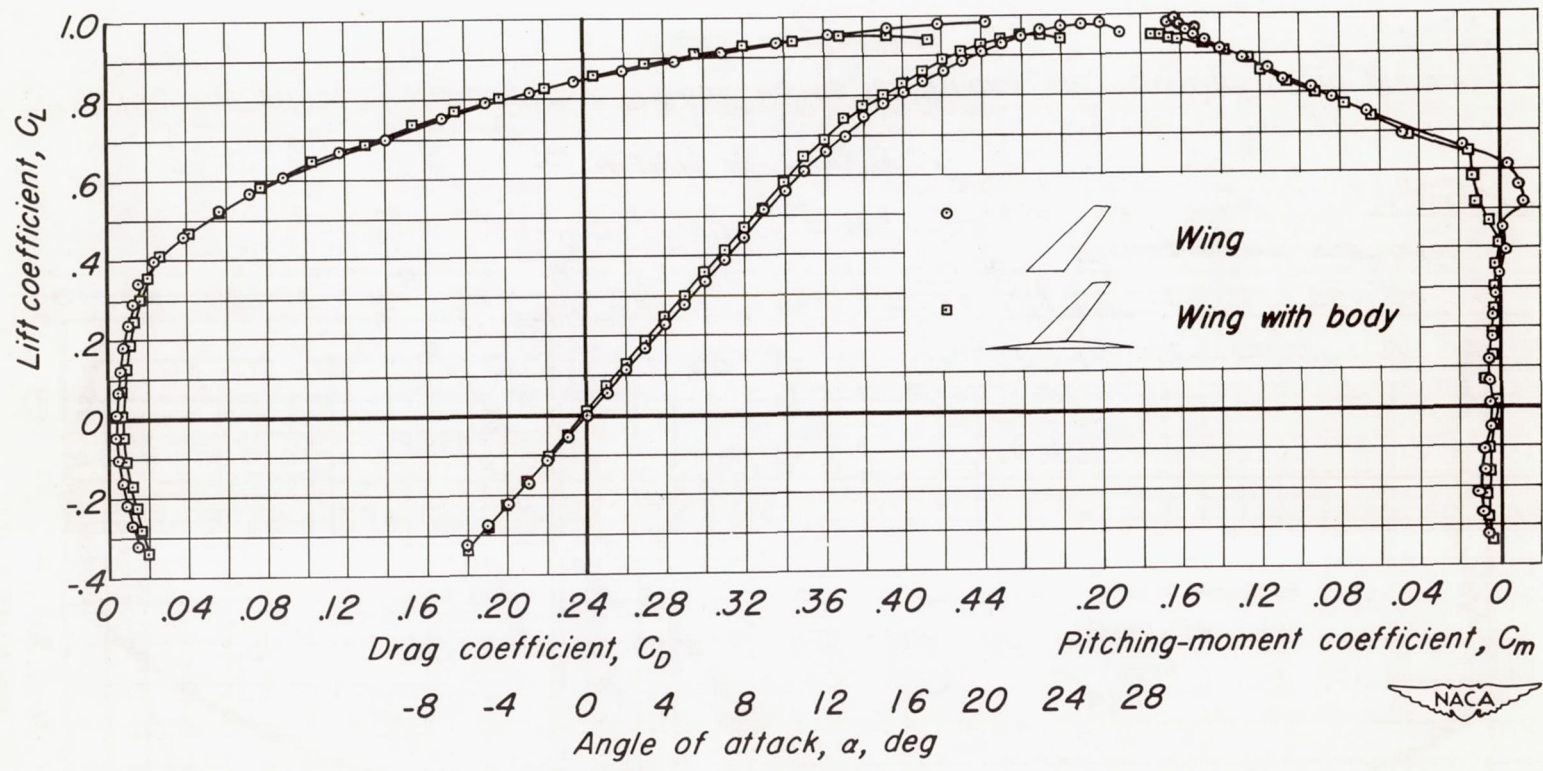


(c) $M, 0.60$
Figure 17.-Concluded.



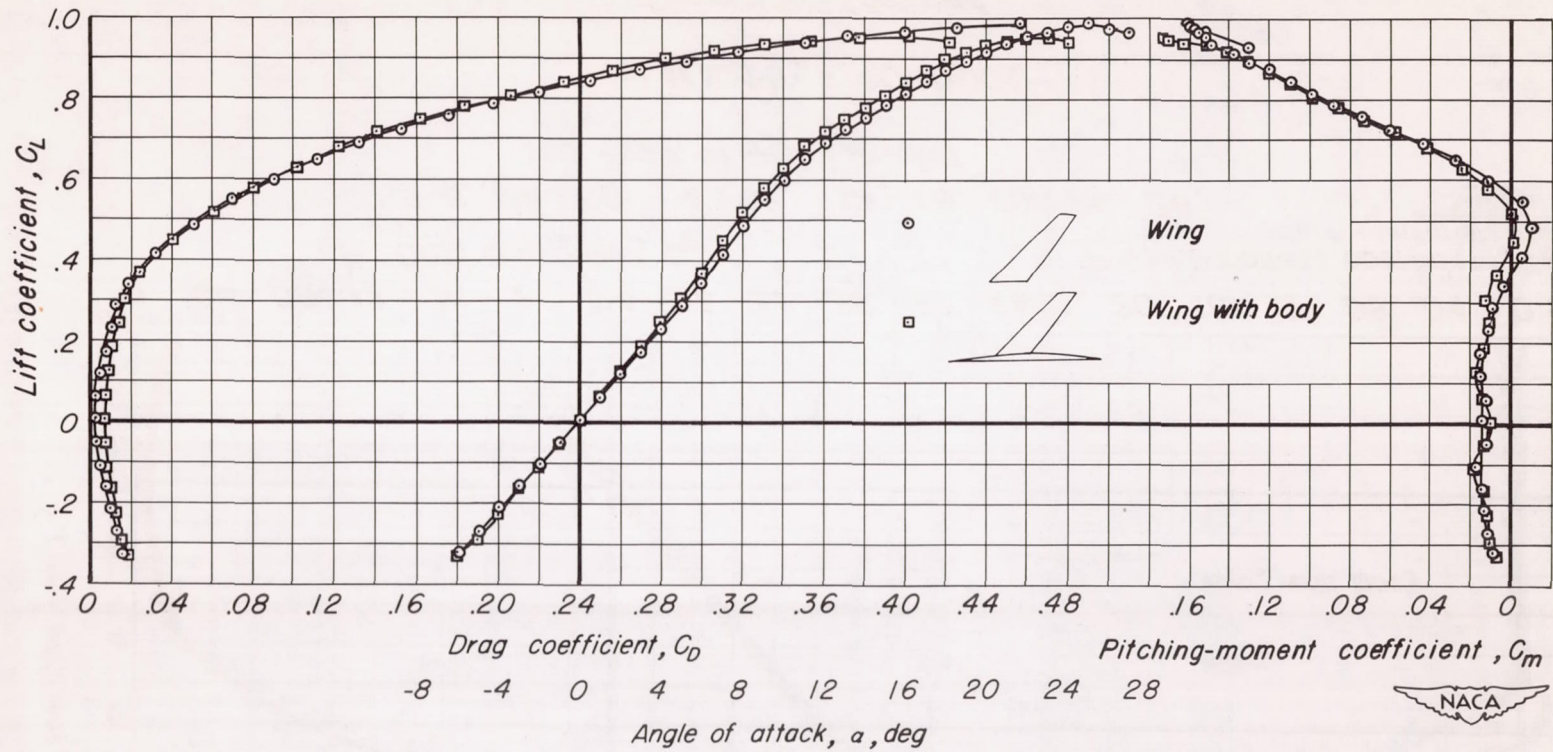
(a) $M, 0.25; R, 10,000,000$

Figure 18. - The effect of the addition of the body on the aerodynamic characteristics of the plane wing.



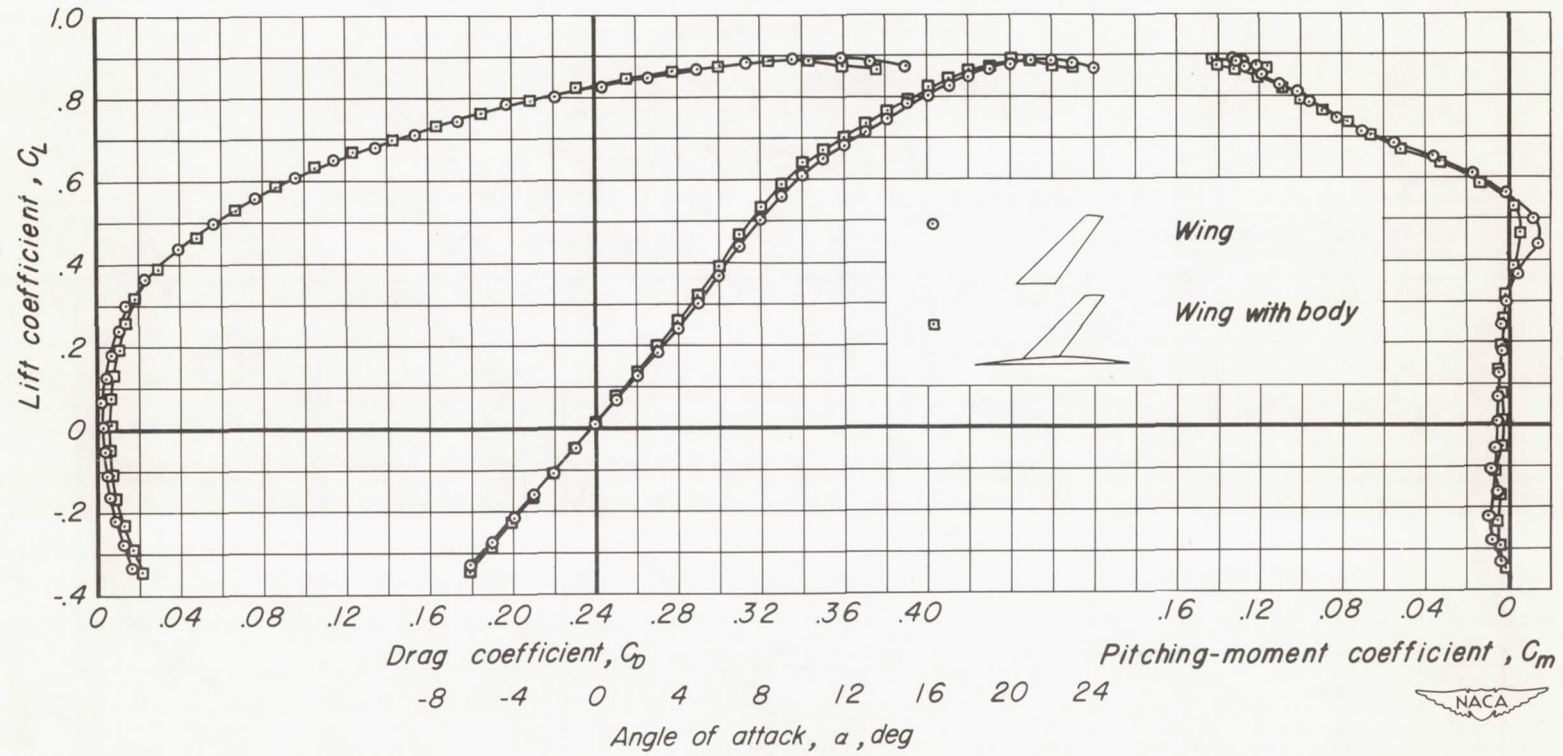
(b) $M, 0.25; R, 4,000,000$

Figure 18. - Continued.



(c) $M, 0.25 ; R, 2,000,000$

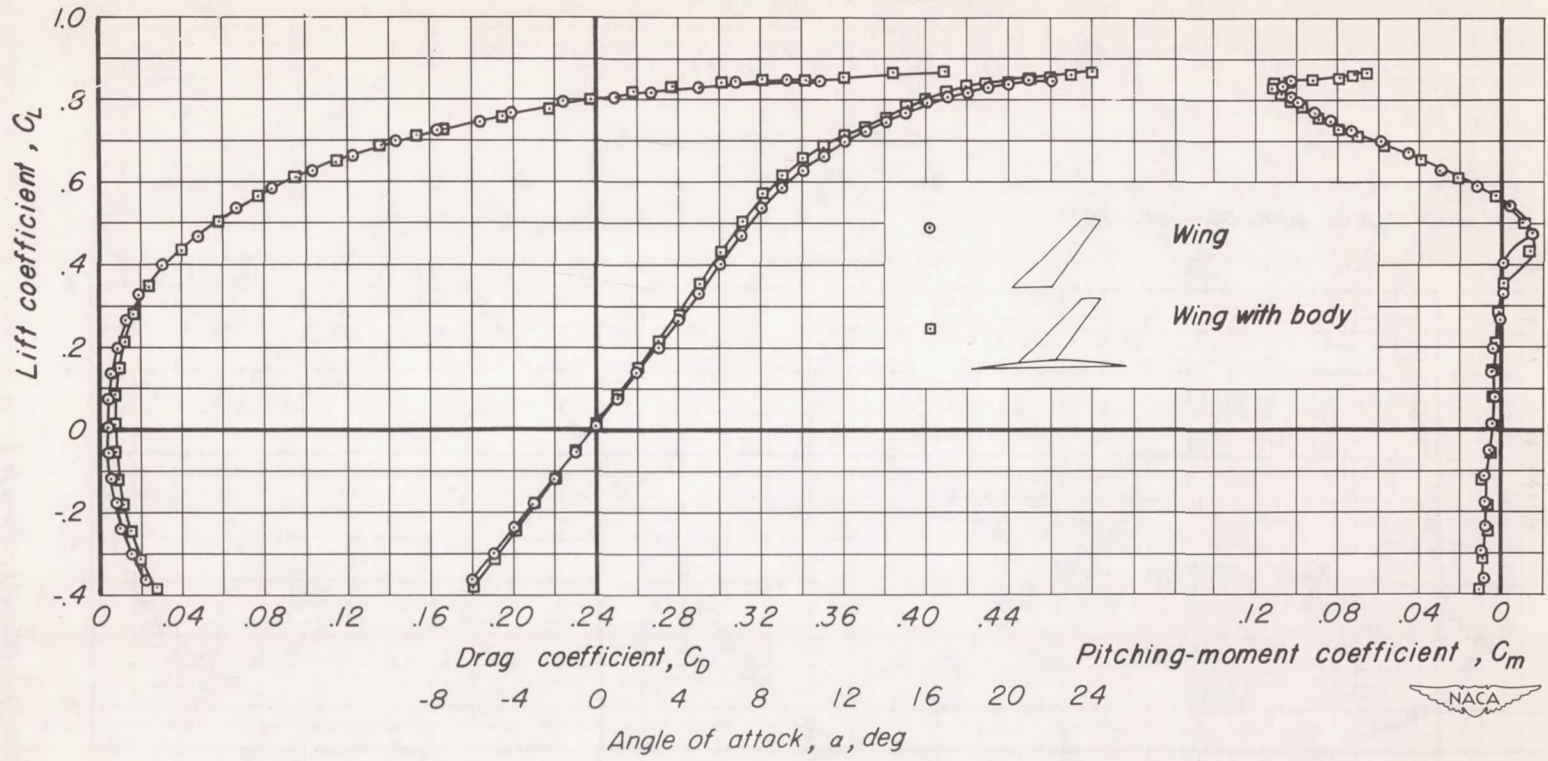
Figure 18. - Continued.



(d) $M, 0.60$; $R, 2,000,000$

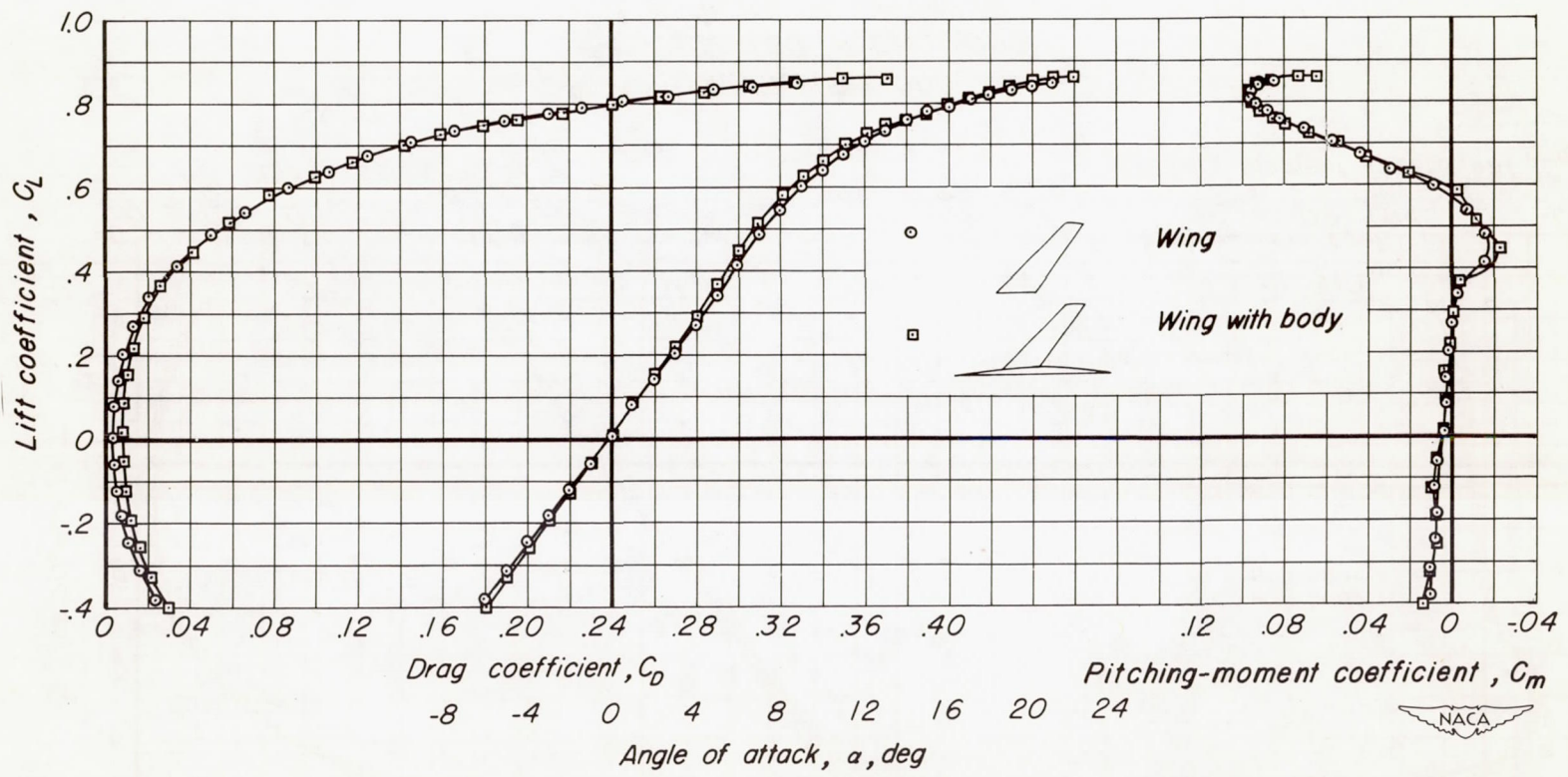
Figure 18. - Continued.





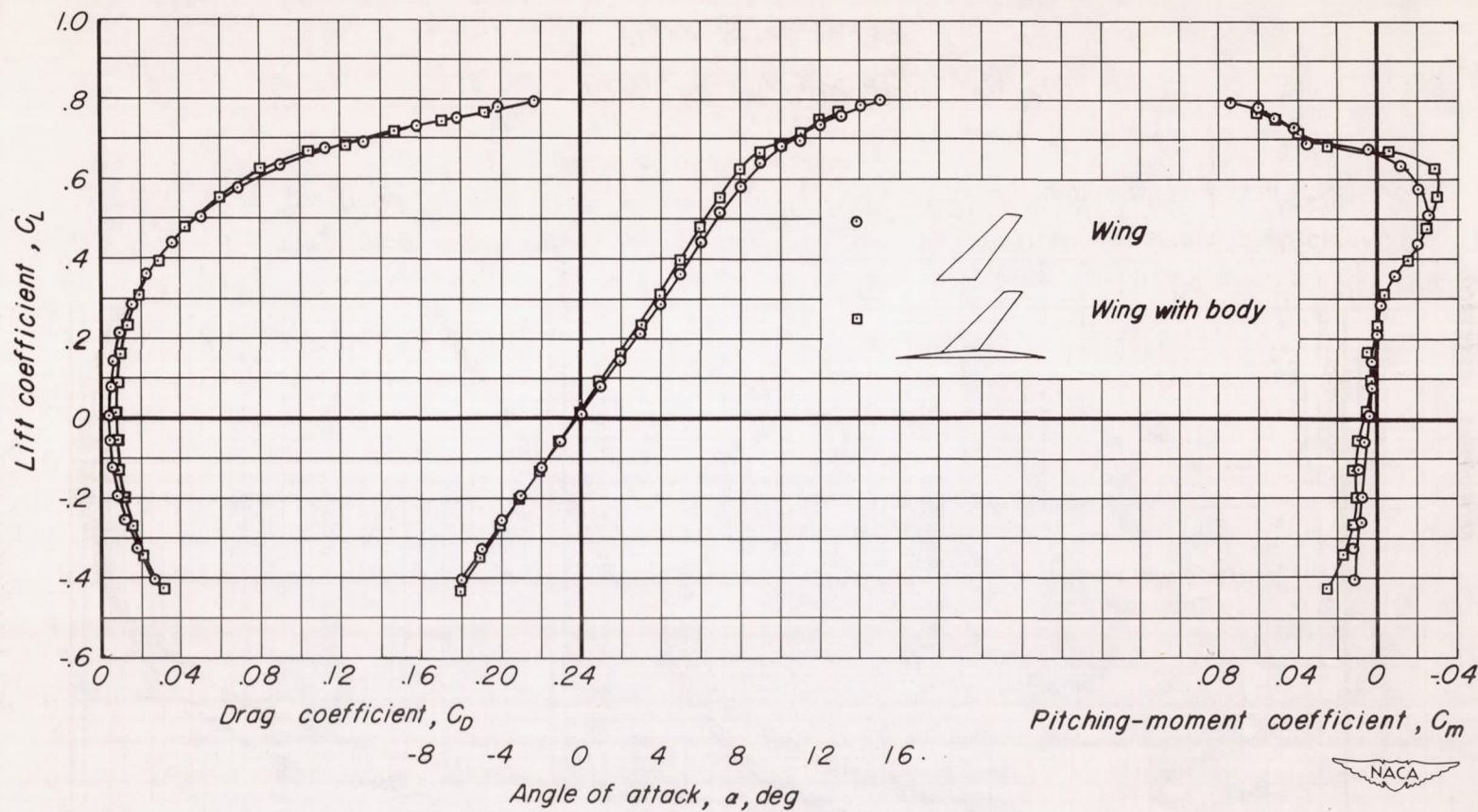
(e) $M, 0.80 ; R, 2,000,000$

Figure 18. - Continued.



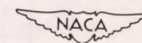
(f) $M, 0.85 ; R, 2,000,000$

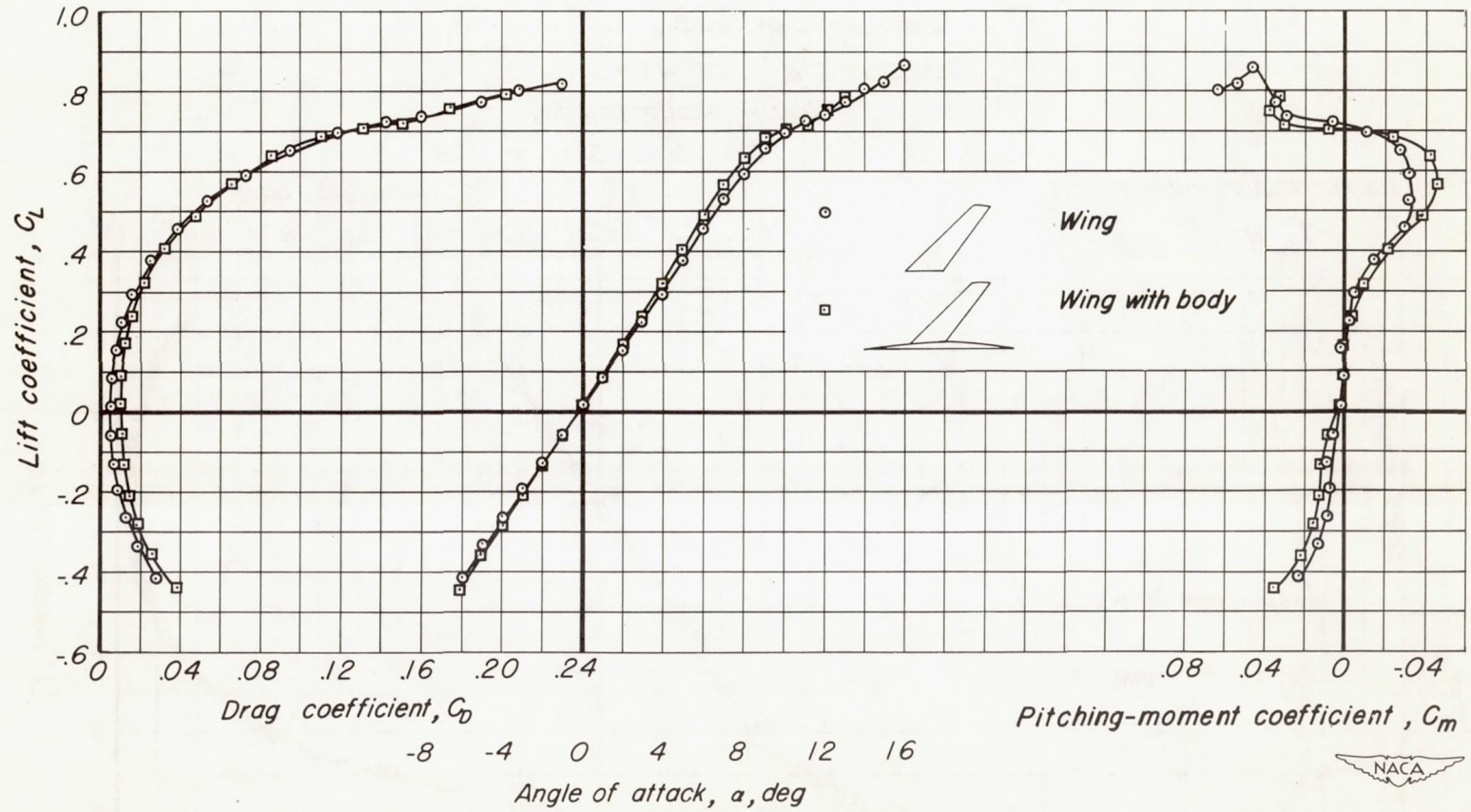
Figure 18. - Continued.



(g) $M, 0.90 ; R, 2,000,000$

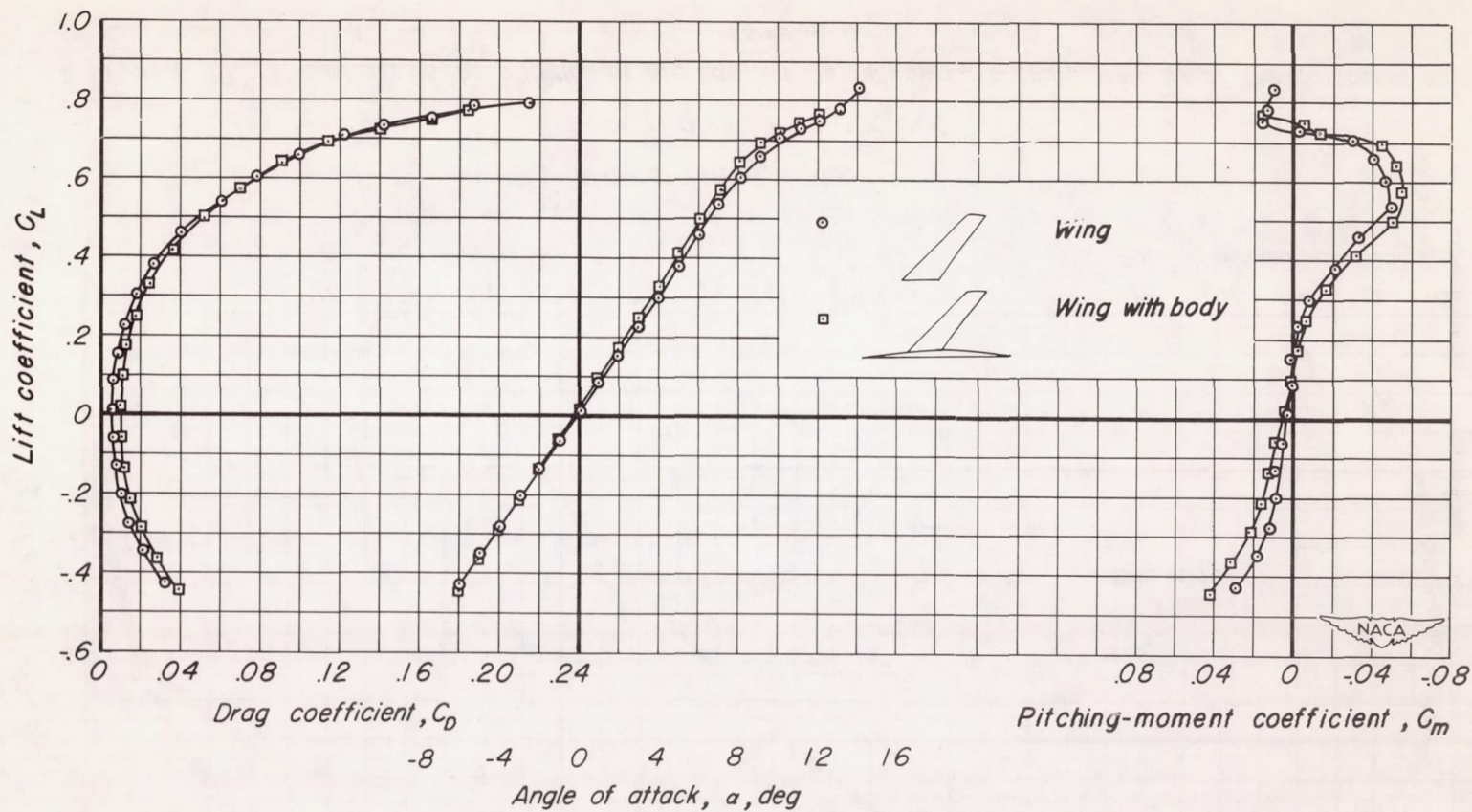
Figure 18. - Continued.





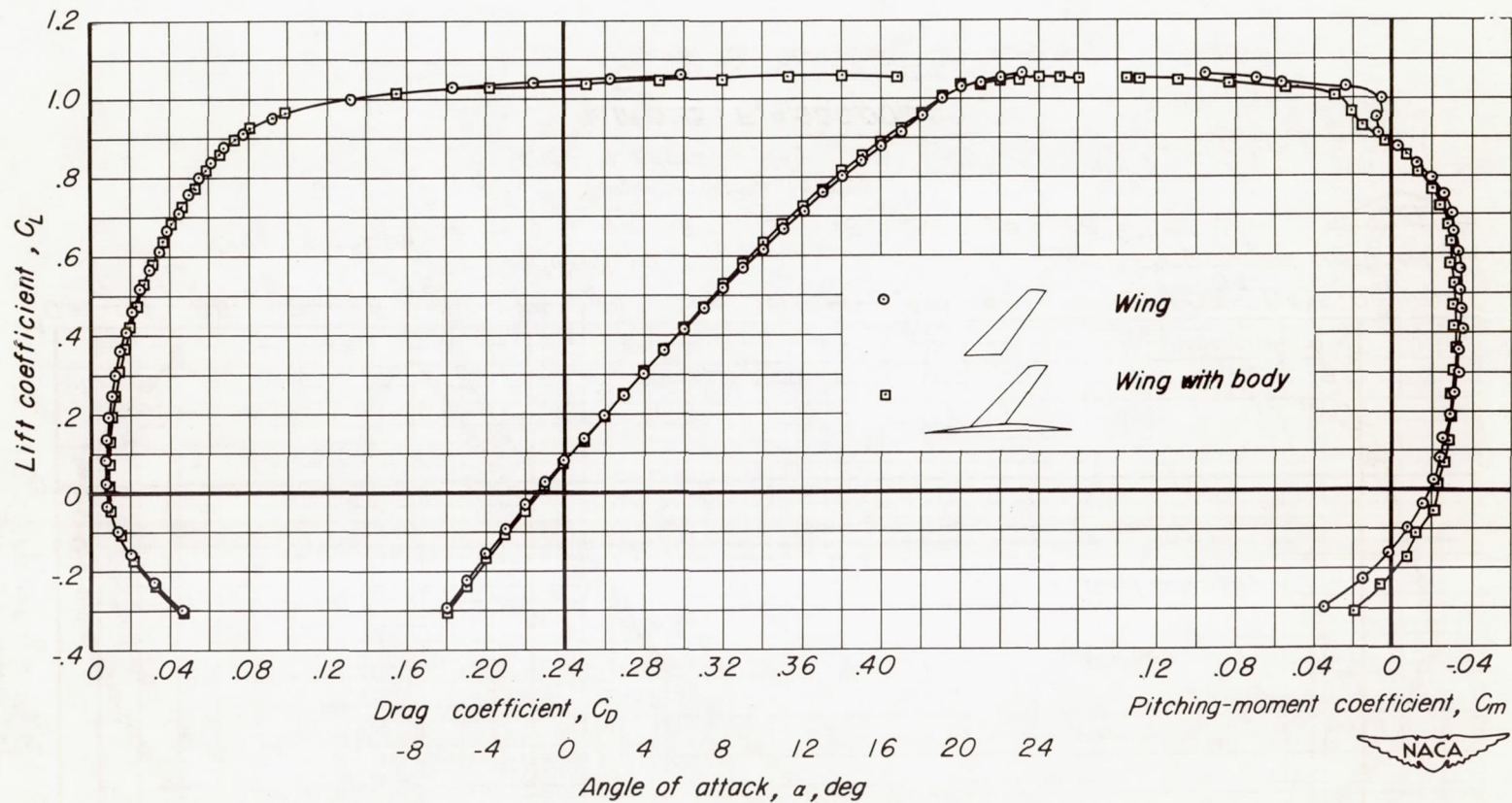
(h) $M, 0.92$; $R, 2,000,000$

Figure 18. - Continued.



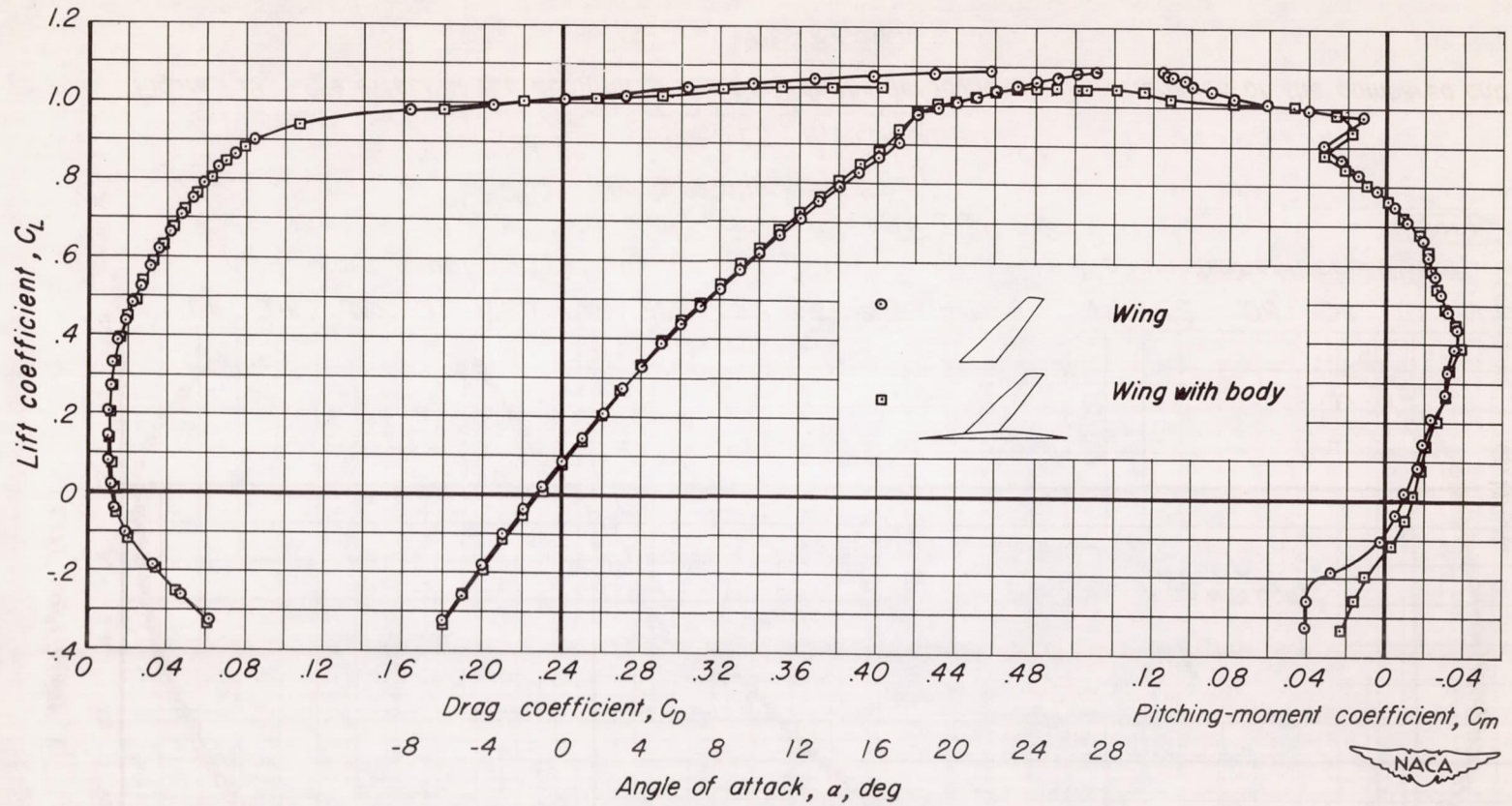
(i) $M, 0.94$; $R, 2,000,000$

Figure 18. - Concluded.



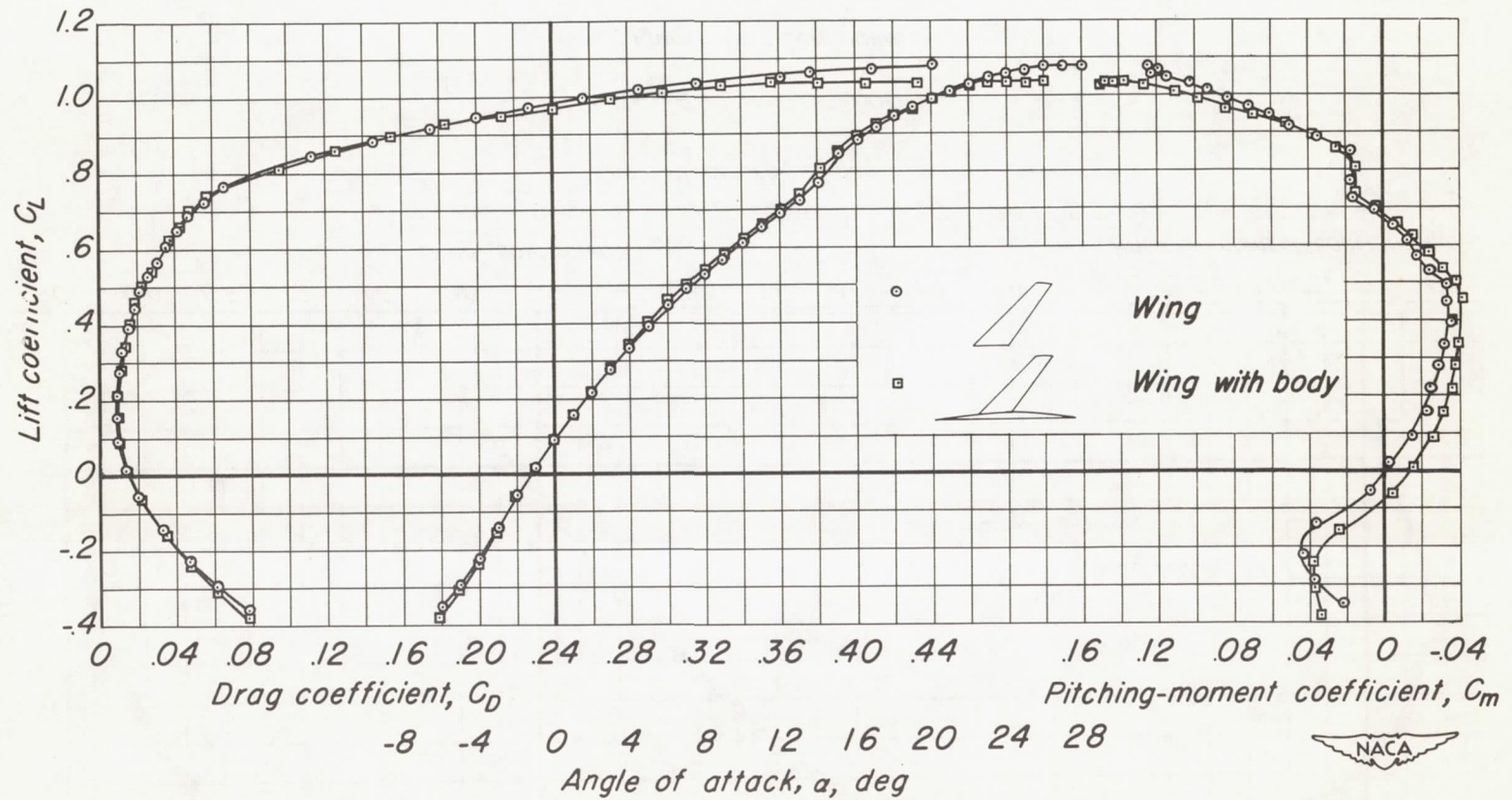
(a) $M, 0.25$; $R, 10,000,000$

Figure 19. - The effect of the addition of the body on the aerodynamic characteristics of the cambered and twisted wing.



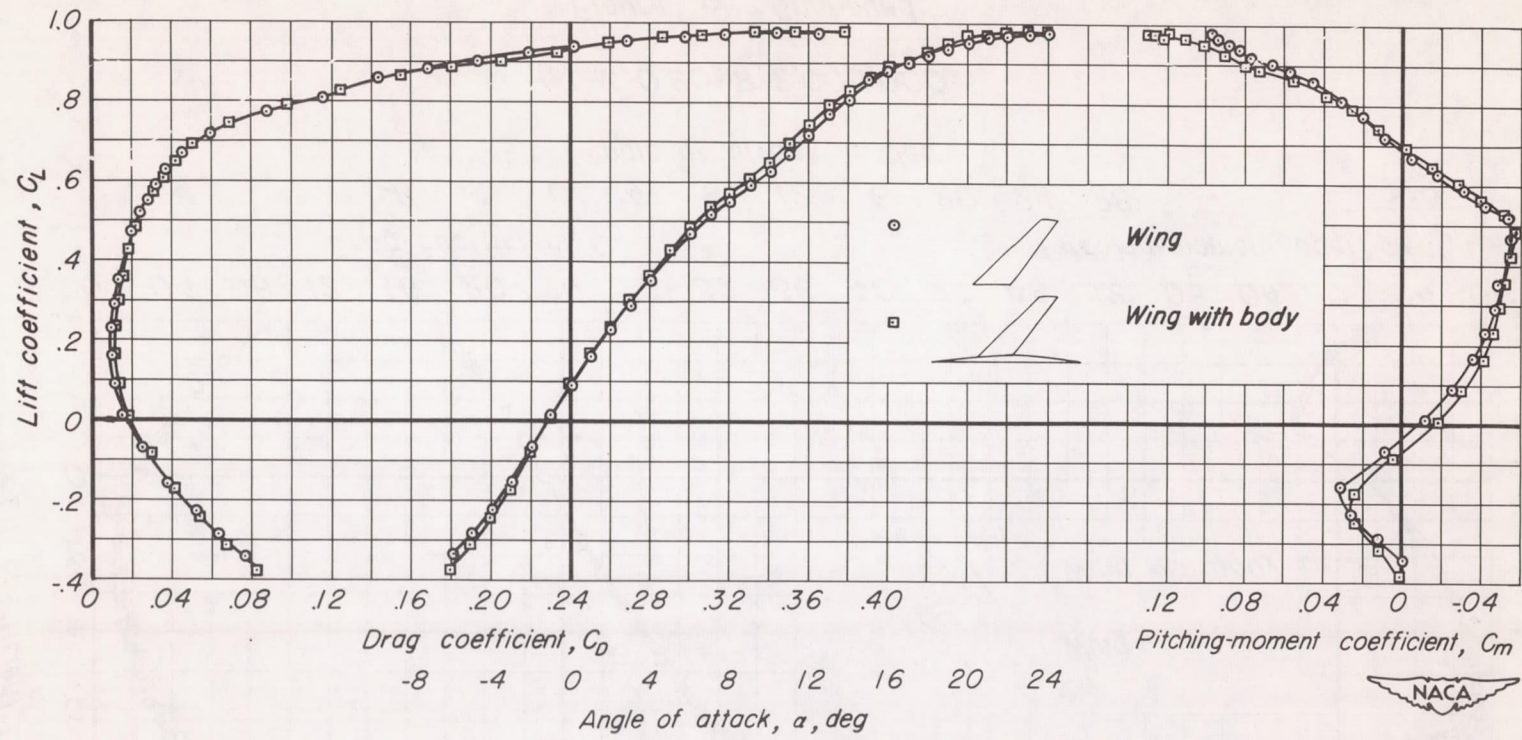
(b) $M, 0.25 ; R, 4,000,000$

Figure 19. -Continued.



(c) $M, 0.25; R, 2,000,000$

Figure 19.-Continued.



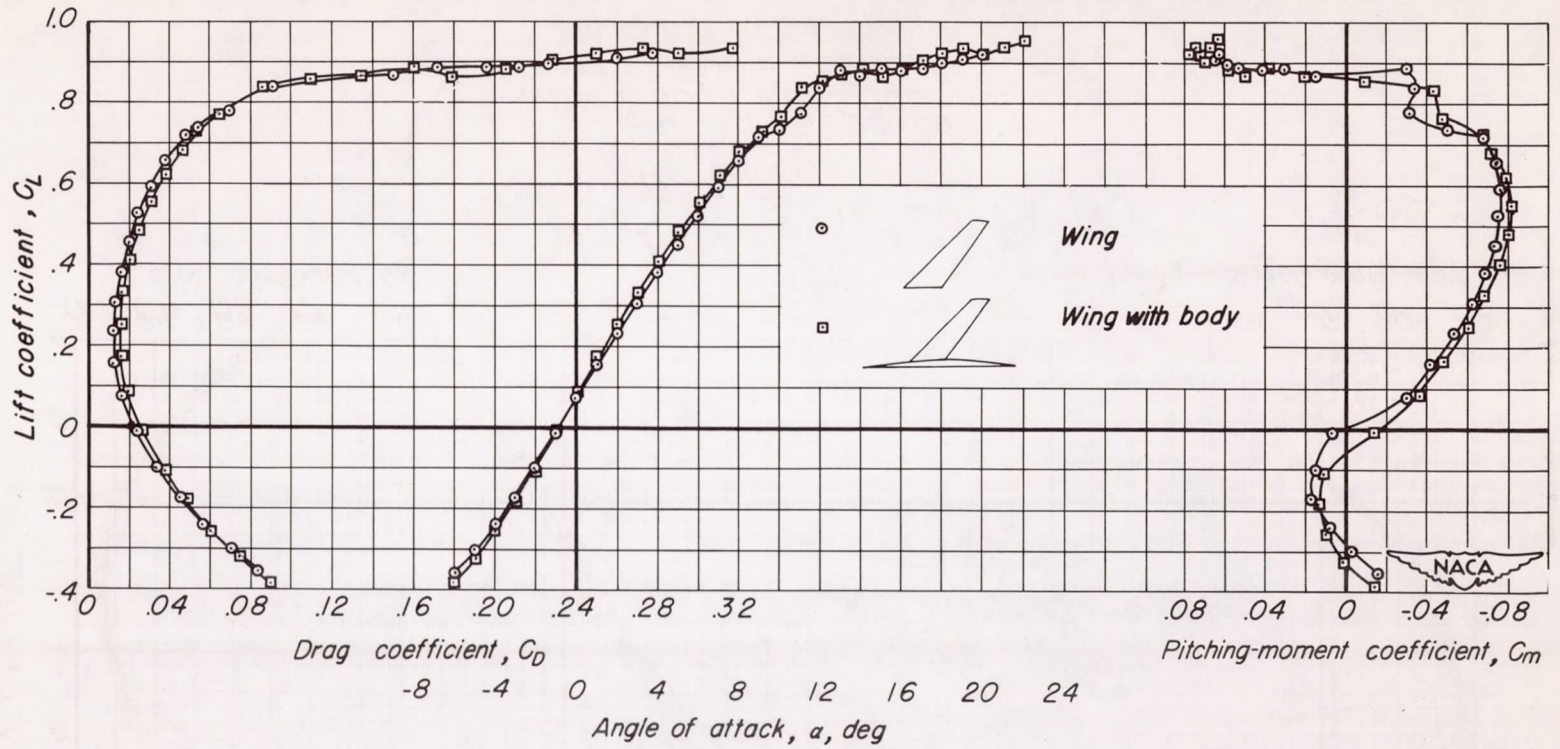
(d) $M, 0.60$; $R, 2,000,000$.

Figure 19.-Continued.



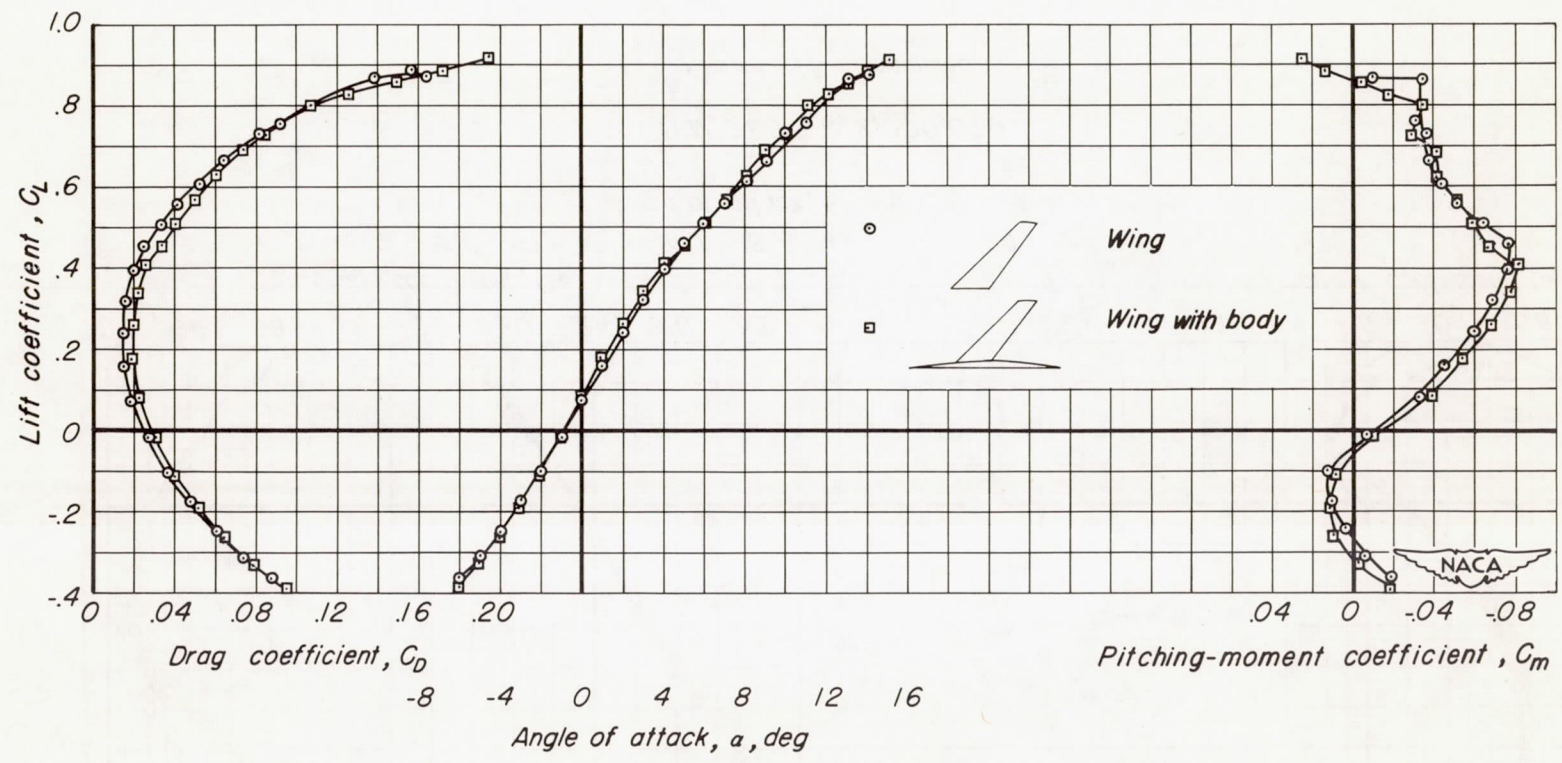
(e) $M, 0.80; R, 2,000,000$

Figure 19.-Continued.



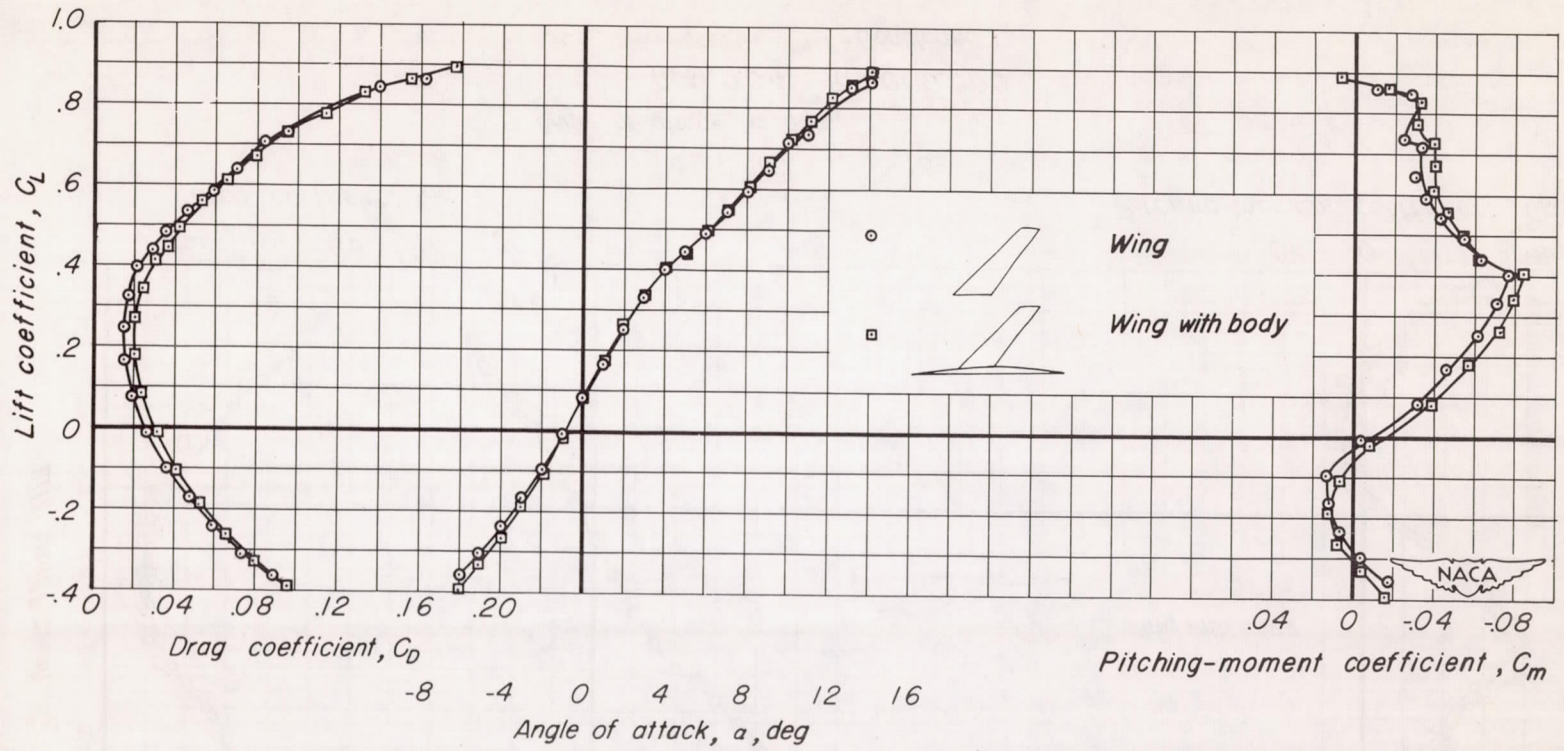
(f) $M, 0.85 ; R, 2,000,000$

Figure 19.-Continued.



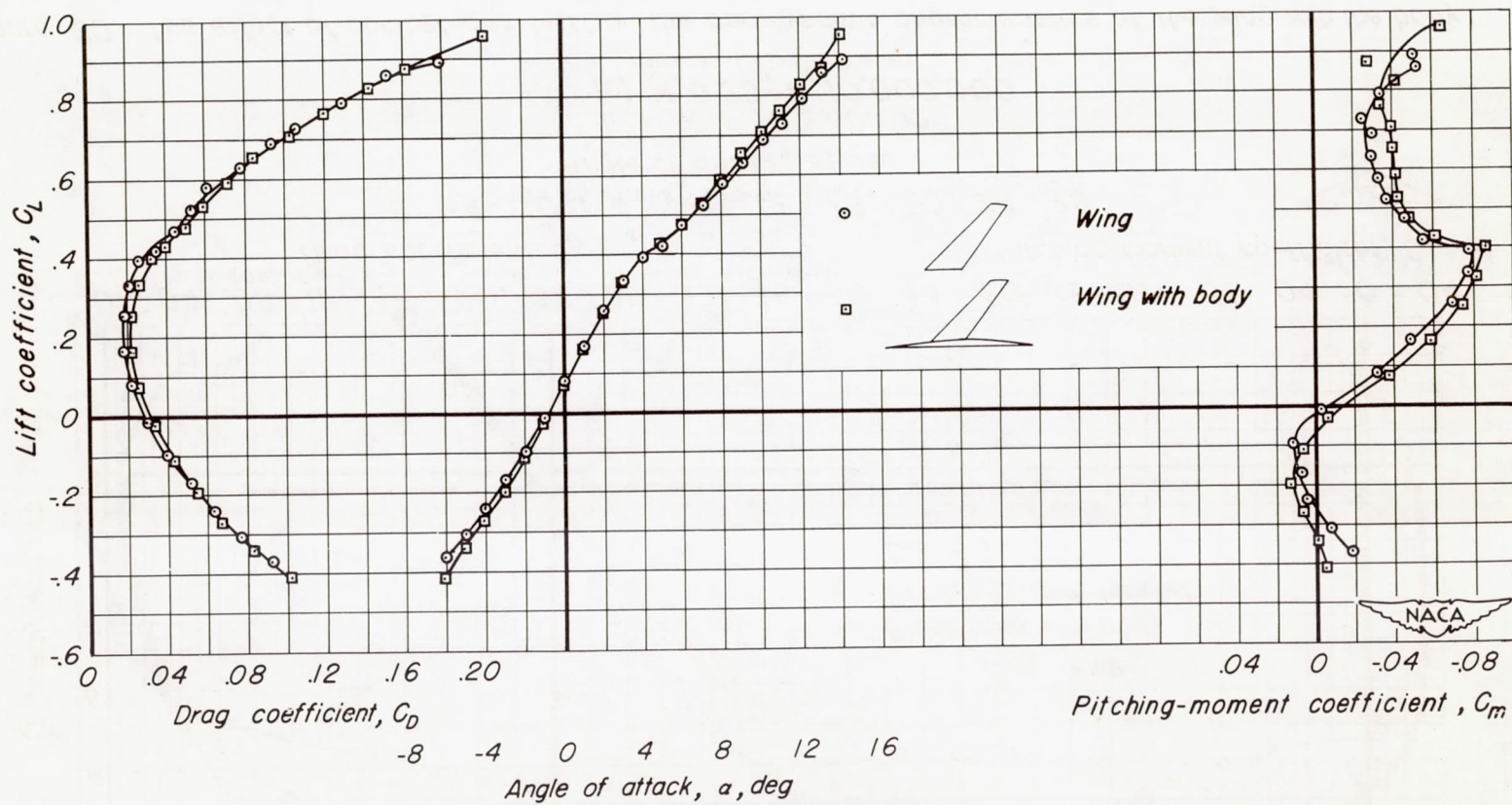
(g) $M, 0.90 ; R, 2,000,000$

Figure 19. - Continued.



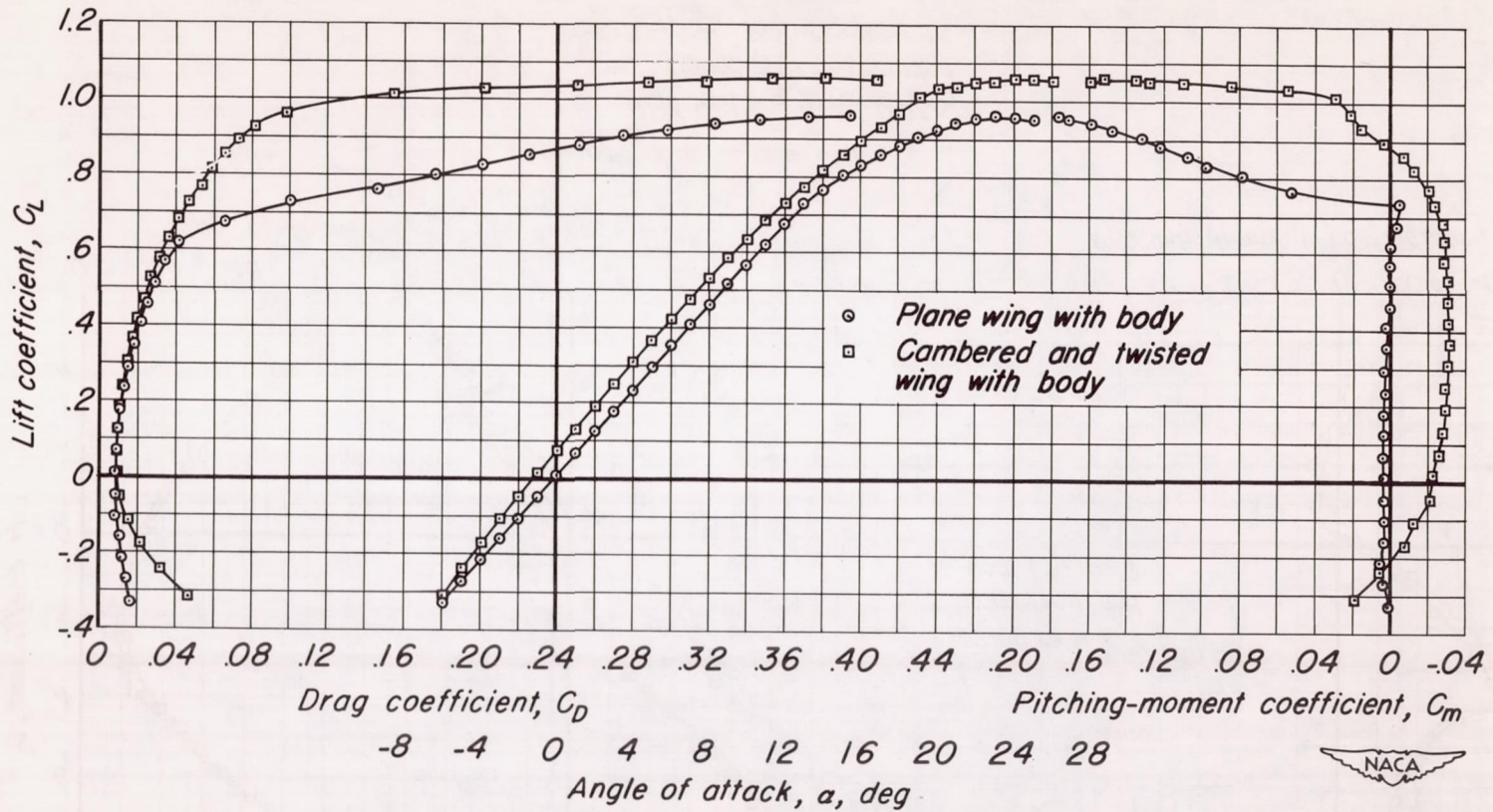
(h) $M, 0.92 ; R, 2,000,000$

Figure 19. -Continued.



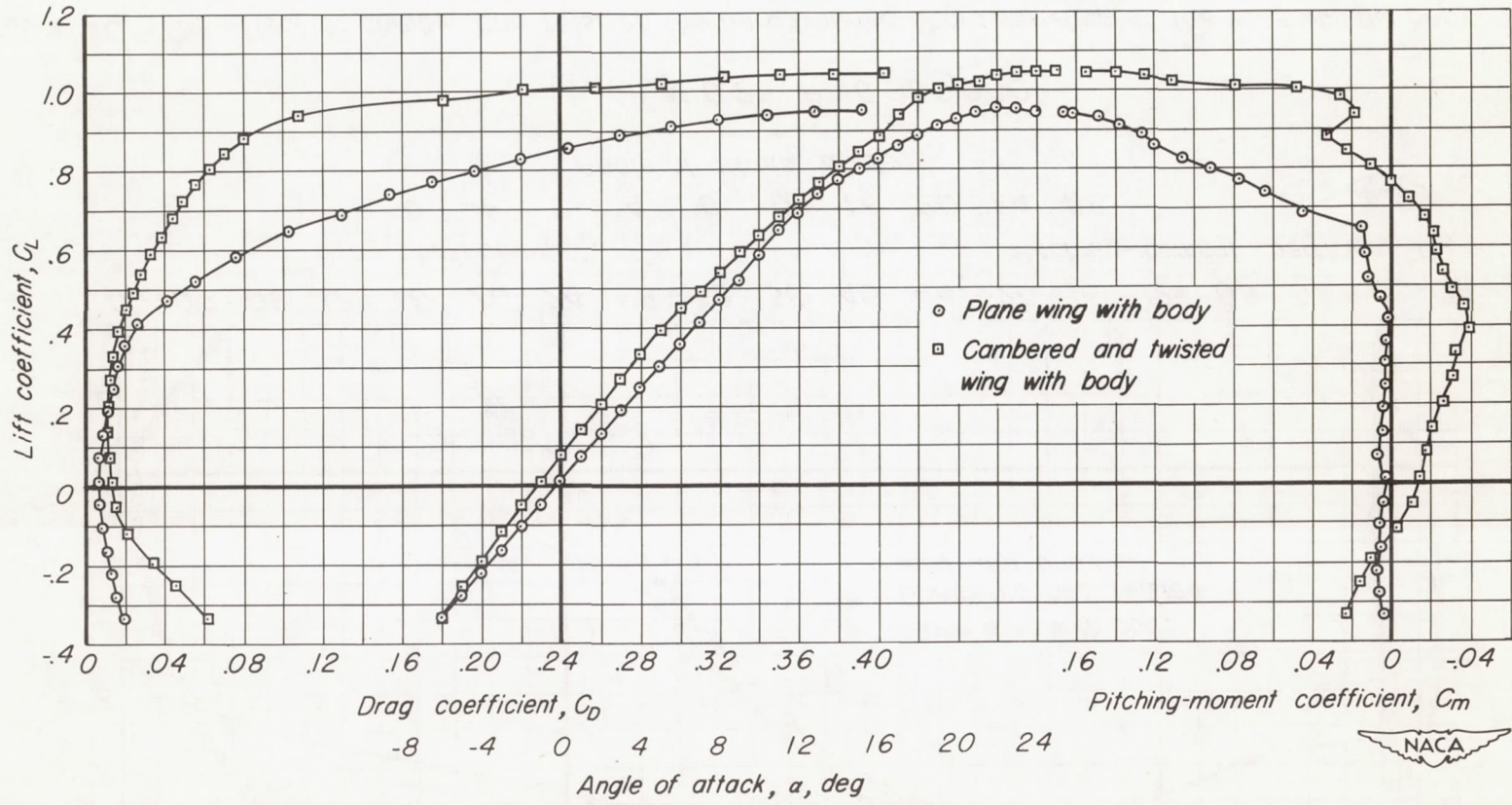
(i) $M, 0.94$; $R, 2,000,000$

Figure 19.-Concluded.



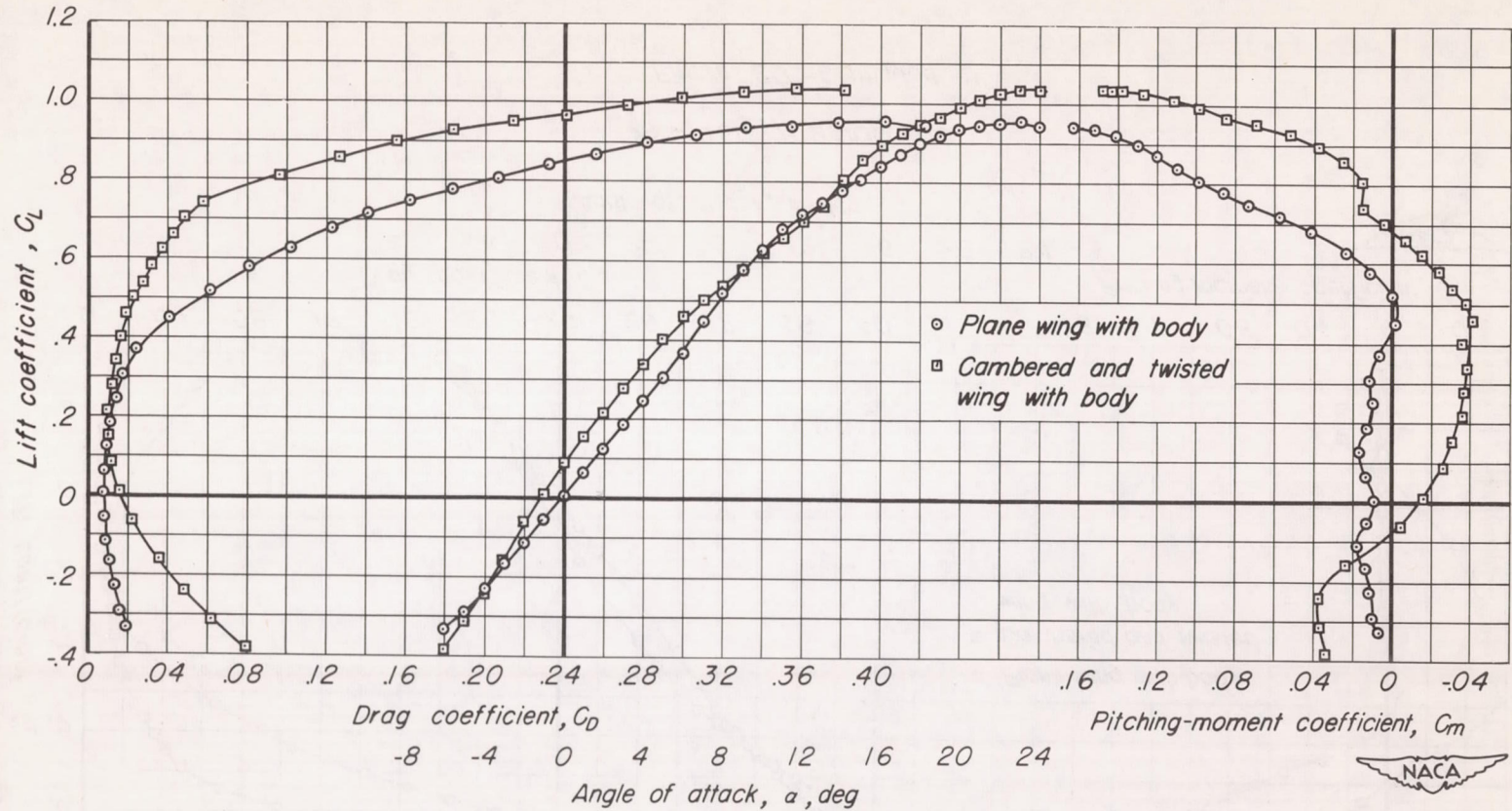
(a) $M, 0.25; R, 10,000,000$

Figure 20. - The effect of camber and twist on the aerodynamic characteristics of the wing with the body.



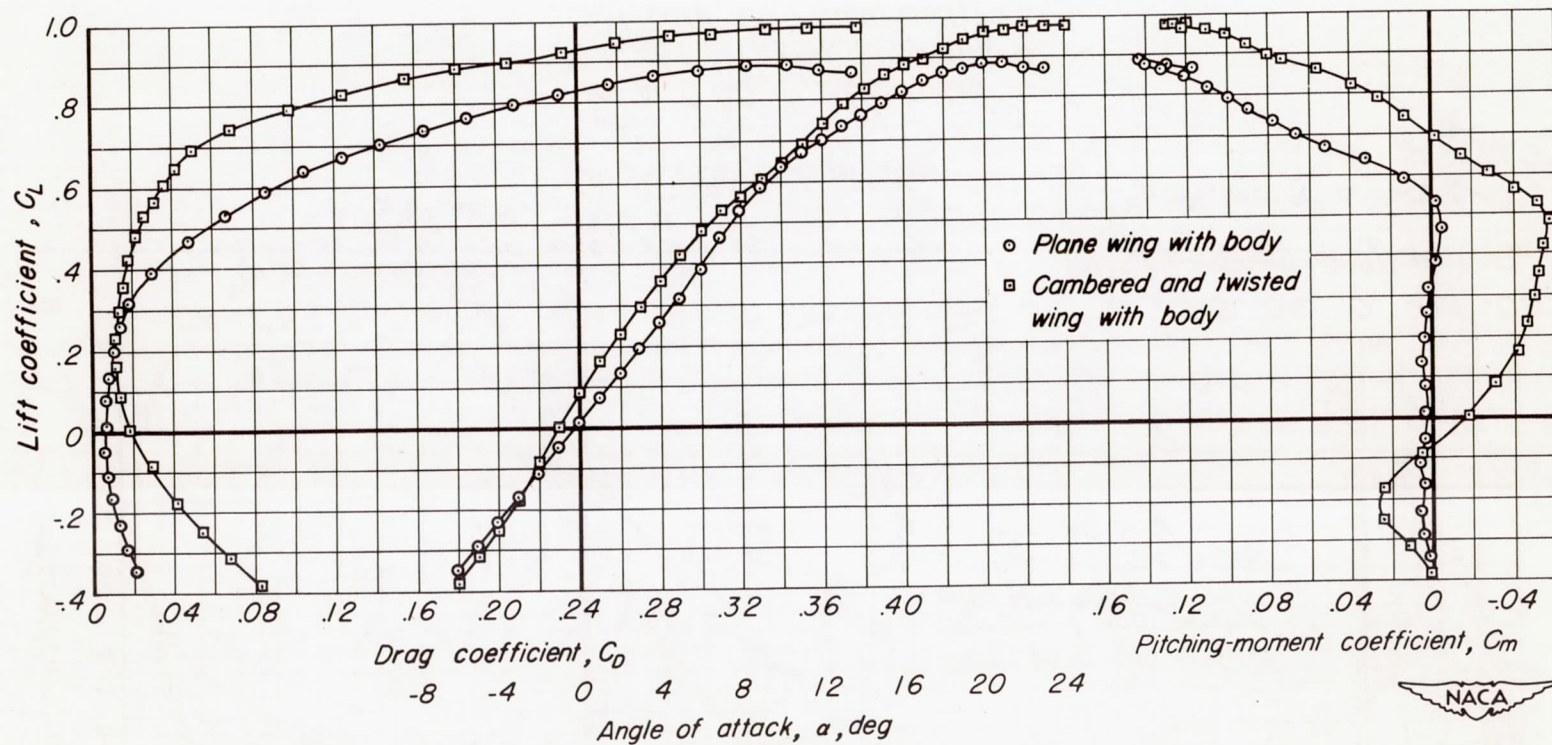
(b) $M, 0.25 ; R, 4,000,000$

Figure 20.-Continued.



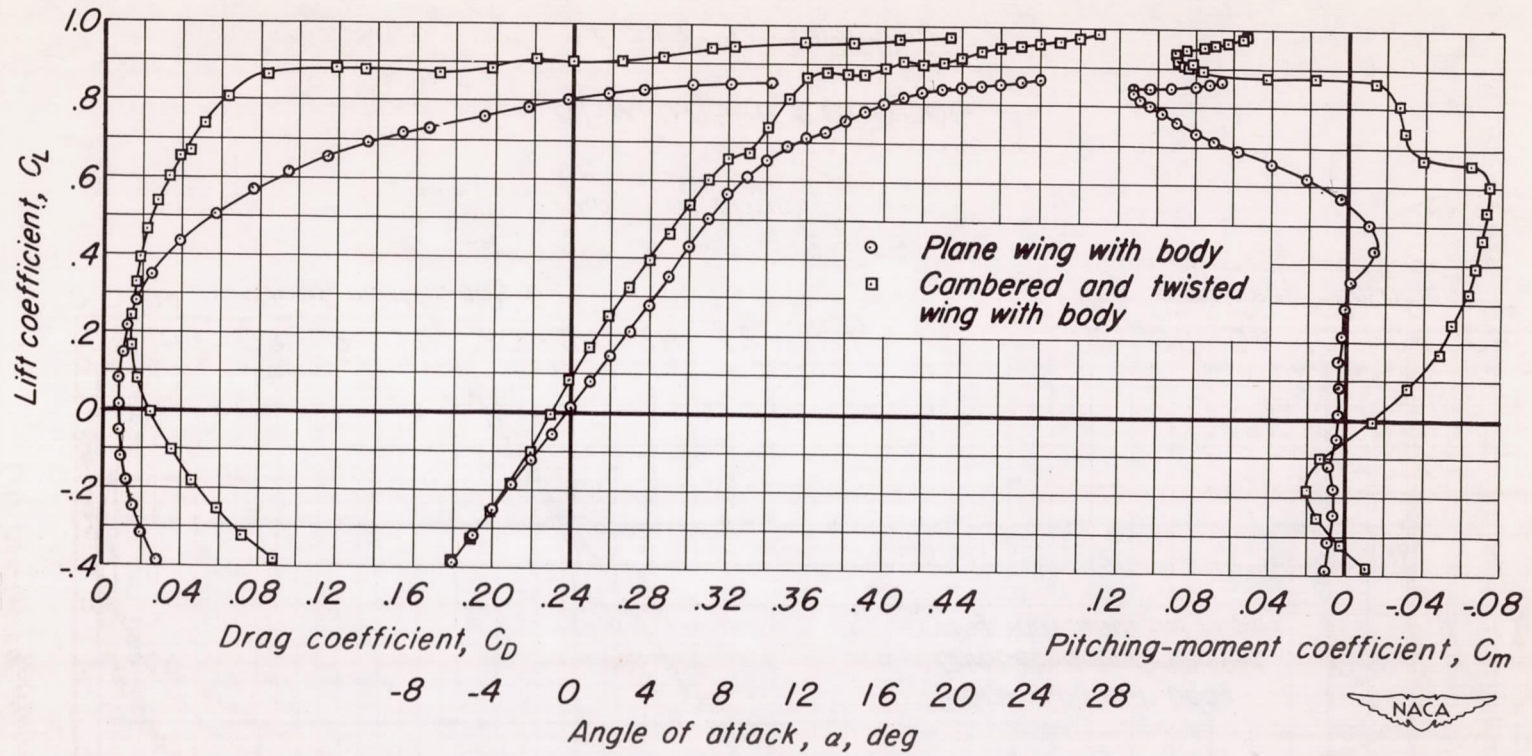
(c) $M, 0.25 ; R, 2,000,000$

Figure 20. -Continued.

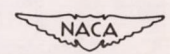


(d) $M, 0.60$; $R, 2,000,000$

Figure 20. -Continued.

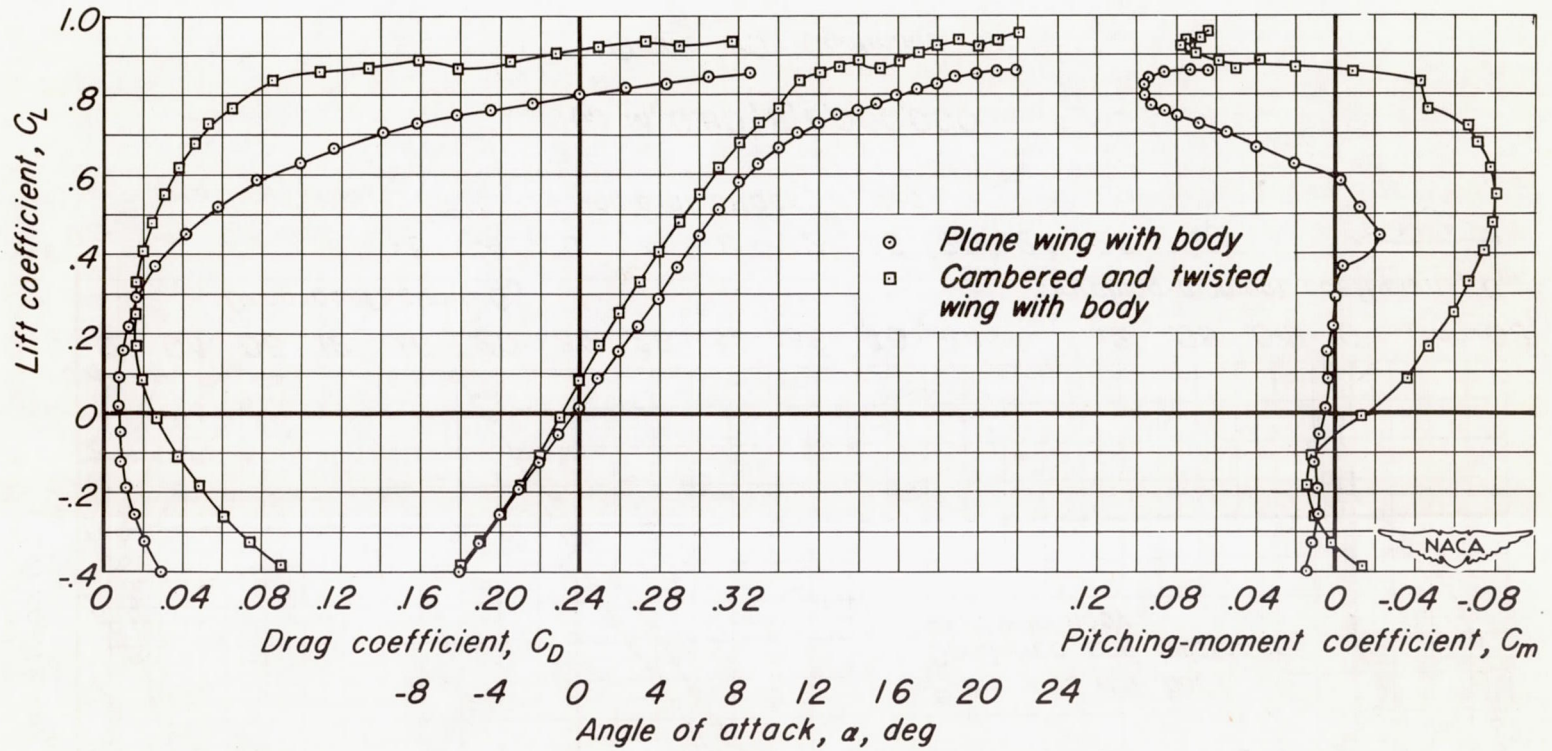


-8 -4 0 4 8 12 16 20 24 28
 Angle of attack, α , deg



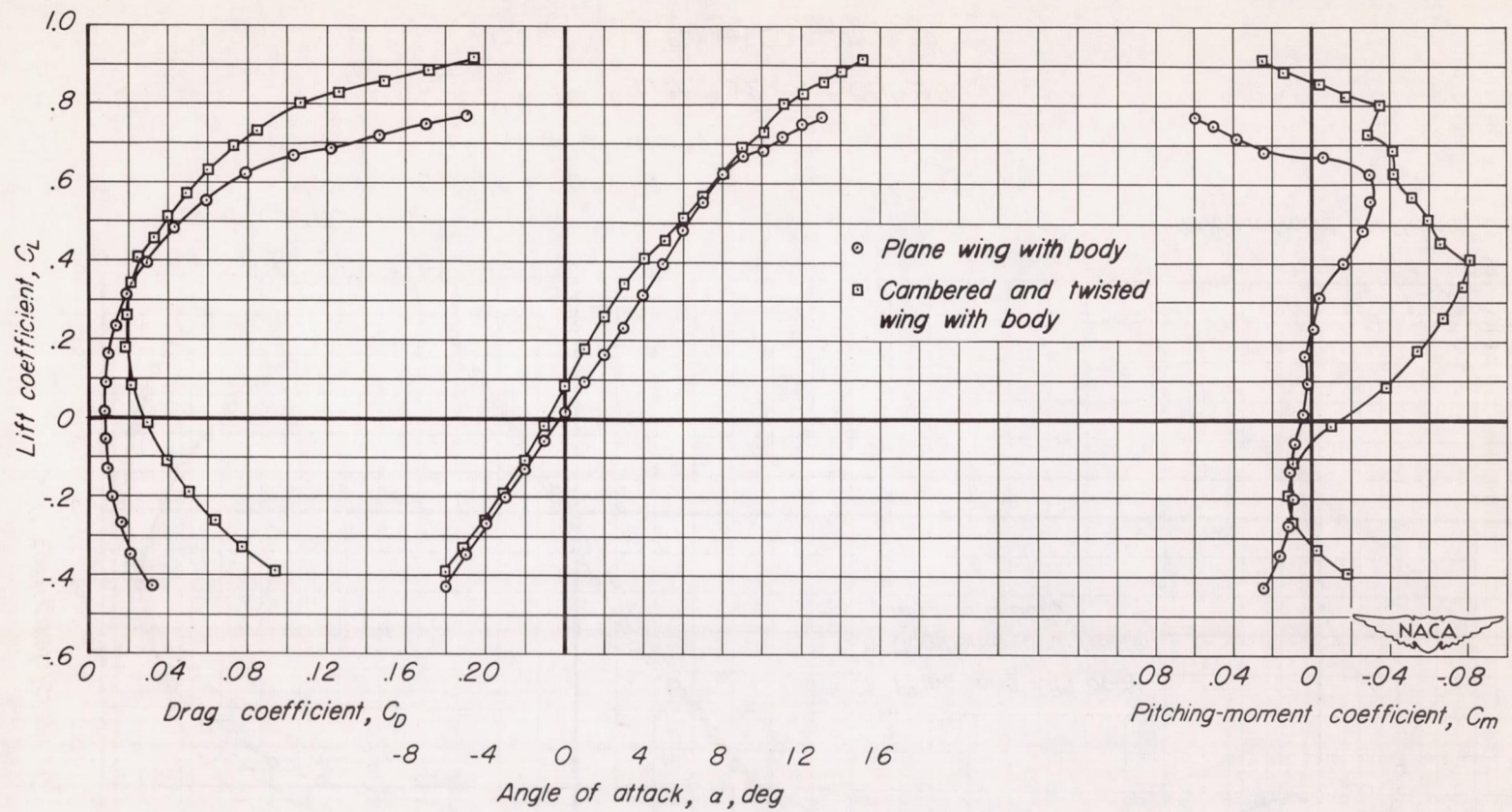
(e) $M, 0.80; R, 2,000,000$

Figure 20.-Continued.

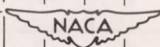


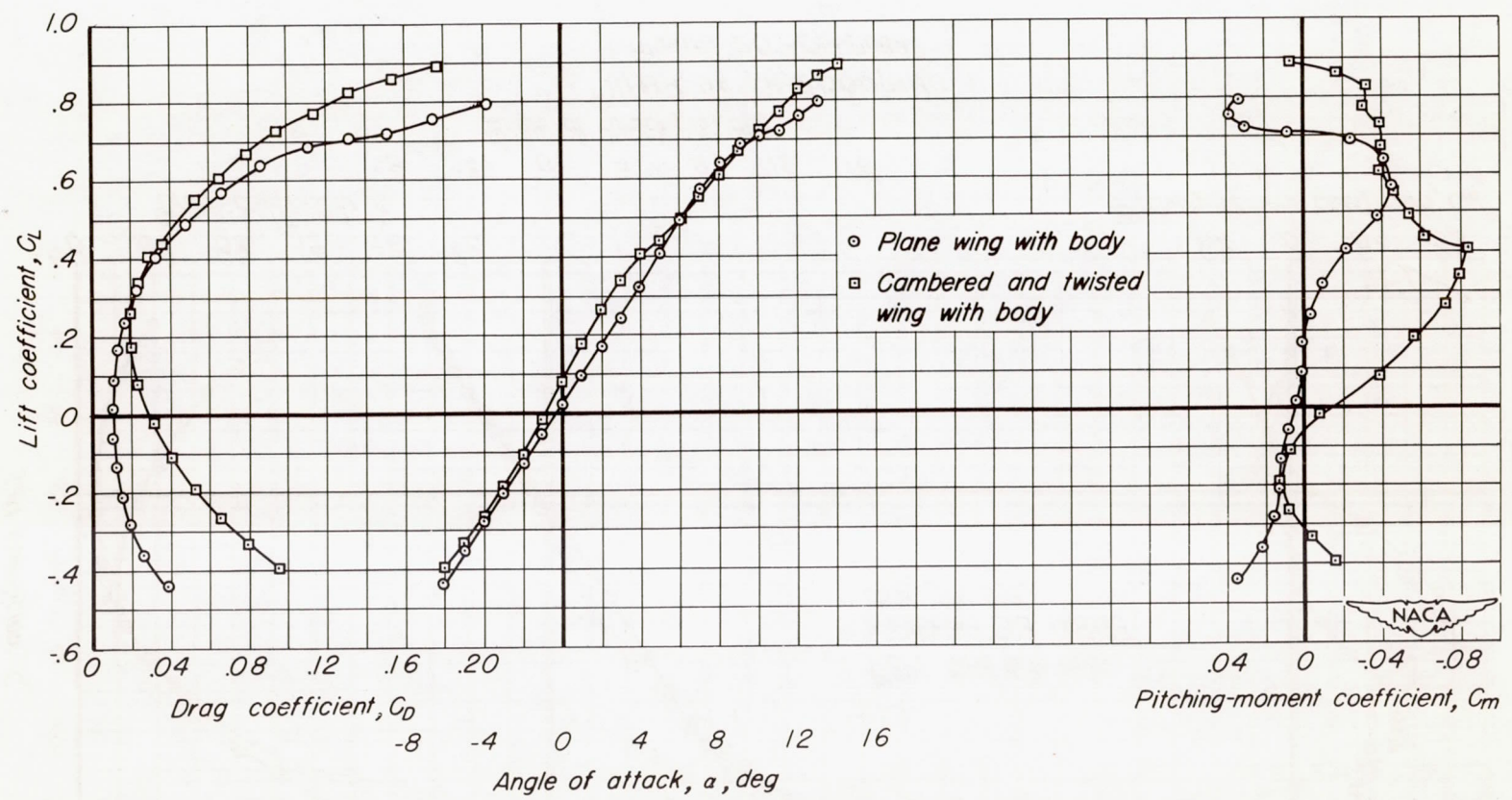
(f) $M, 0.85; R, 2,000,000$

Figure 20. - Continued.



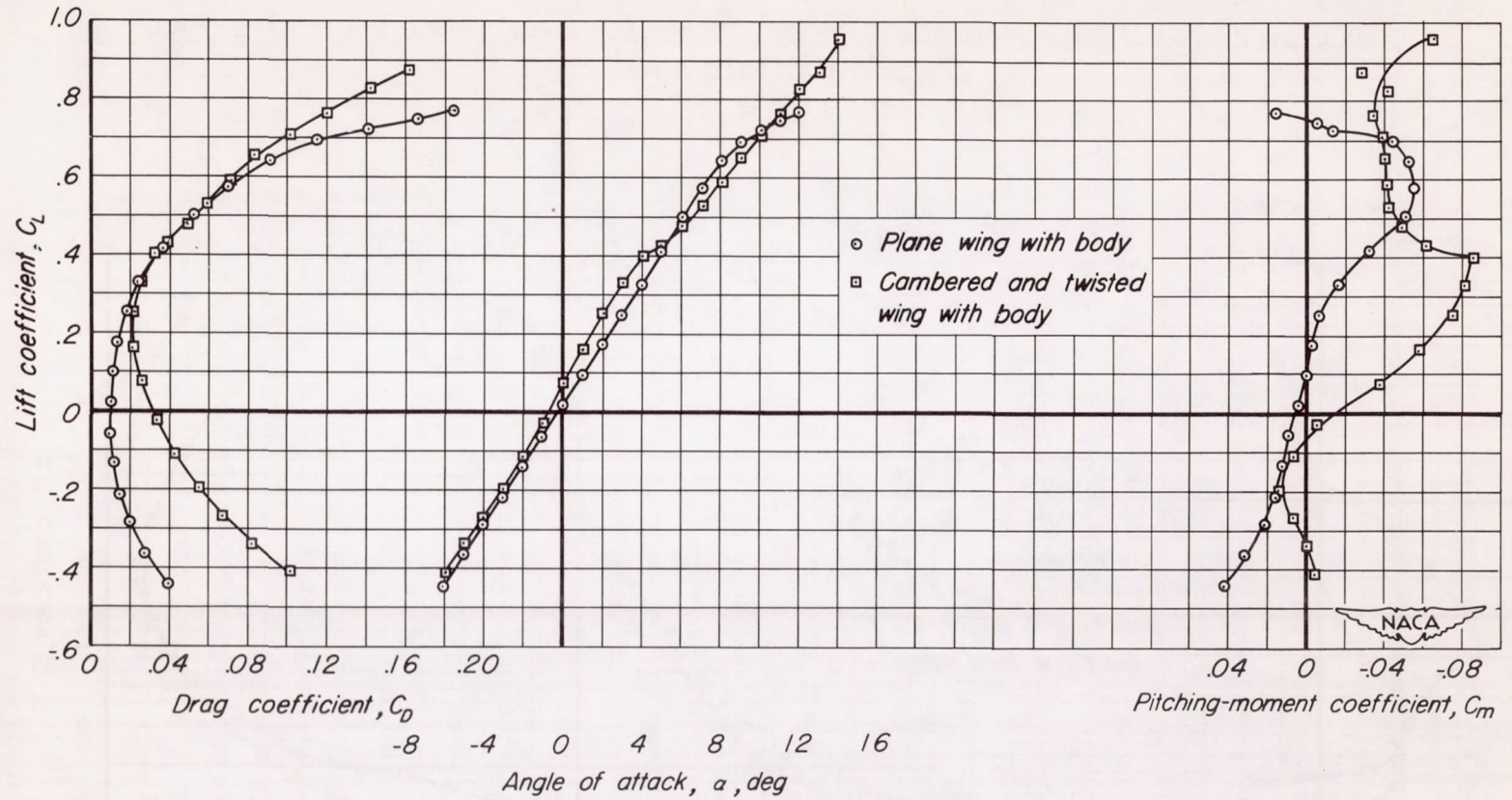
(g) $M, 0.90$; $R, 2,000,000$
 Figure 20.-Continued.





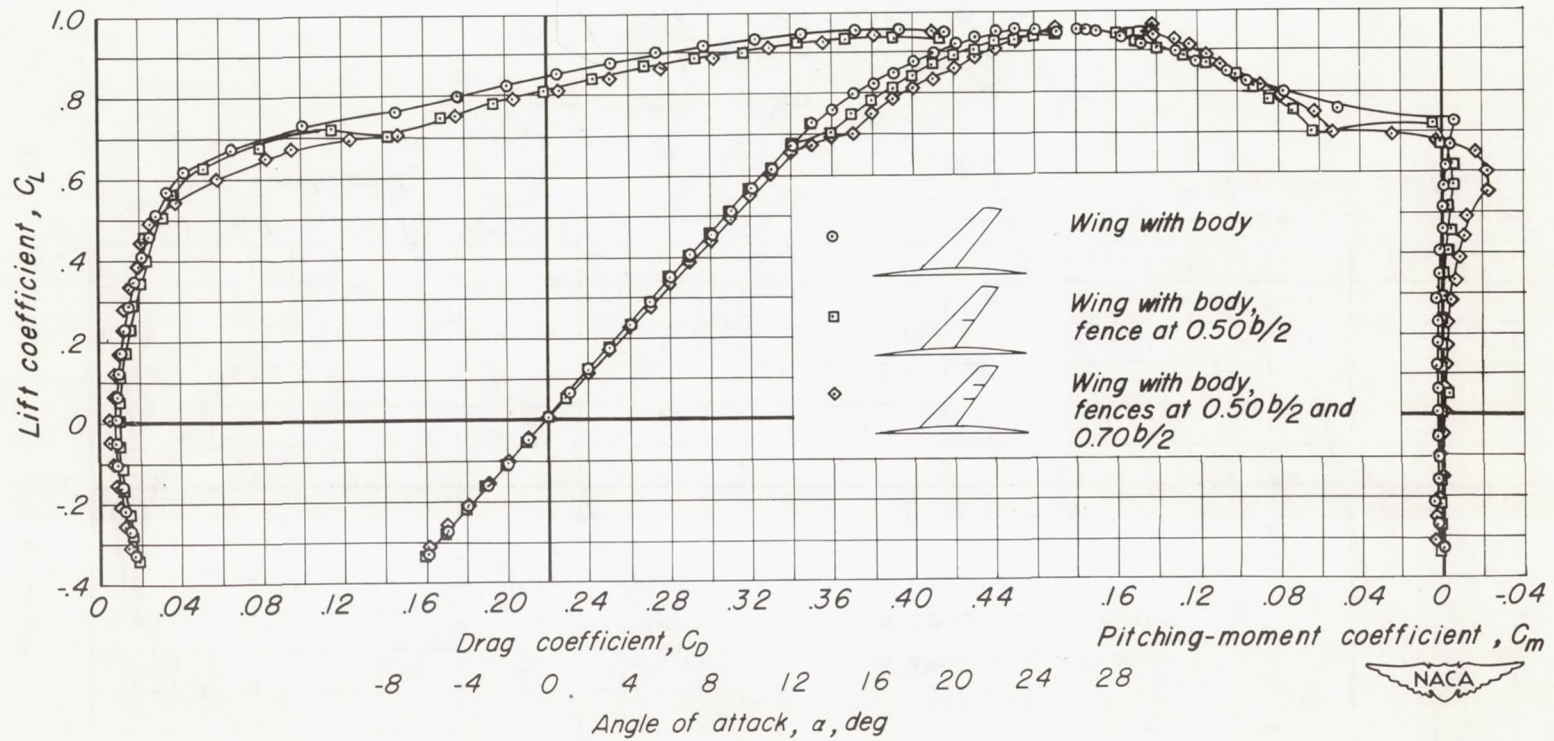
(h) $M, 0.92 ; R, 2,000,000$

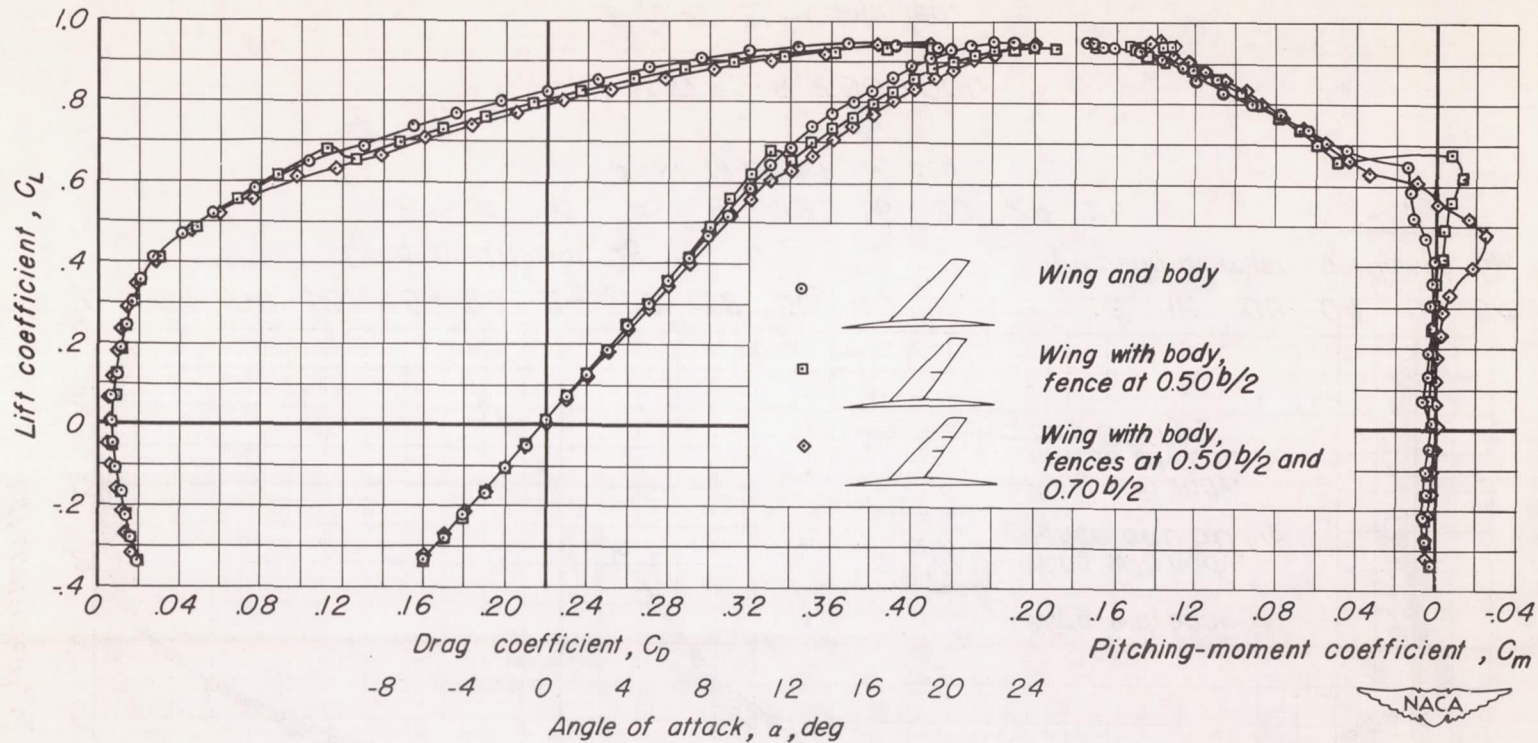
Figure 20.-Continued.



(i) $M, 0.94 ; R, 2,000,000$

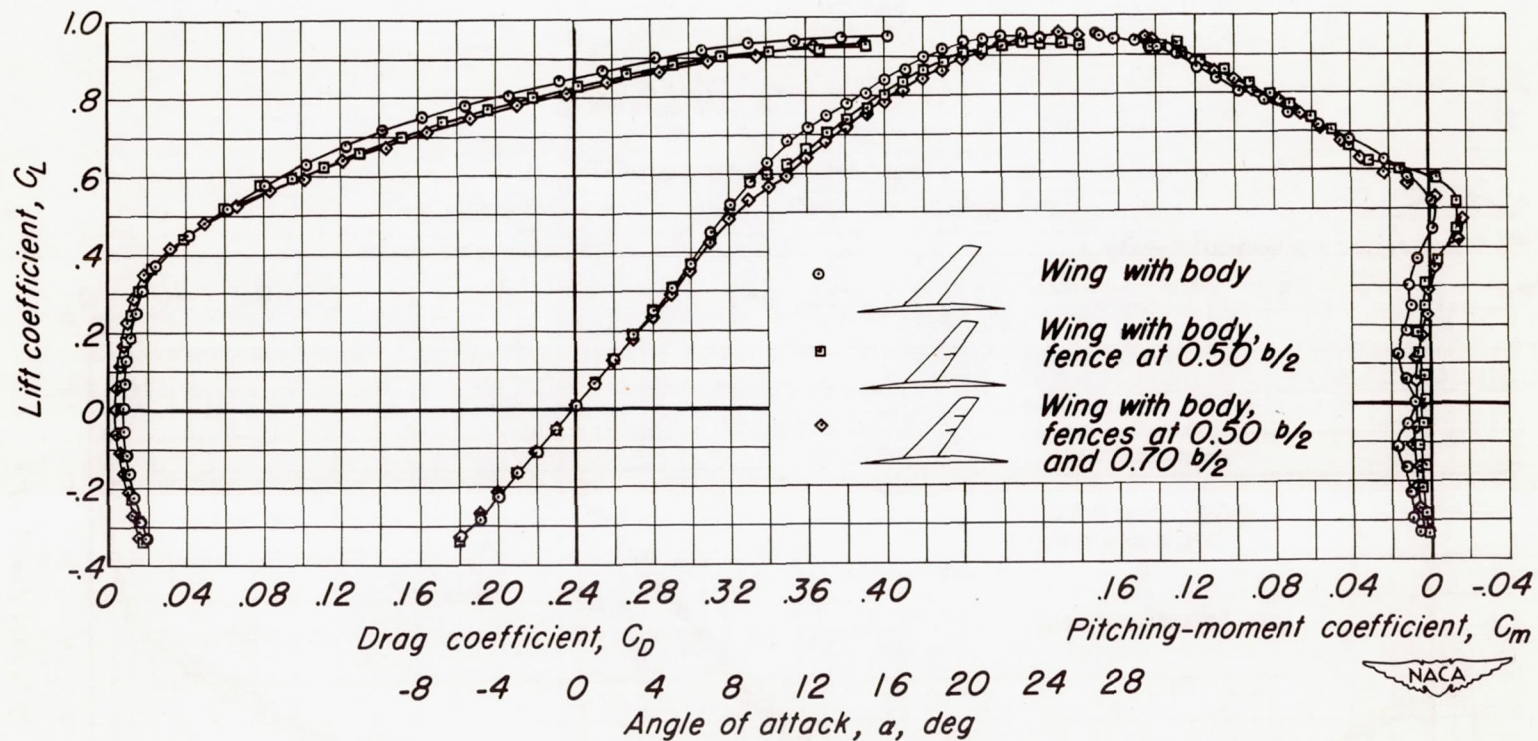
Figure 20. - Concluded.





(b) $M, 0.25 ; R, 4,000,000$

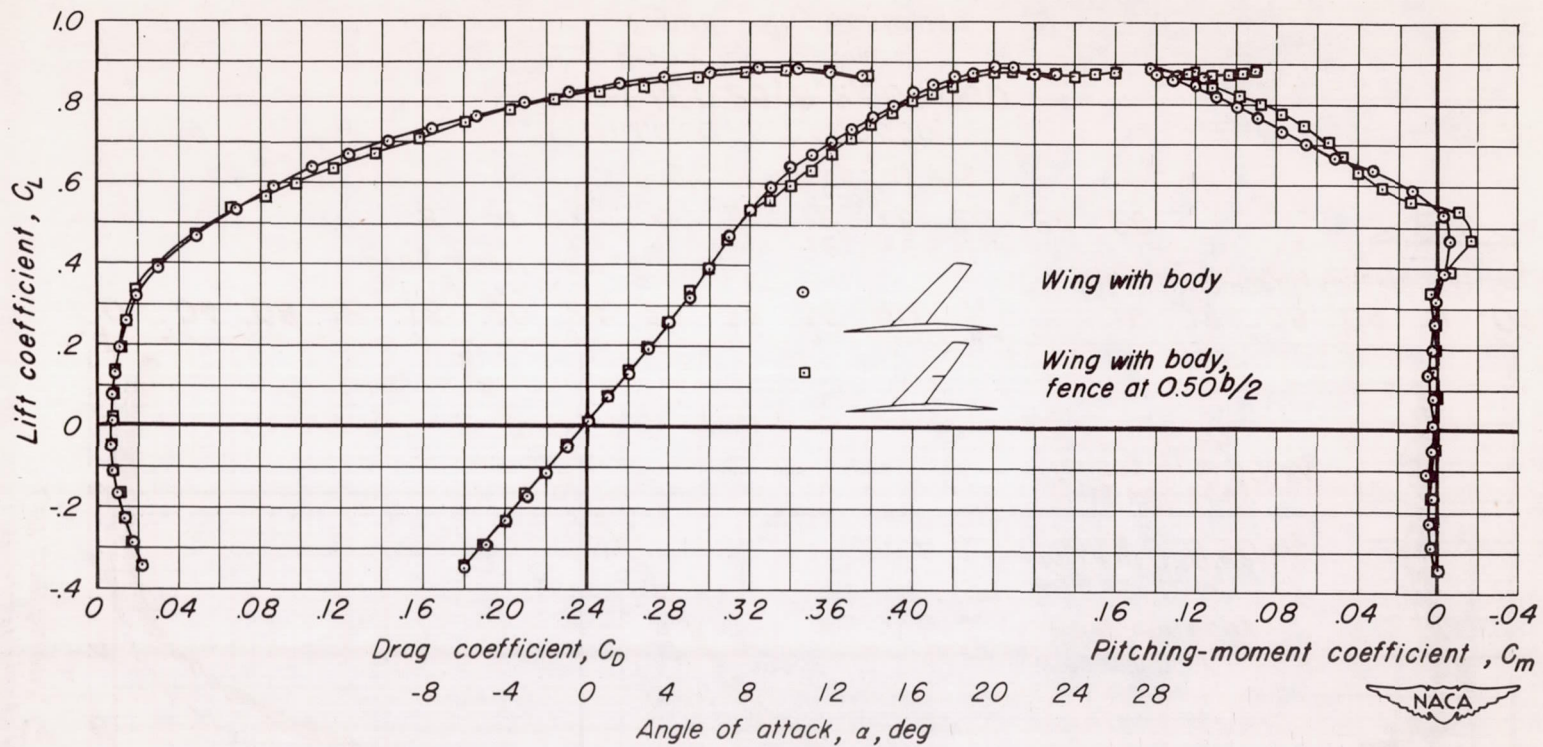
Figure 21. - Continued.



(c) $M, 0.25; R, 2,000,000$

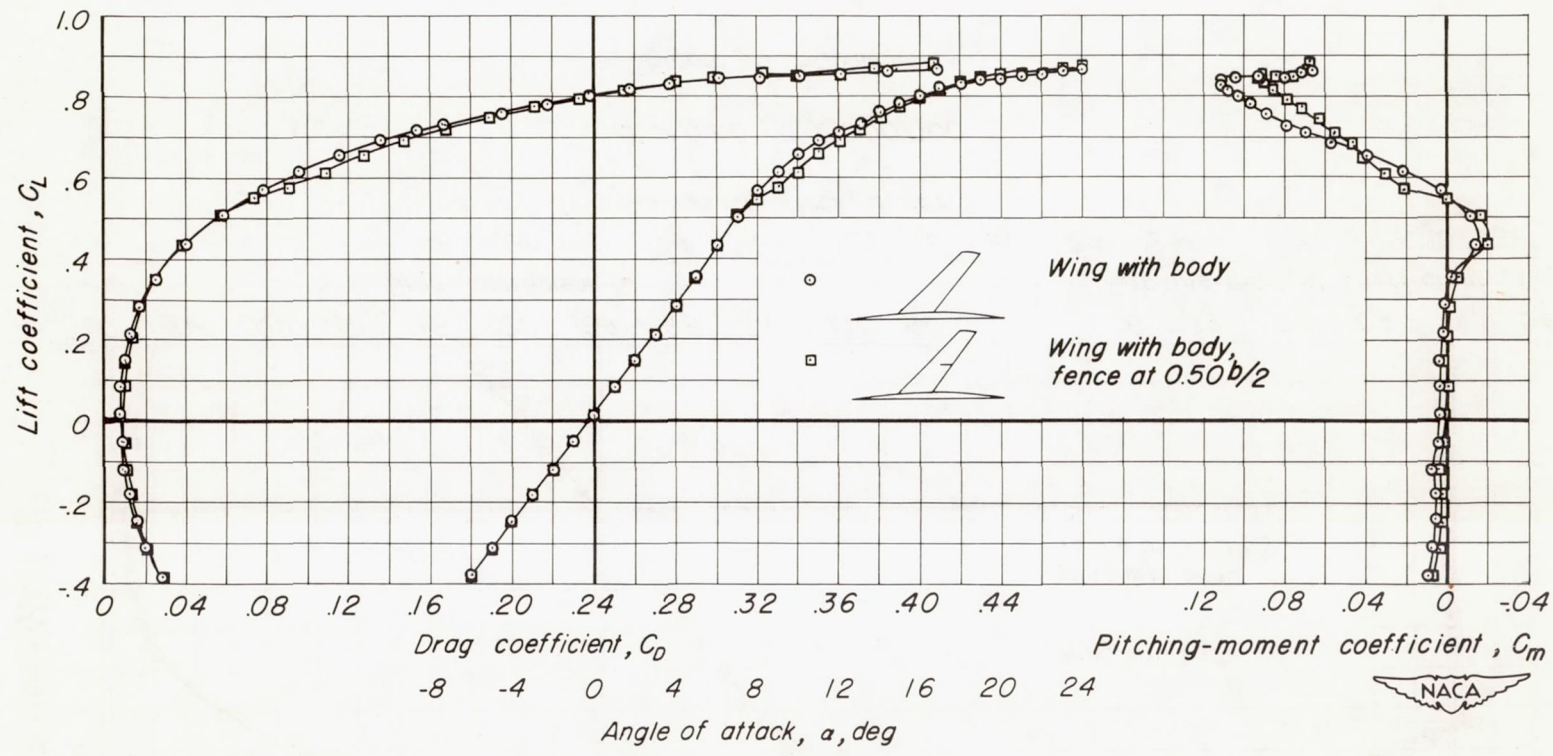
Figure 21. - Continued.





(d) $M, 0.60$; $R, 2,000,000$

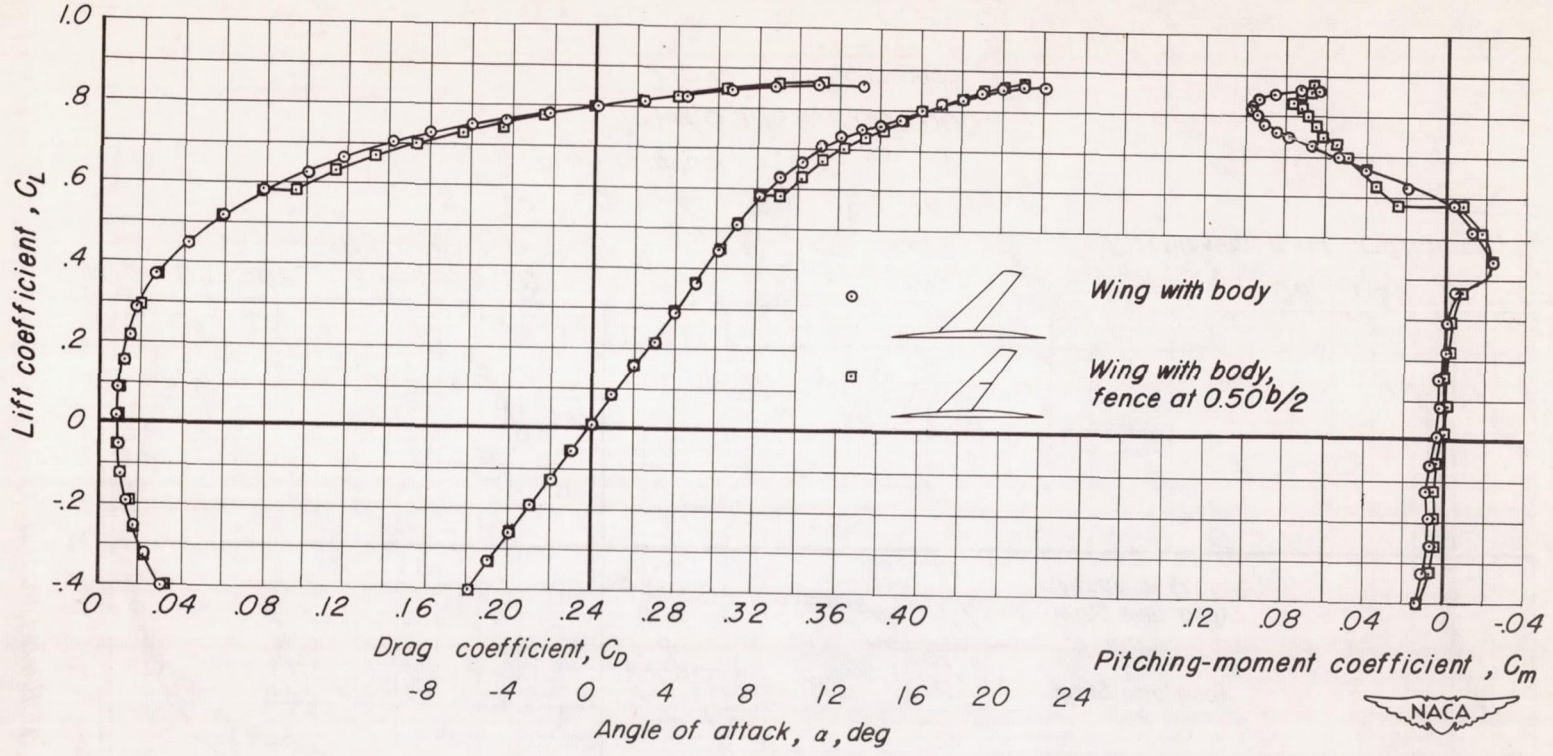
Figure 21. - Continued.



(e) $M, 0.80$; $R, 2,000,000$

Figure 21.-Continued.

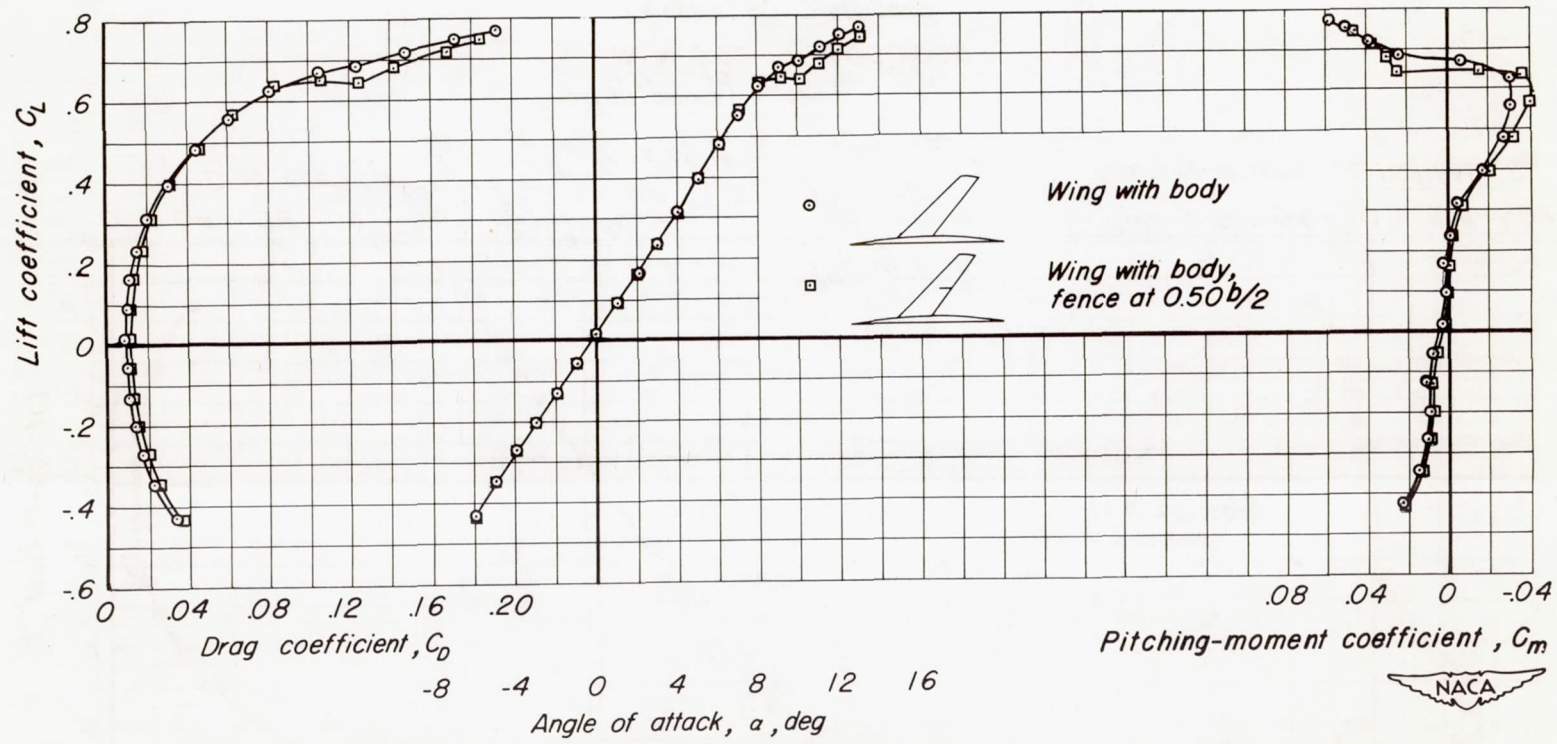




(f) $M, 0.85 ; R, 2,000,000$

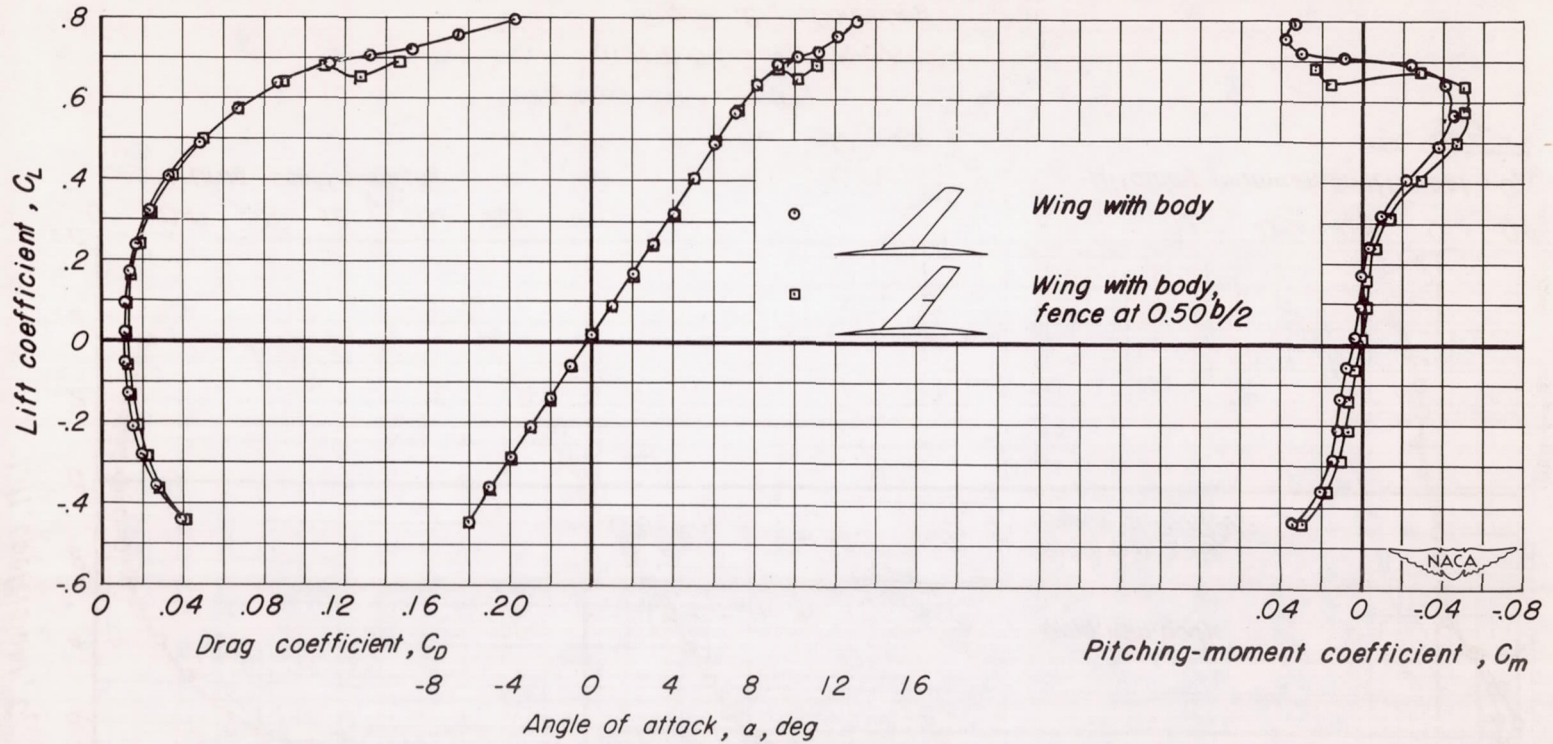
Figure 21. -Continued.



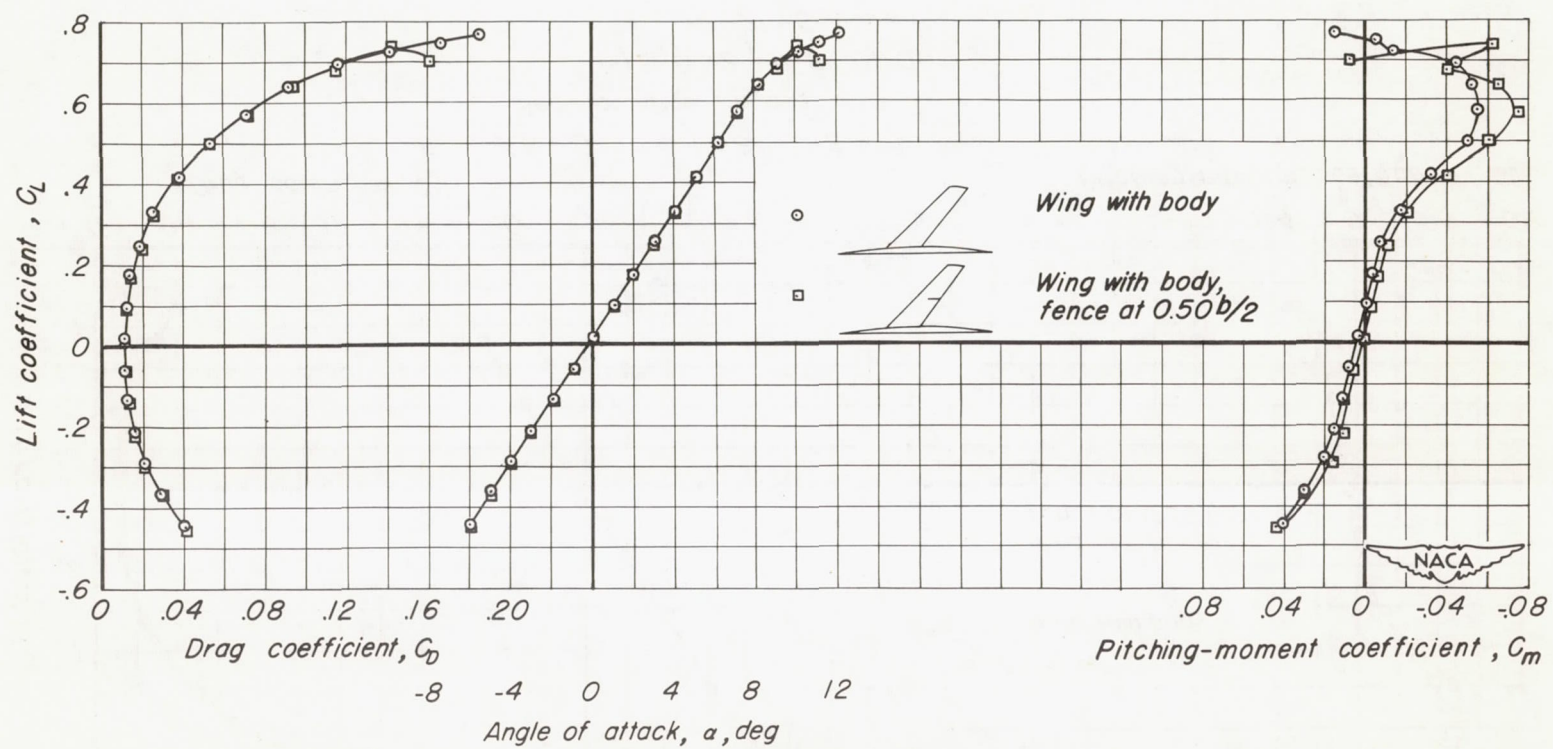


(g) $M, 0.90 ; R, 2,000,000$
Figure 21 - Continued.

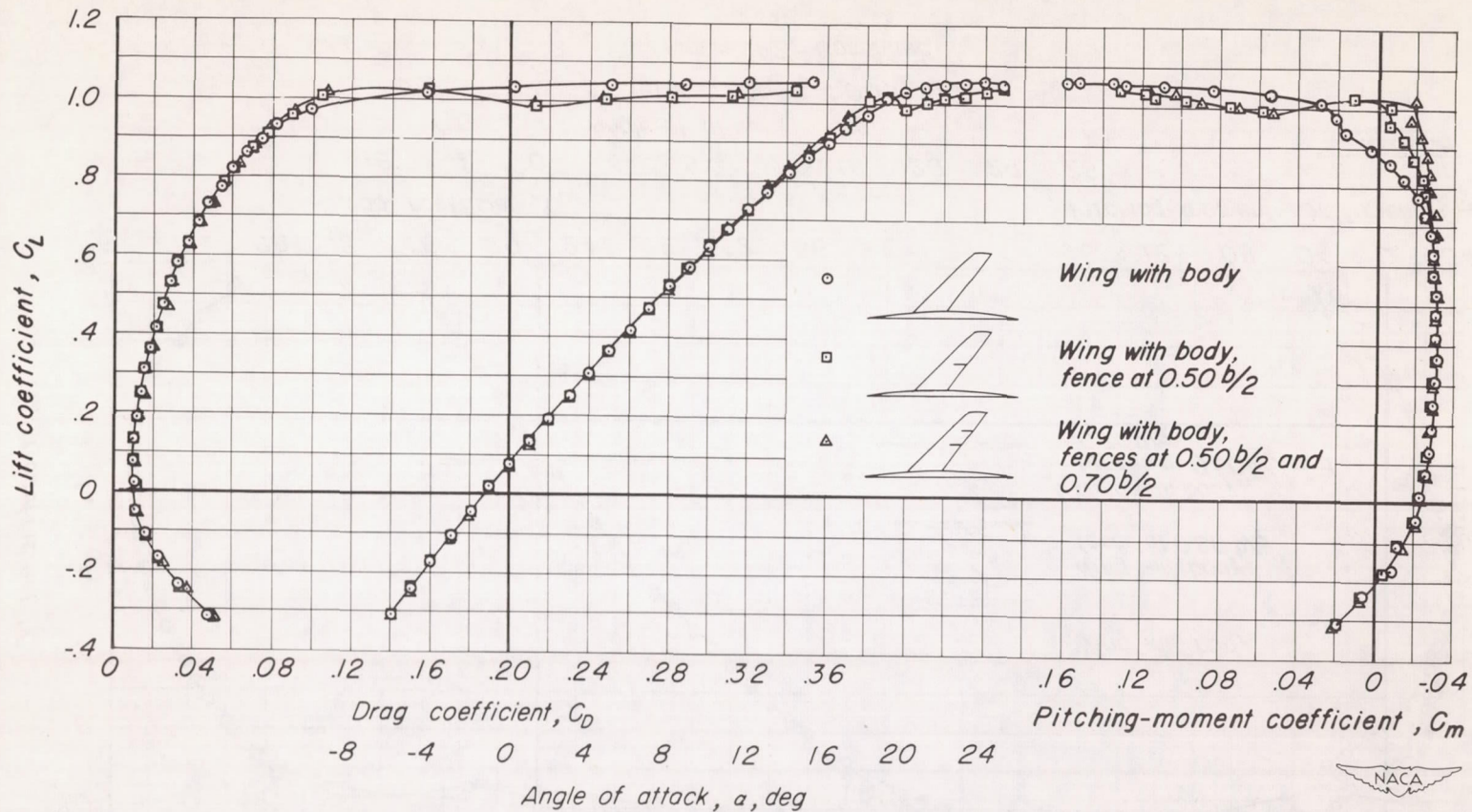




(h) $M, 0.92$; $R, 2,000,000$
 Figure 21.-Continued.

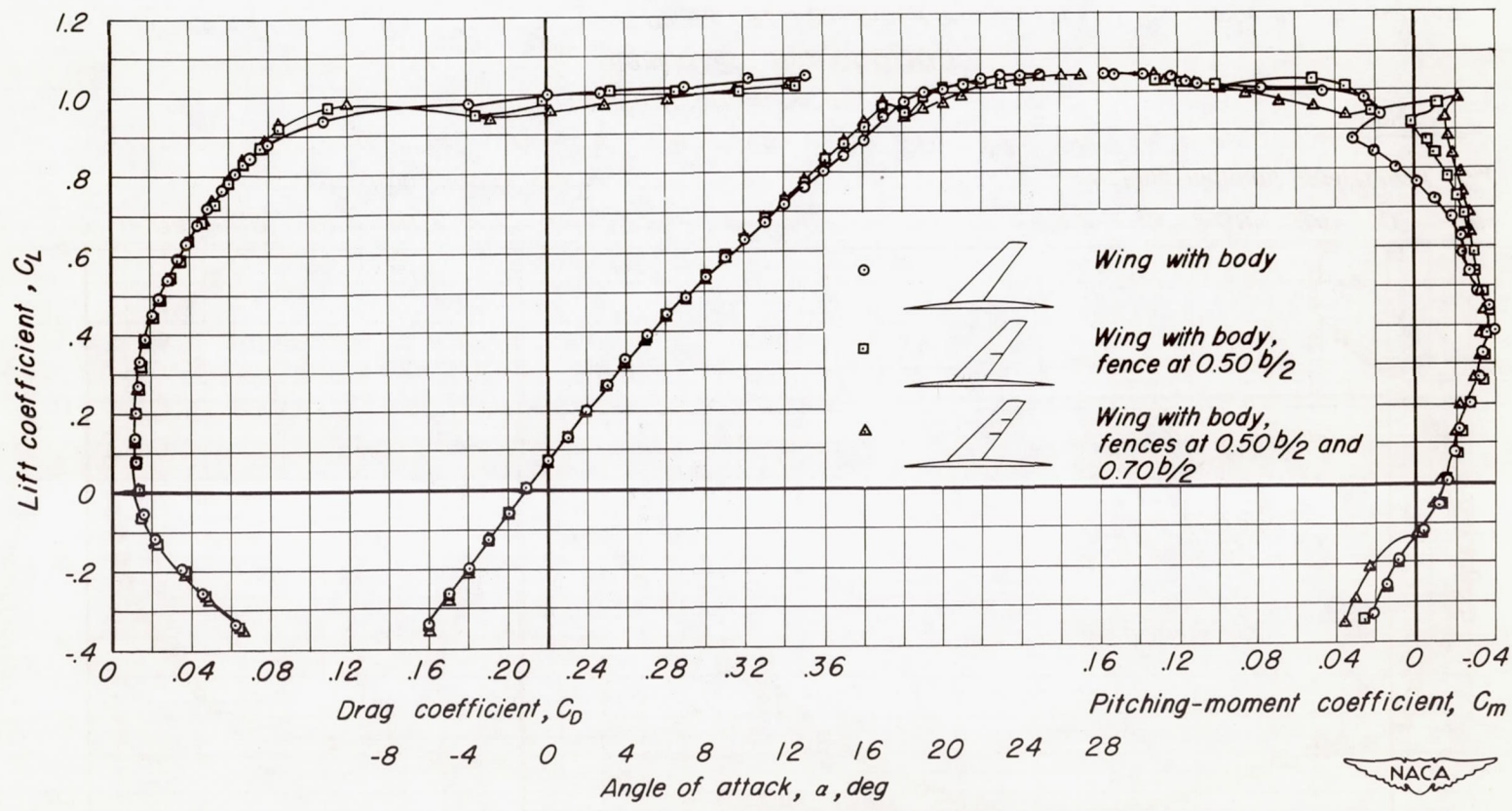


(i) $M, 0.94$; $R, 2,000,000$
 Figure 21.- Concluded.



(a) $M, 0.25$; $R, 10,000,000$

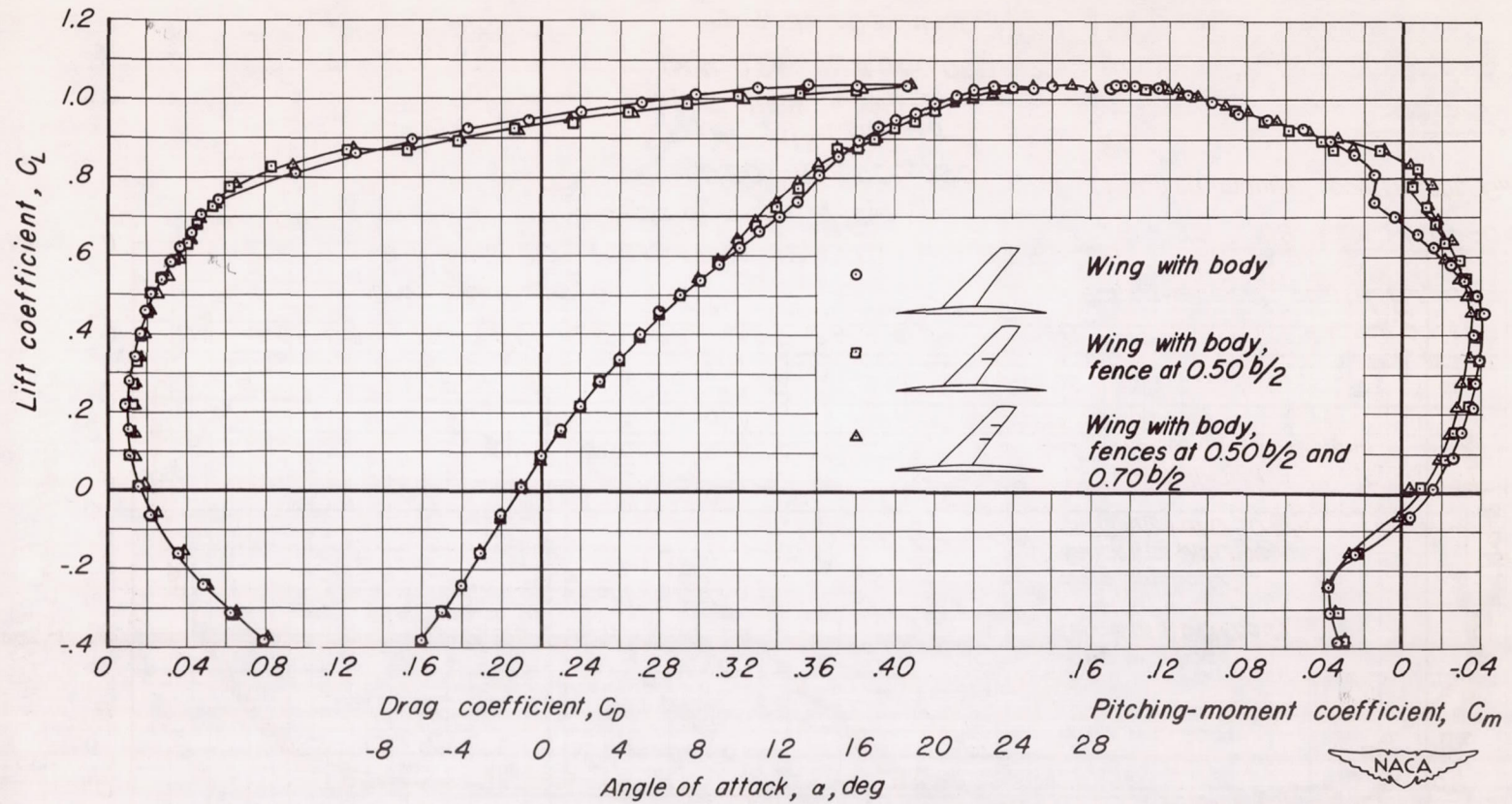
Figure 22. - The effect of high fences on the aerodynamic characteristics of the cambered and twisted wing with the body.



(b) $M, 0.25$; $R, 4,000,000$

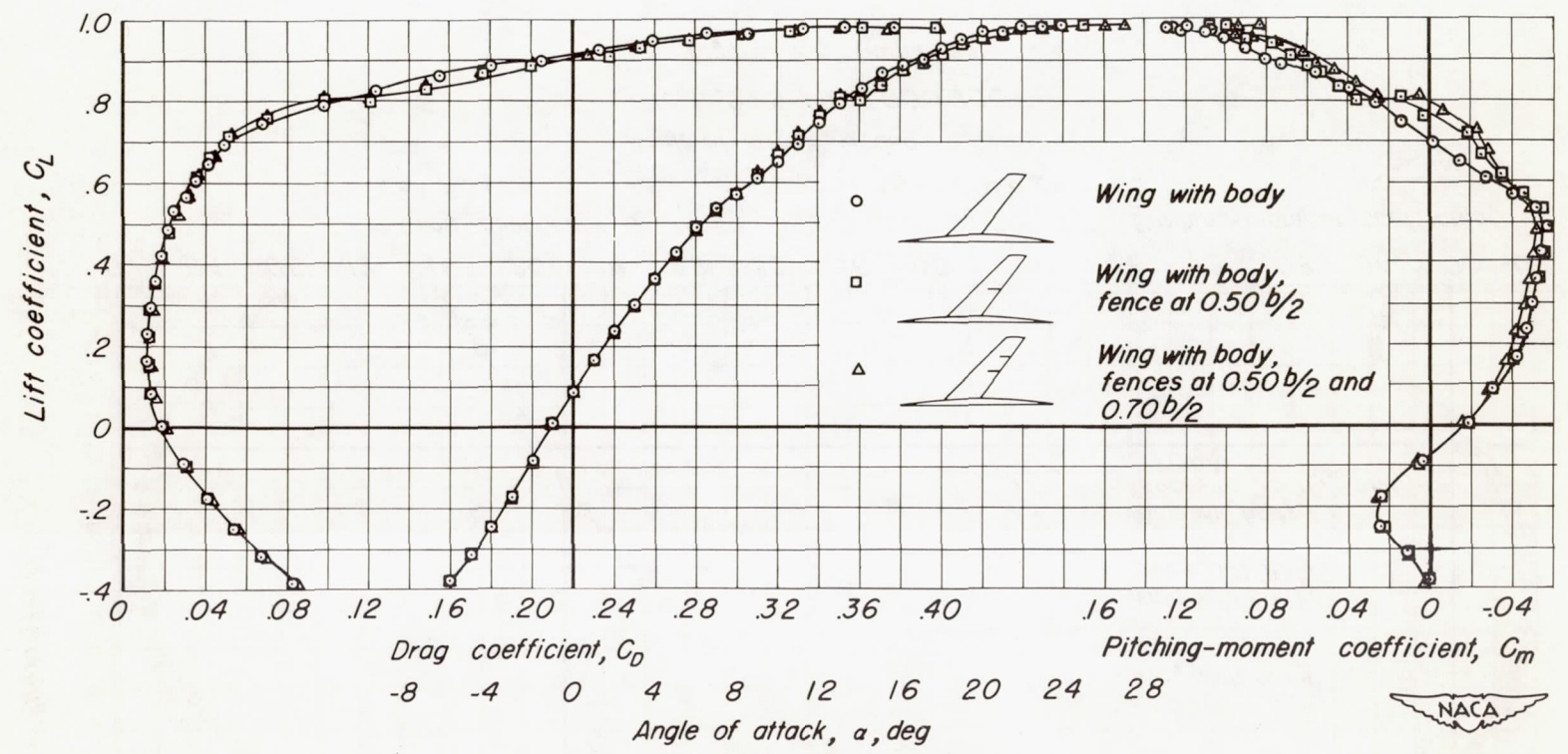
Figure 22. - Continued.



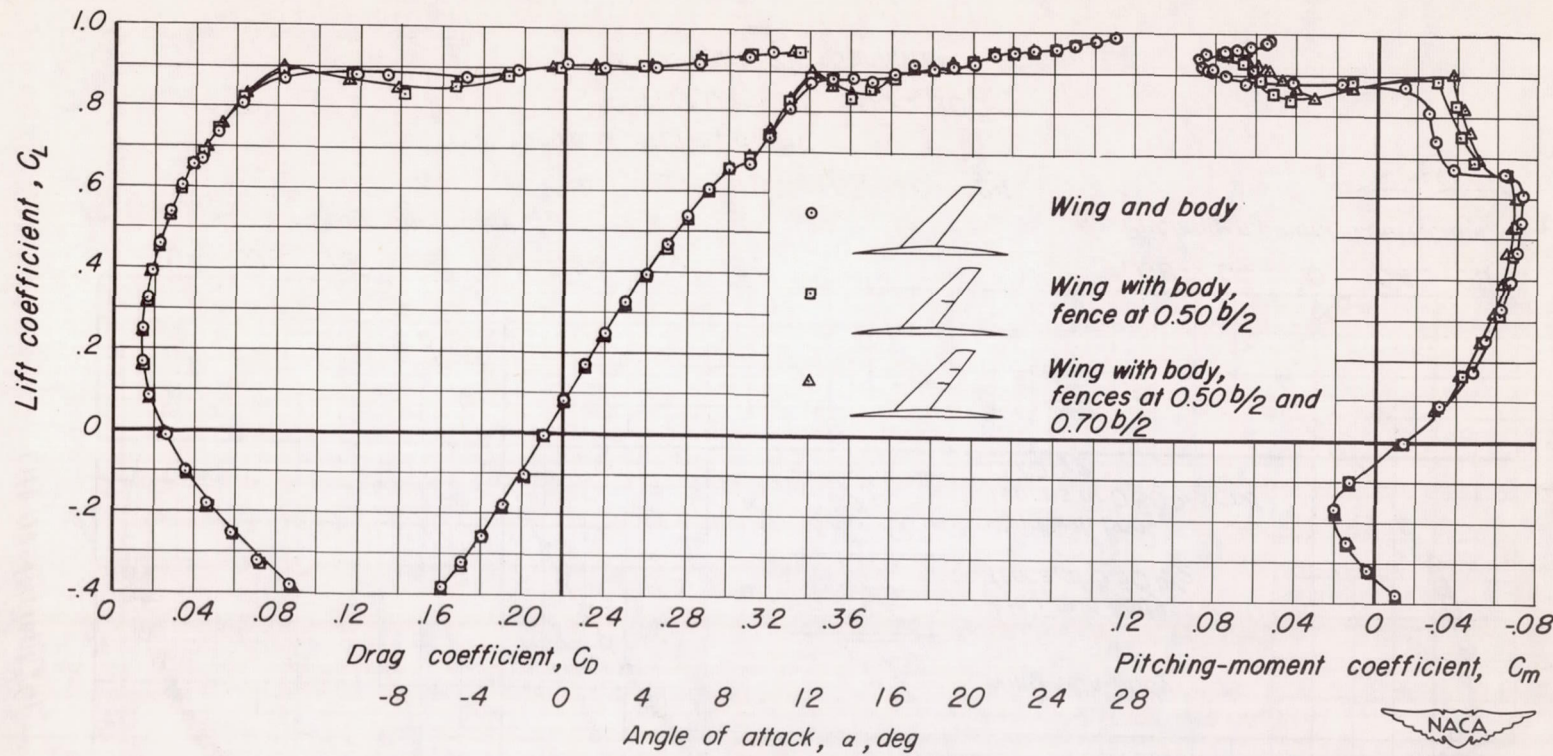


(c) $M, 0.25$; $R, 2,000,000$

Figure 22.-Continued.



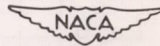
Angle of attack, α , deg
 (d) $M, 0.60$; $R, 2,000,000$
 Figure 22. - Continued.



Drag coefficient, C_D
 -8 -4 0 4 8 12 16 20 24 28
 Pitching-moment coefficient, C_m
 -8 -4 0 4 8 12 16 20 24 28
 Angle of attack, α , deg

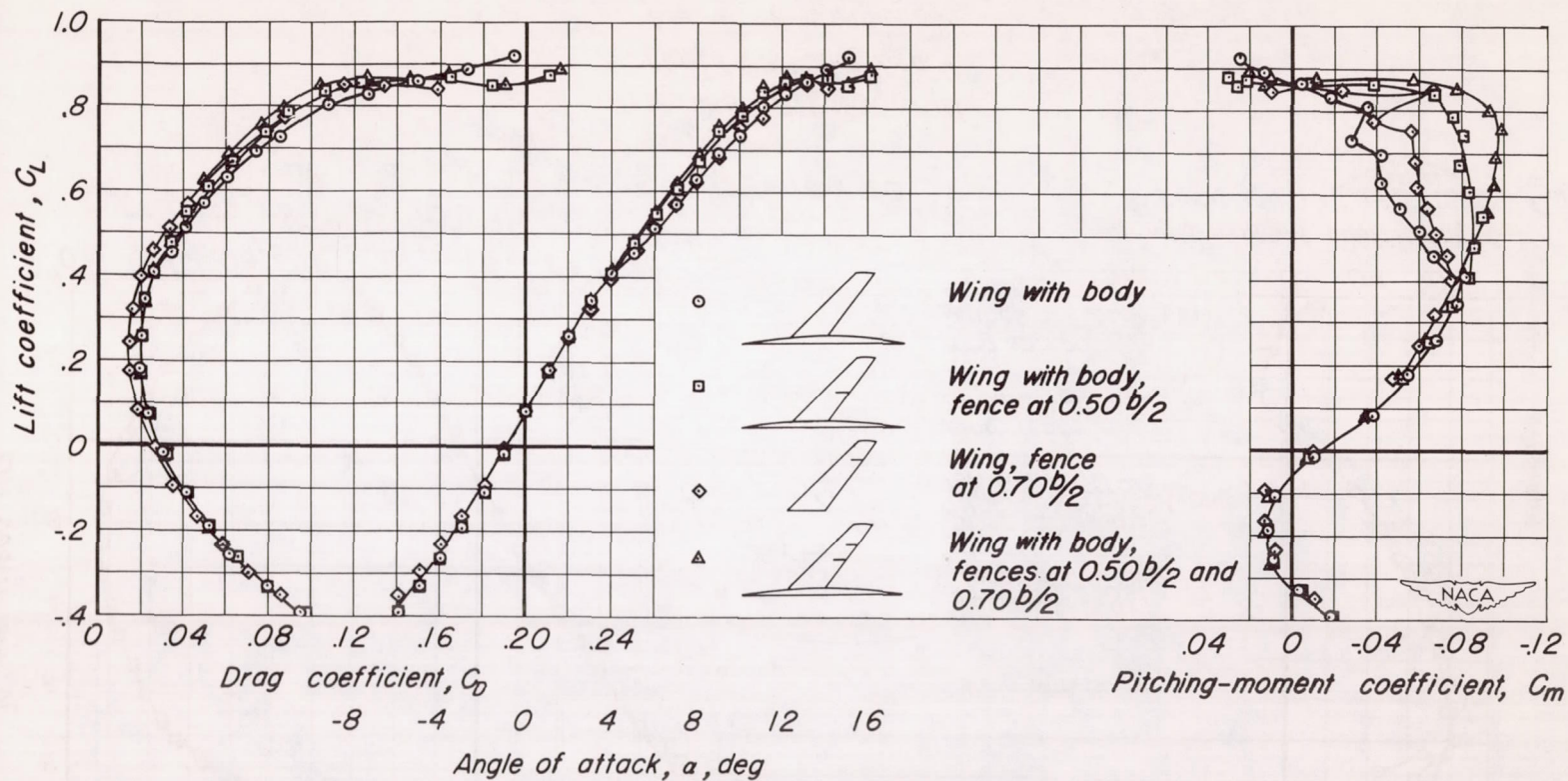
(e) $M, 0.80$; $R, 2,000,000$

Figure 22. - Continued.



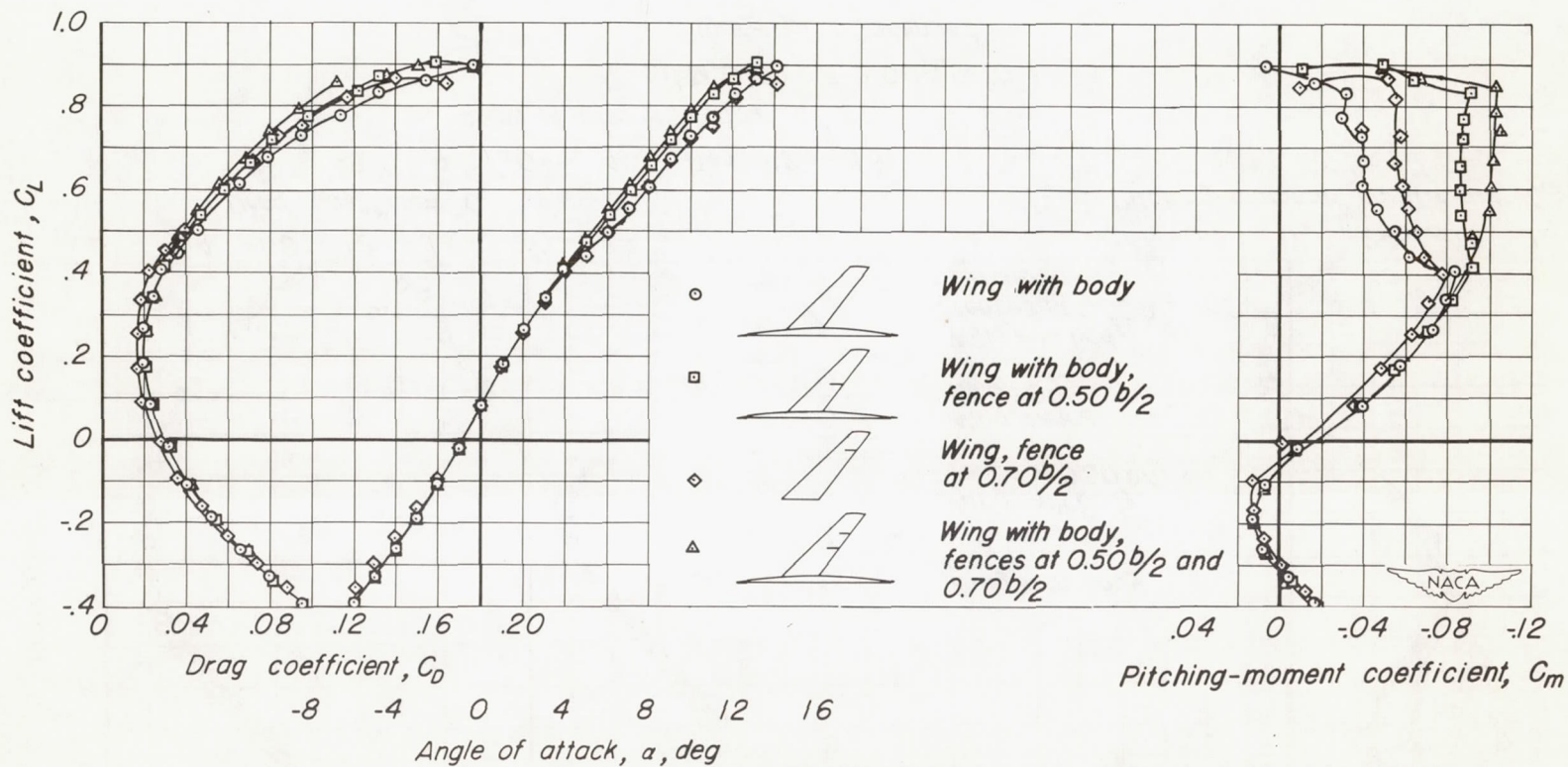


(f) $M, 0.85 ; R, 2,000,000$
 Figure 22.-Continued.



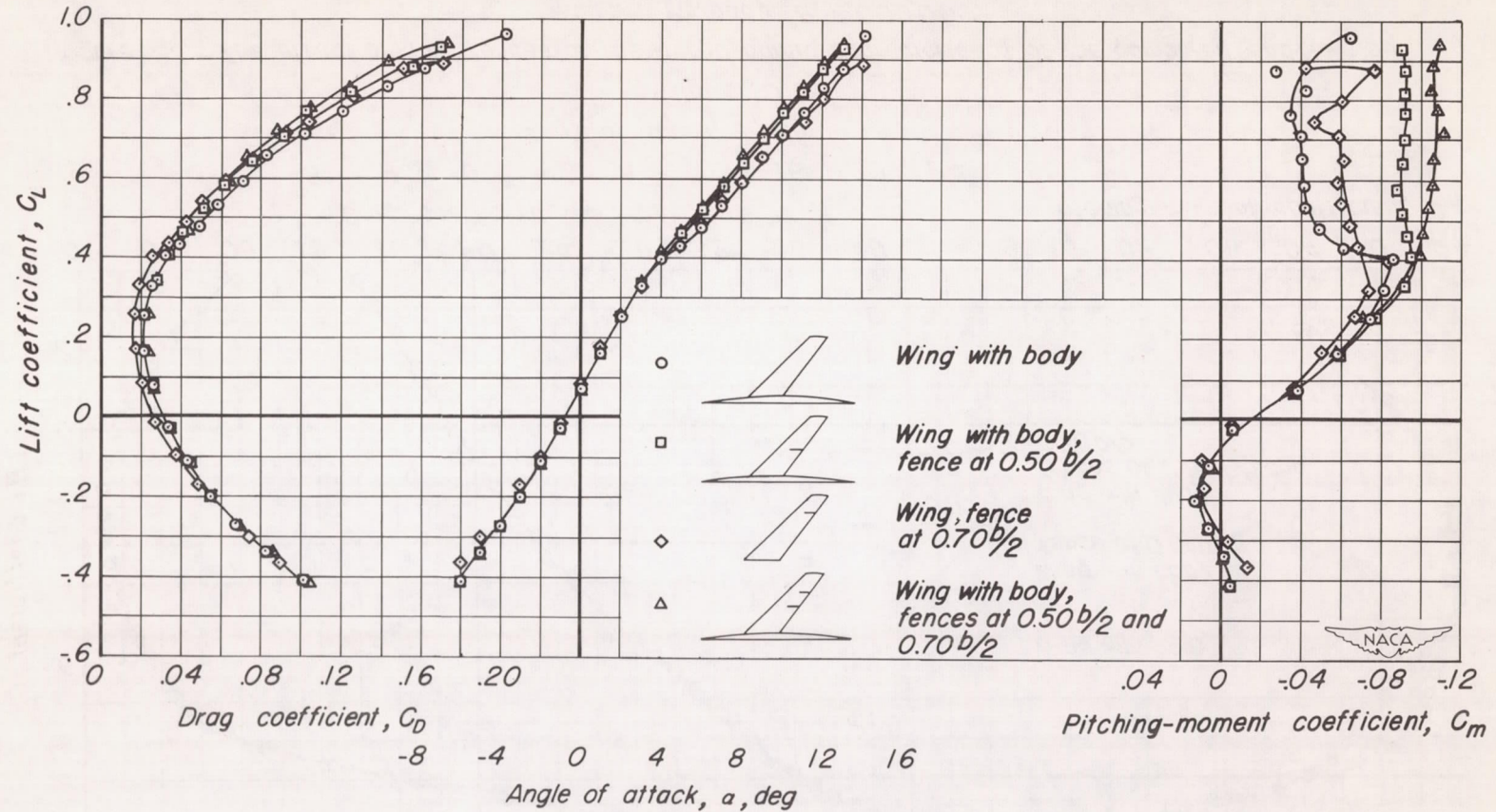
(g) $M, 0.90 ; R, 2,000,000$

Figure 22.-Continued.



(h) $M, 0.92$; $R, 2,000,000$

Figure 22. -Continued.



(i) $M, 0.94$; $R, 2,000,000$
 Figure 22. - Concluded.

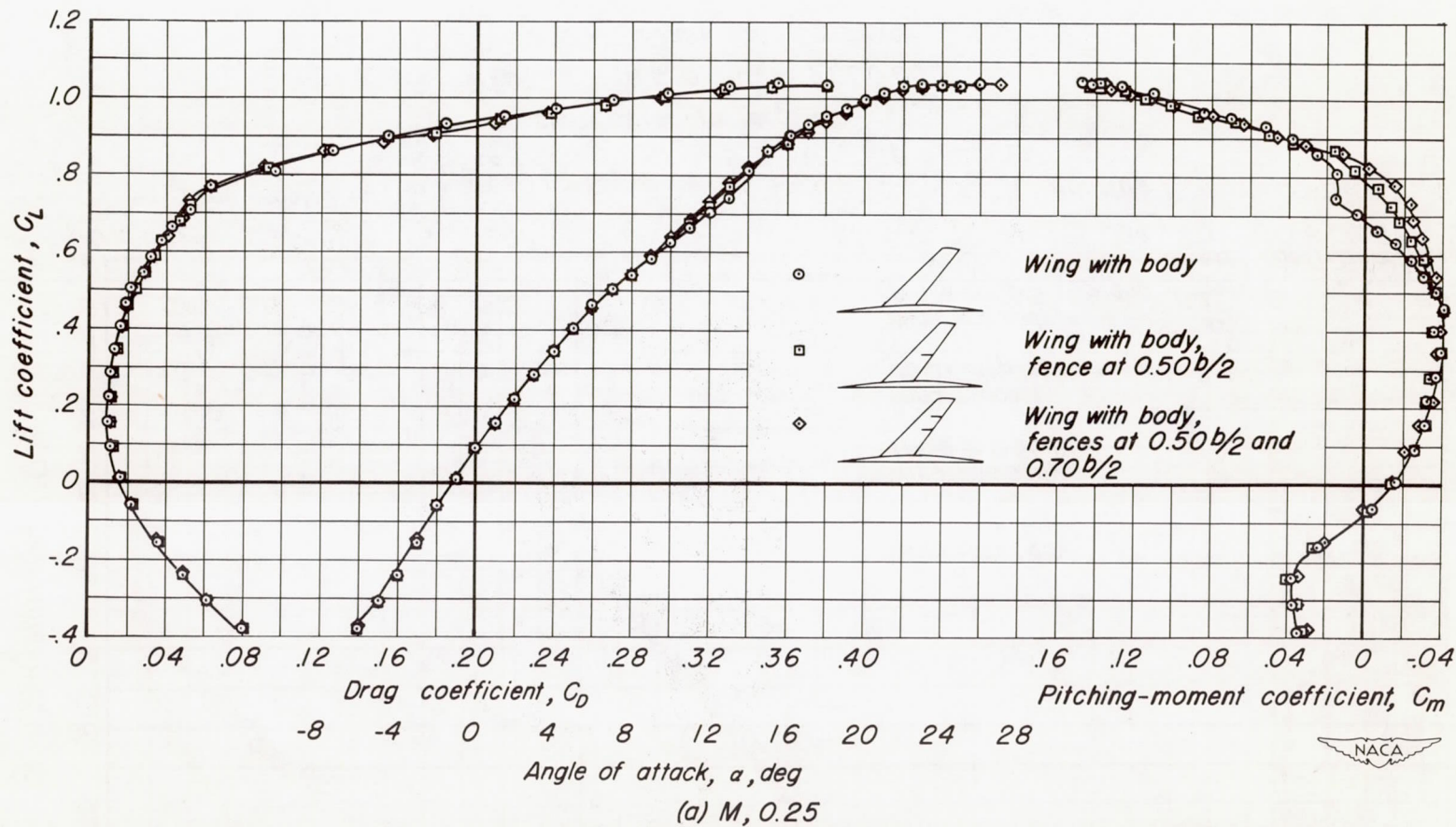
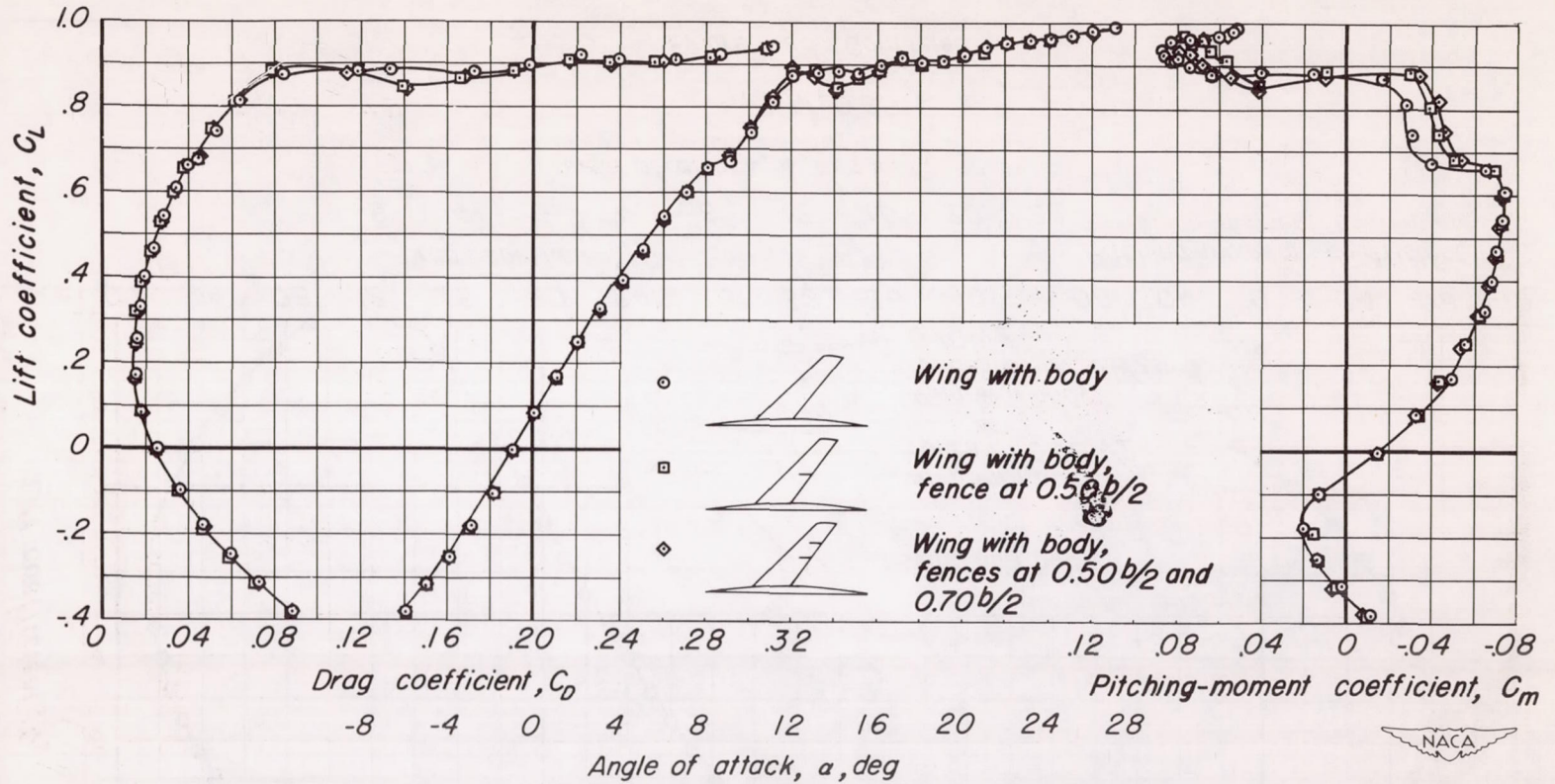
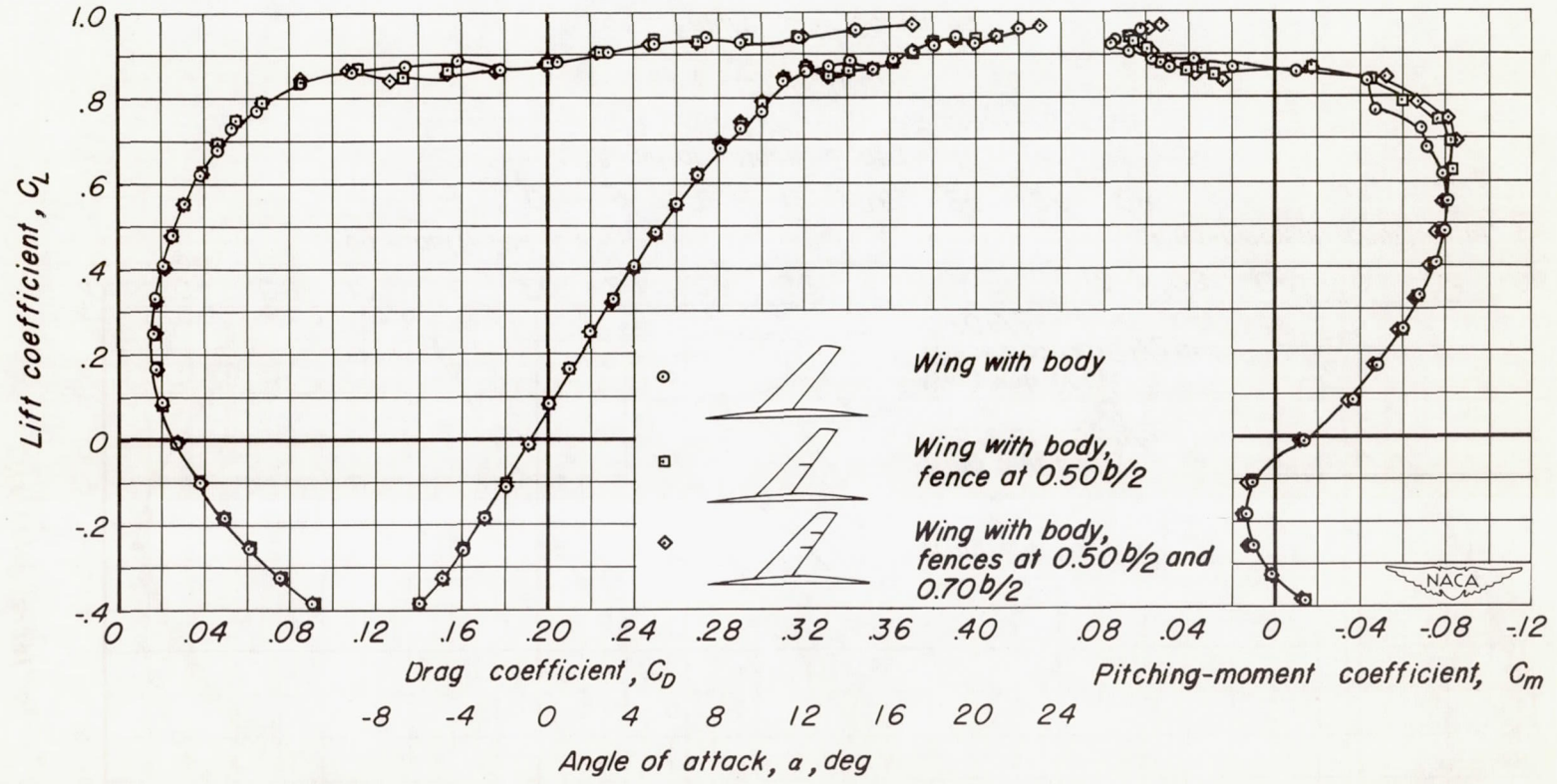


Figure 23.-The effect of low fences on the aerodynamic characteristics of the cambered and twisted wing with the body. $R, 2,000,000$.

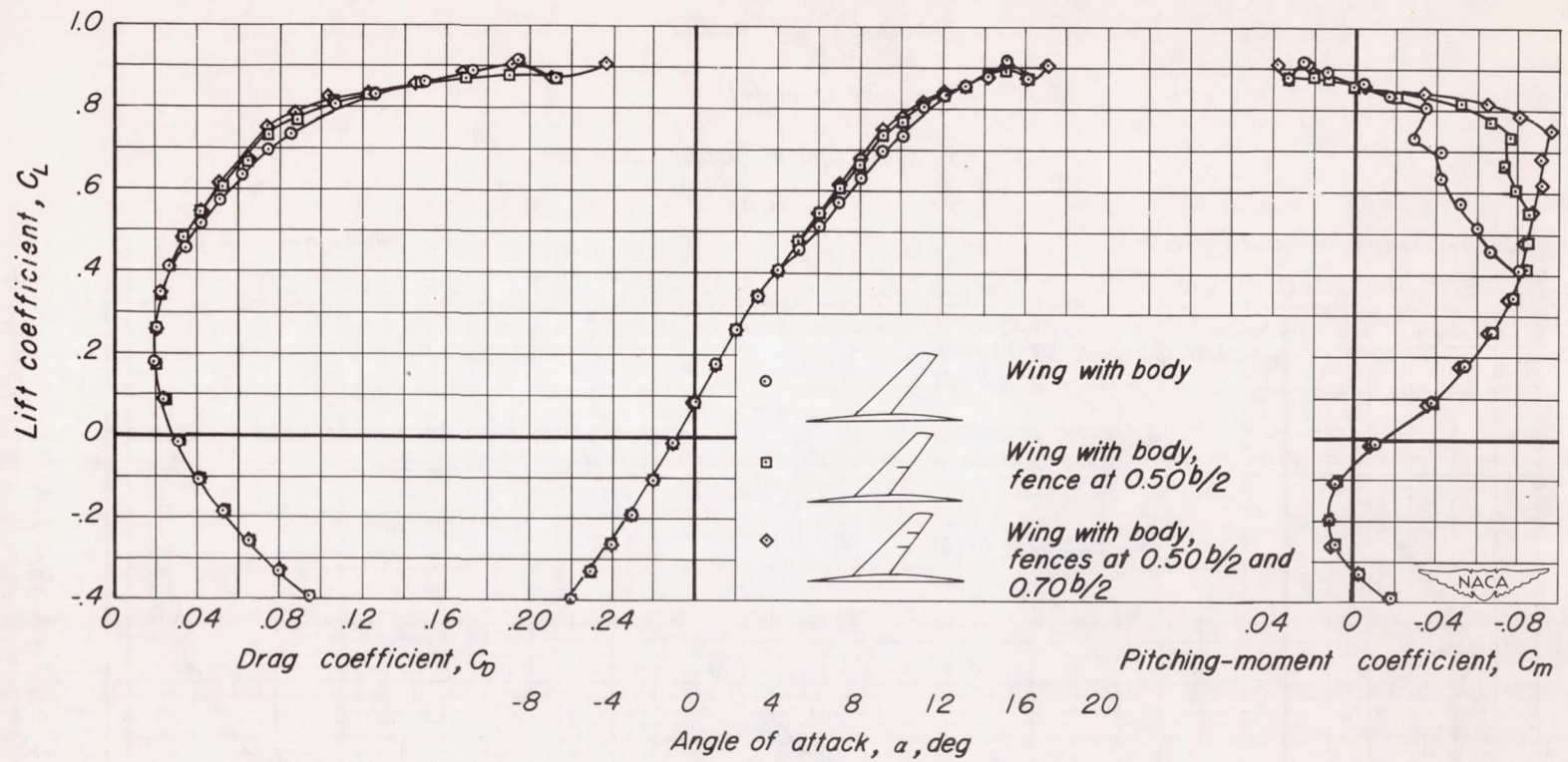


(b) $M, 0.80$

Figure 23.-Continued.

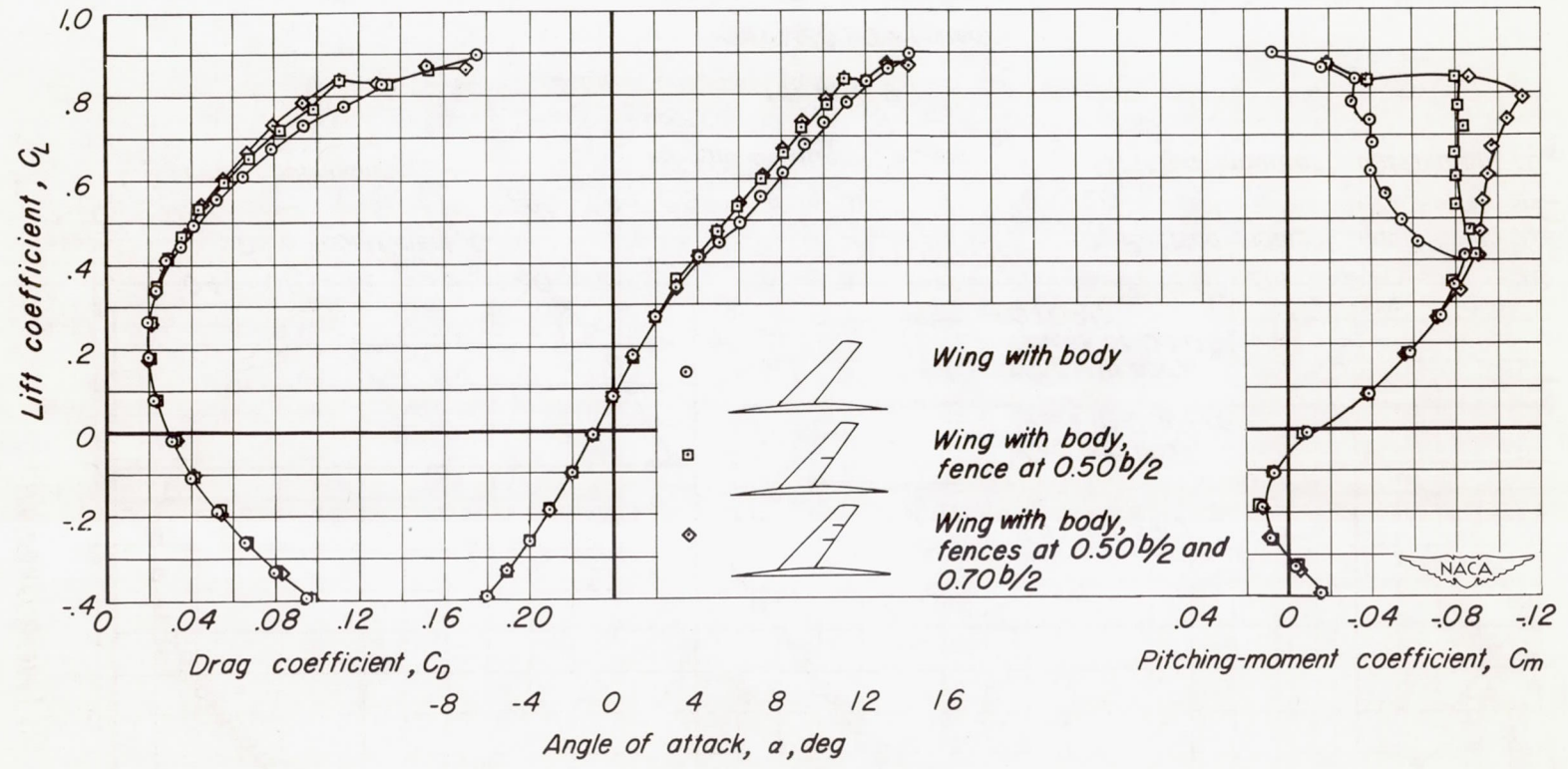


(c) $M, 0.85$
Figure 23.-Continued.



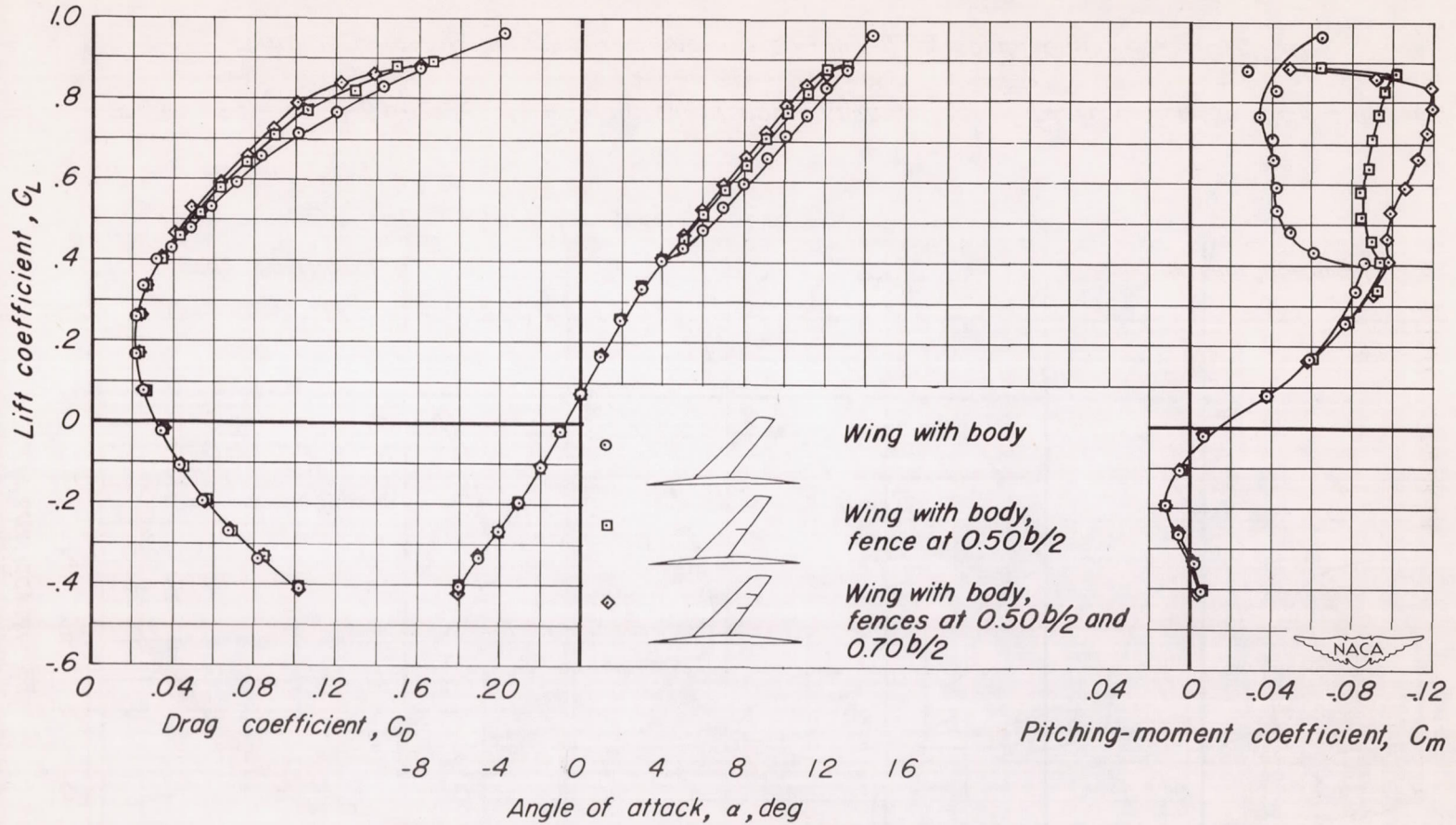
(d) $M, 0.90$

Figure 23.-Continued.



(e) $M, 0.92$

Figure 23.-Continued.



(f) $M, 0.94$

Figure 23.-Concluded.

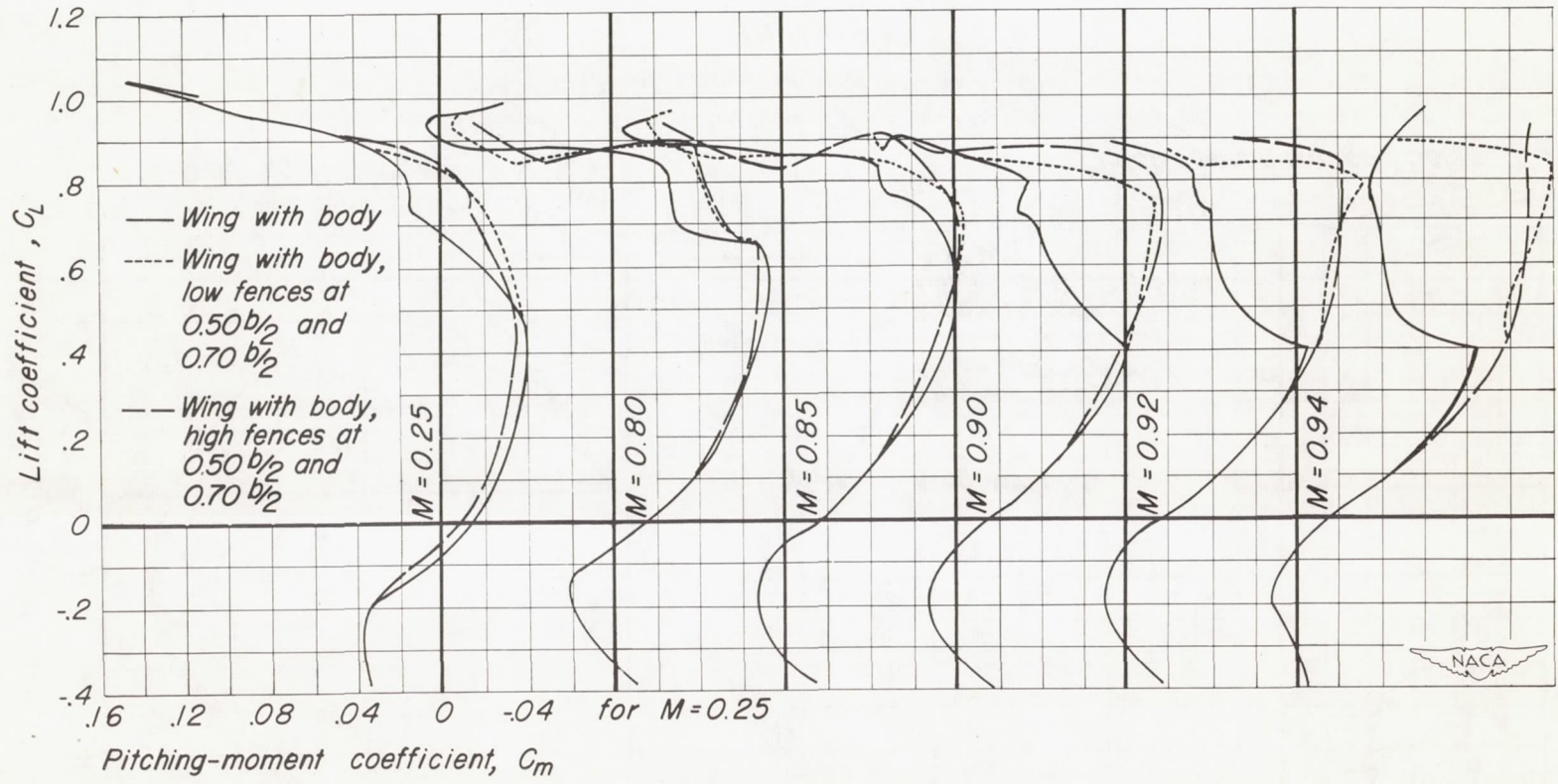
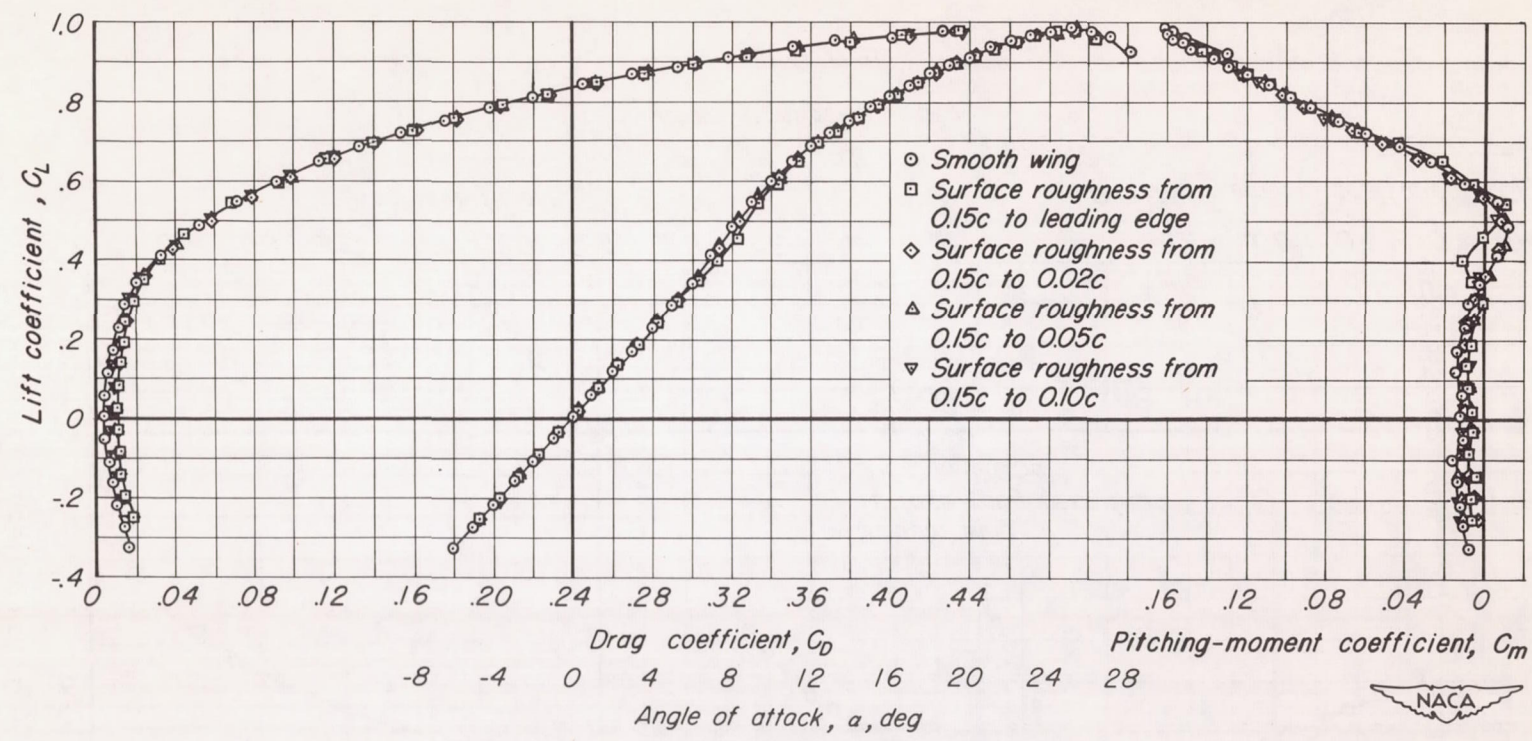


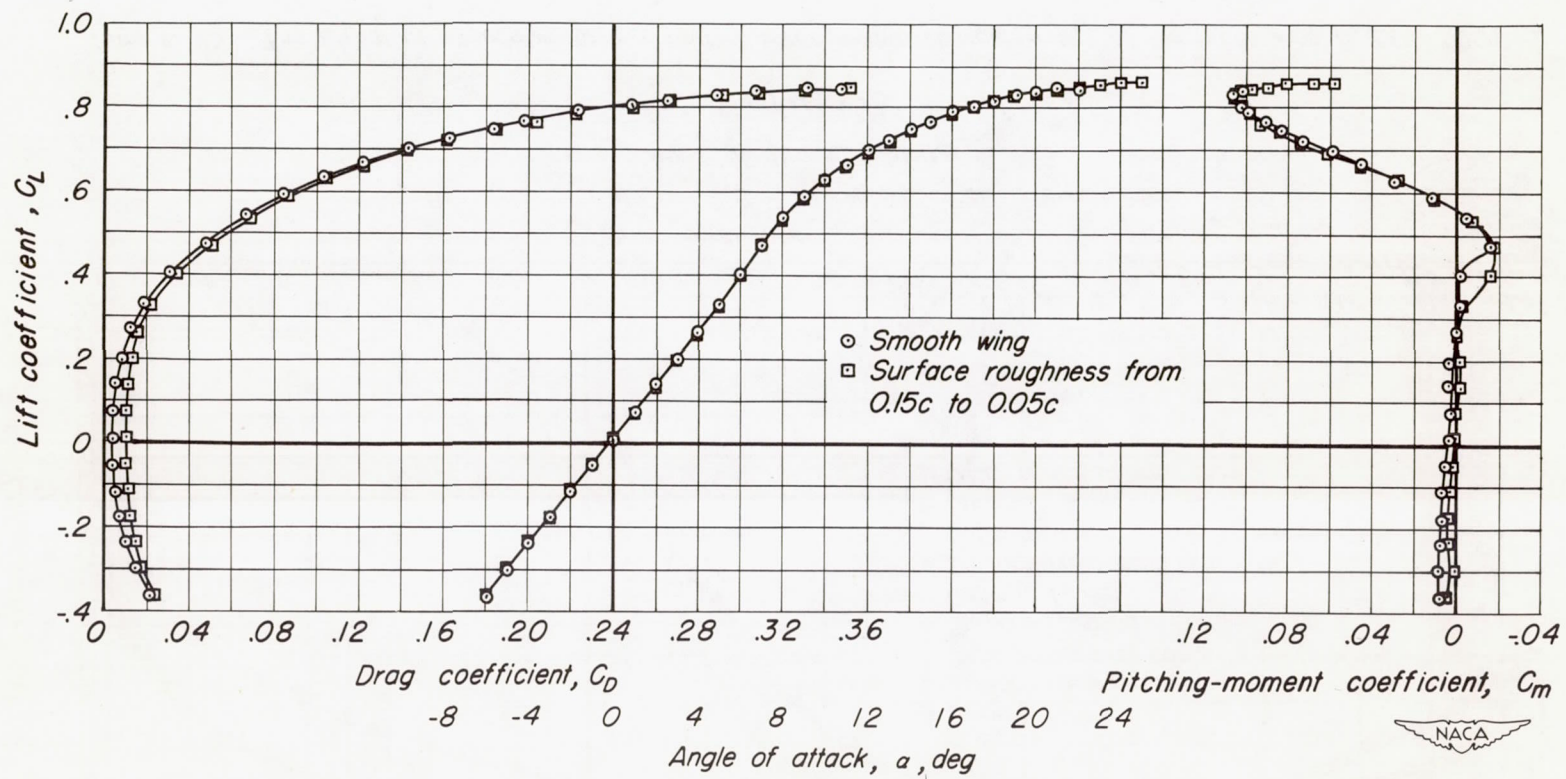
Figure 24. - A comparison of the effect of high fences with the effect of low fences on the pitching-moment characteristics of the cambered and twisted wing-body combination. $R, 2,000,000$.



(a) $M, 0.25$

Figure 25. - The effect of surface roughness on the aerodynamic characteristics of the plane wing. $R, 2,000,000$.

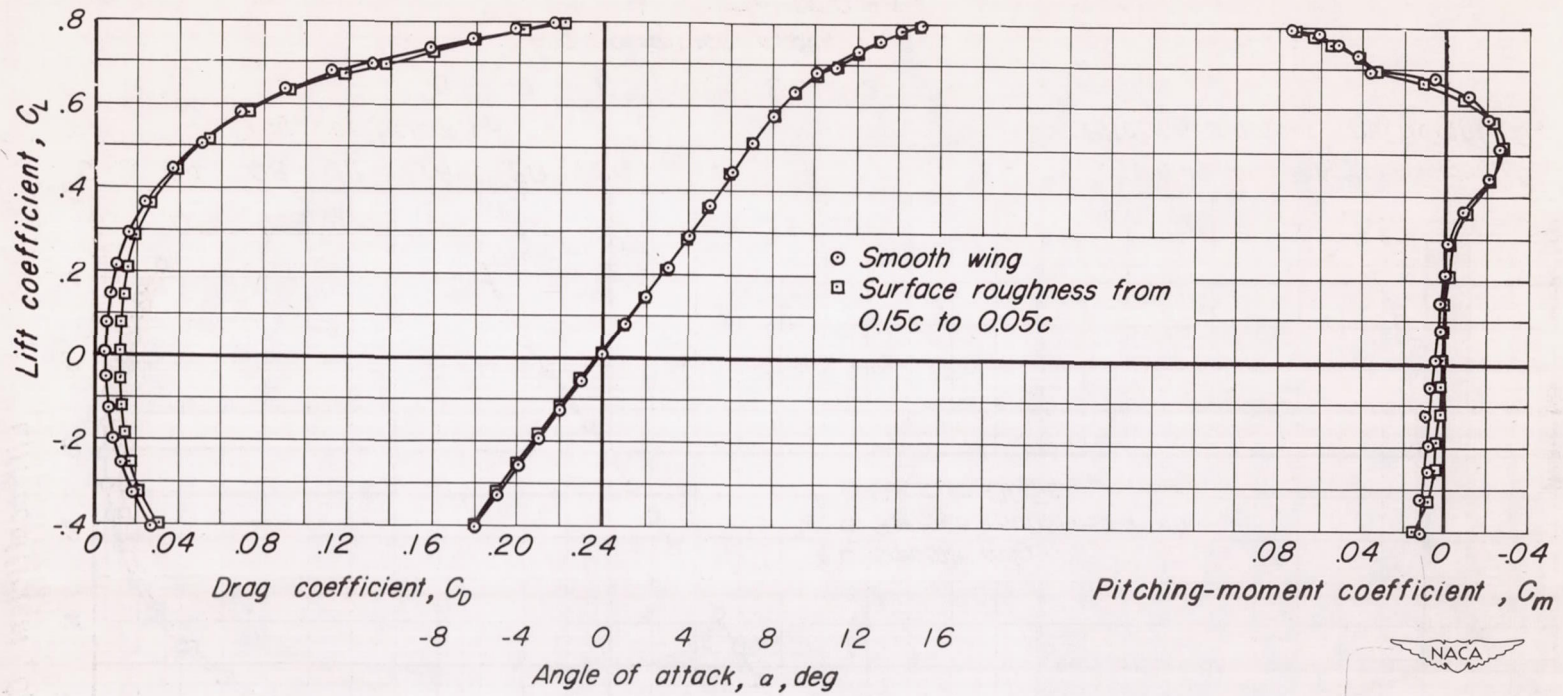




(b) $M, 0.80$

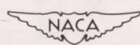
Figure 25.-Continued.

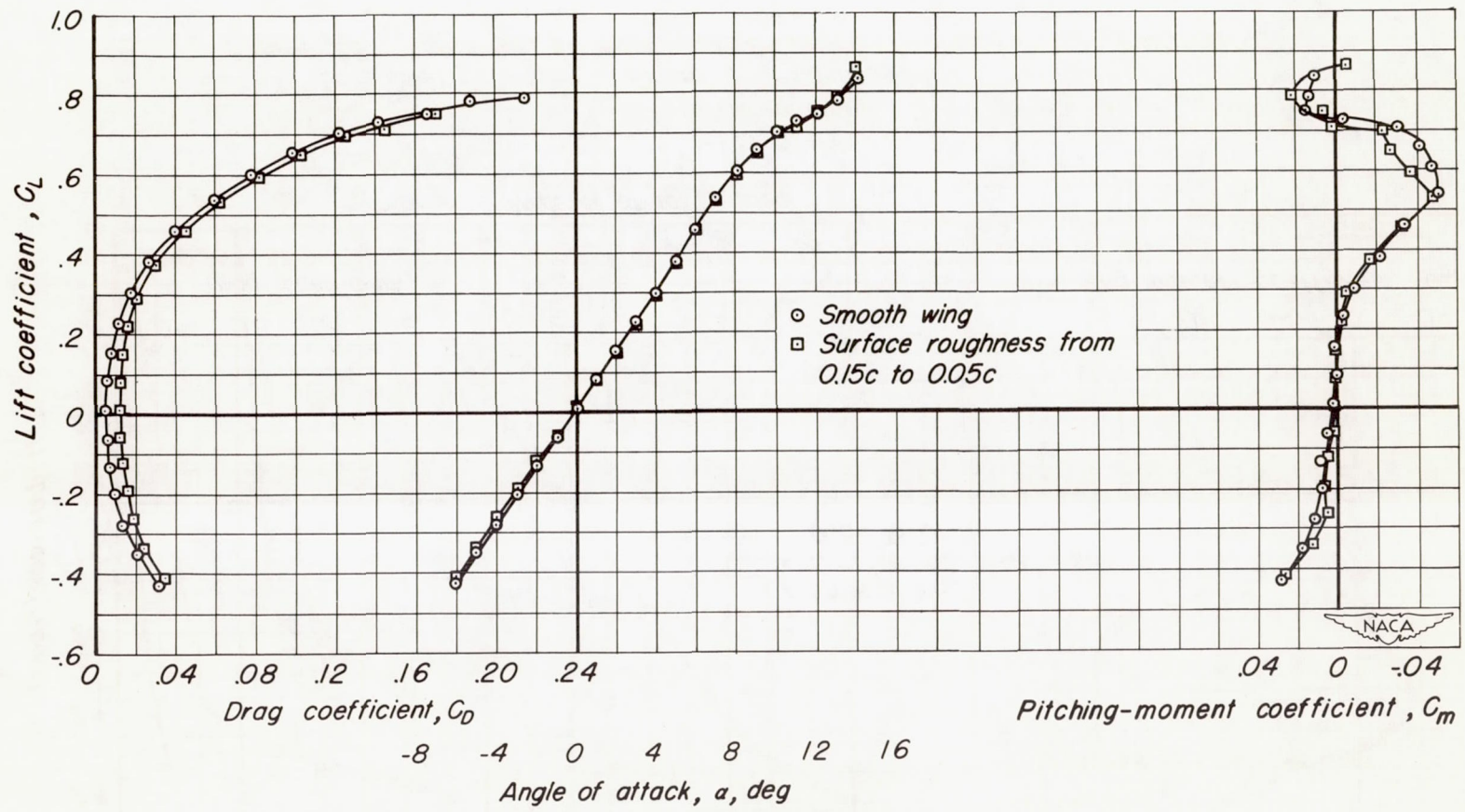




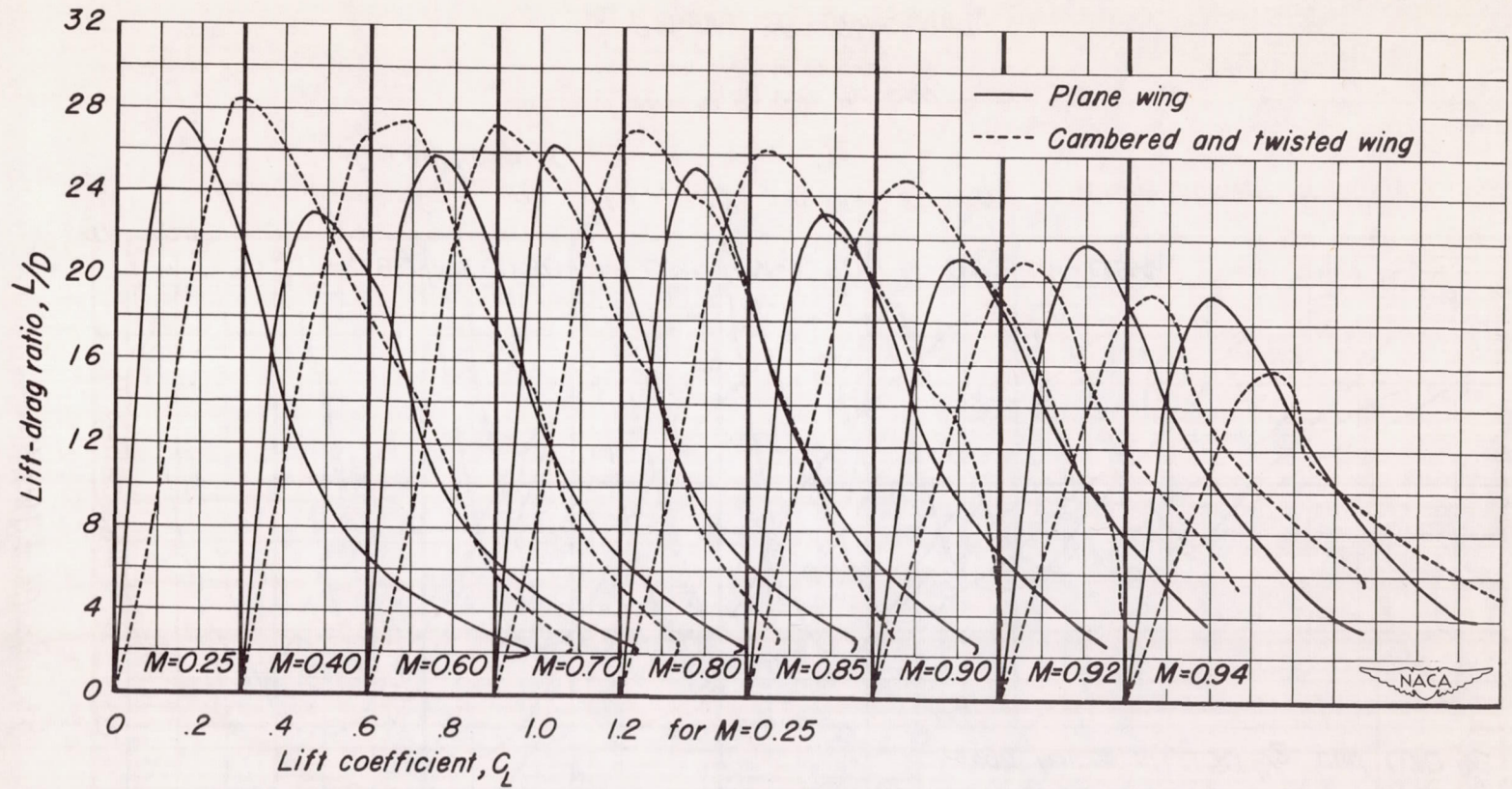
(c) $M, 0.90$

Figure 25.-Continued.



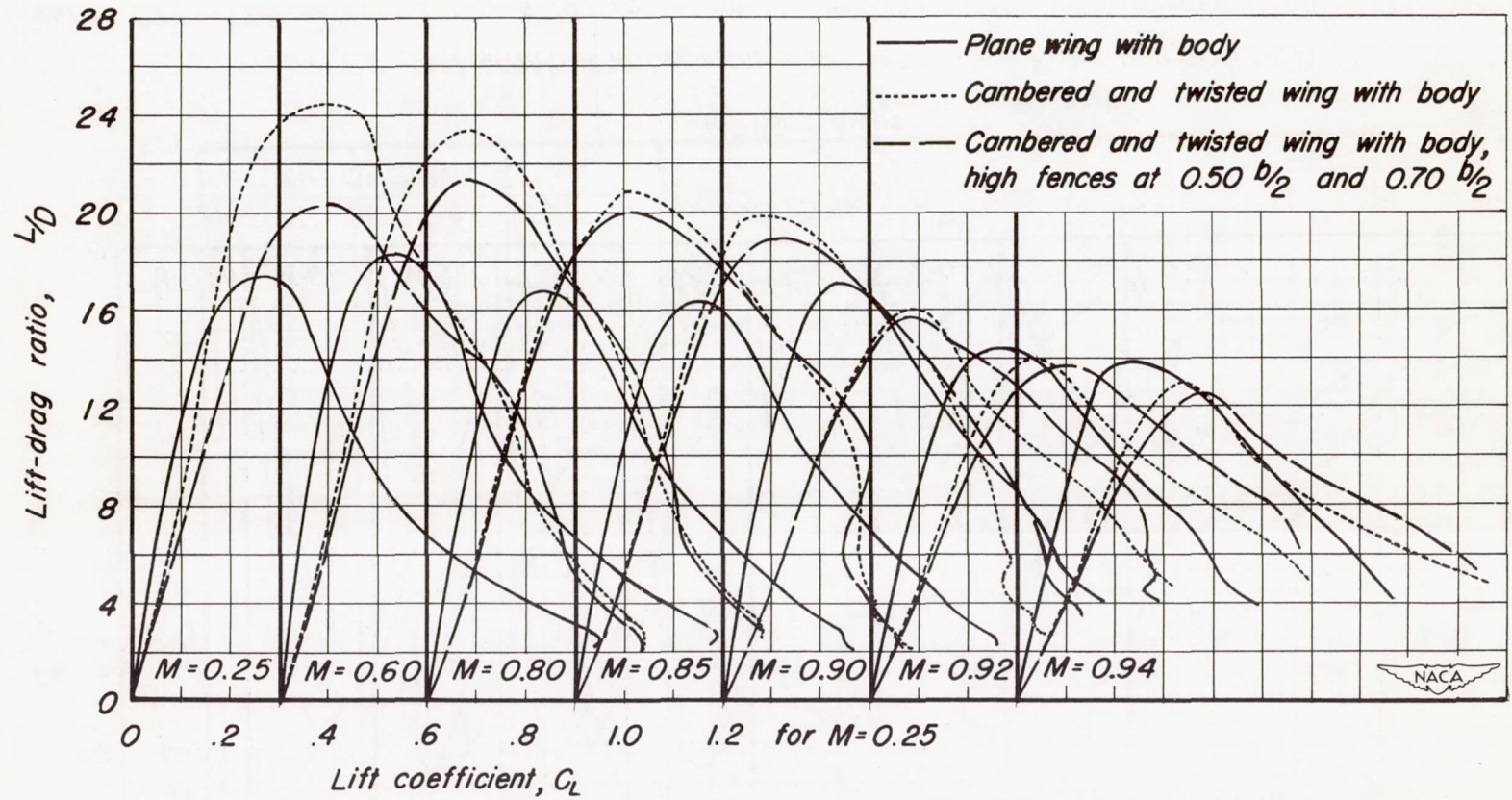


(d) $M, 0.94$
 Figure 25.-Concluded.



(a) Wing alone

Figure 26. - The effect of Mach number on the lift-drag ratio. $R, 2,000,000$.



(b) Wing with the body

Figure 26.—Concluded.

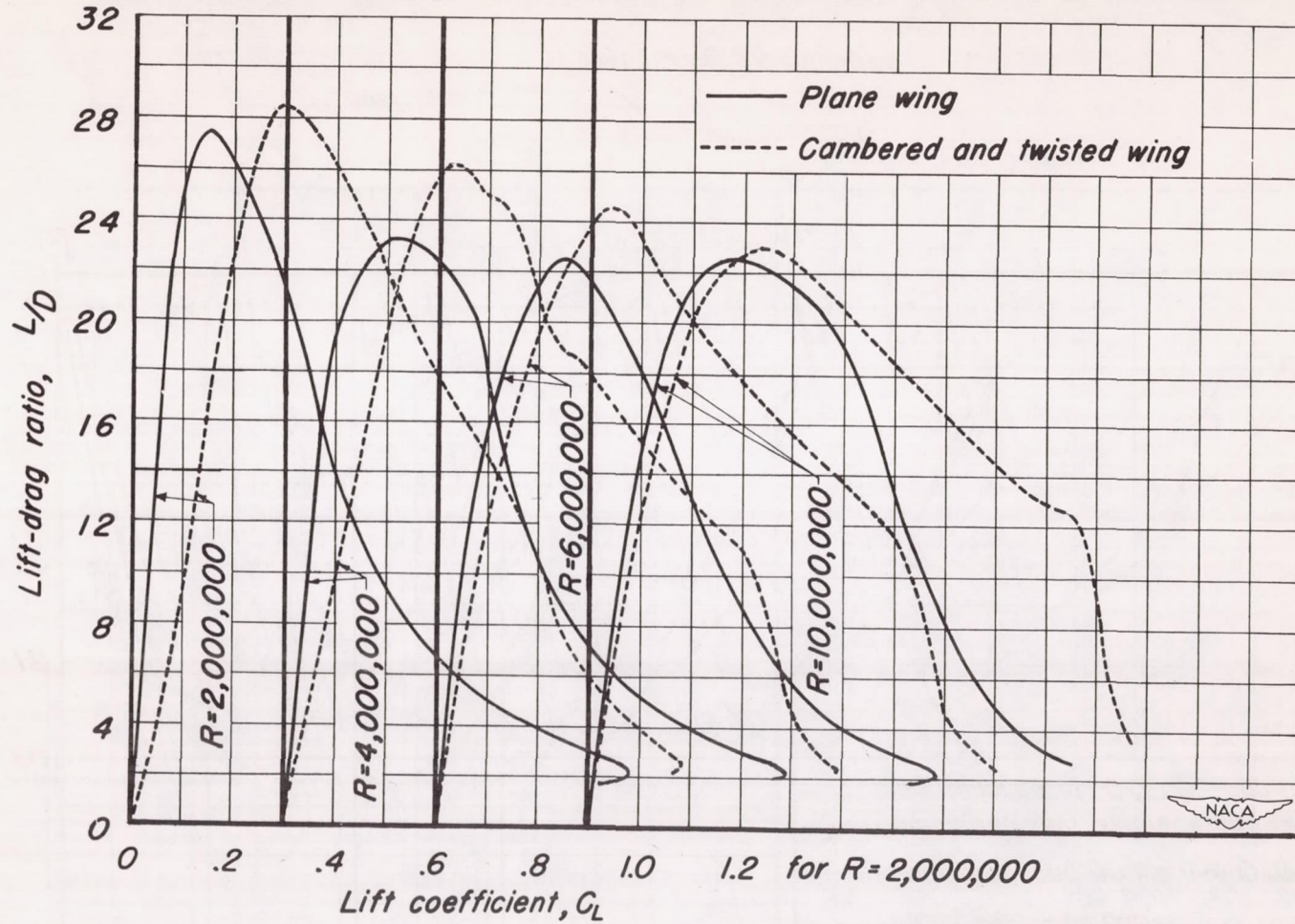
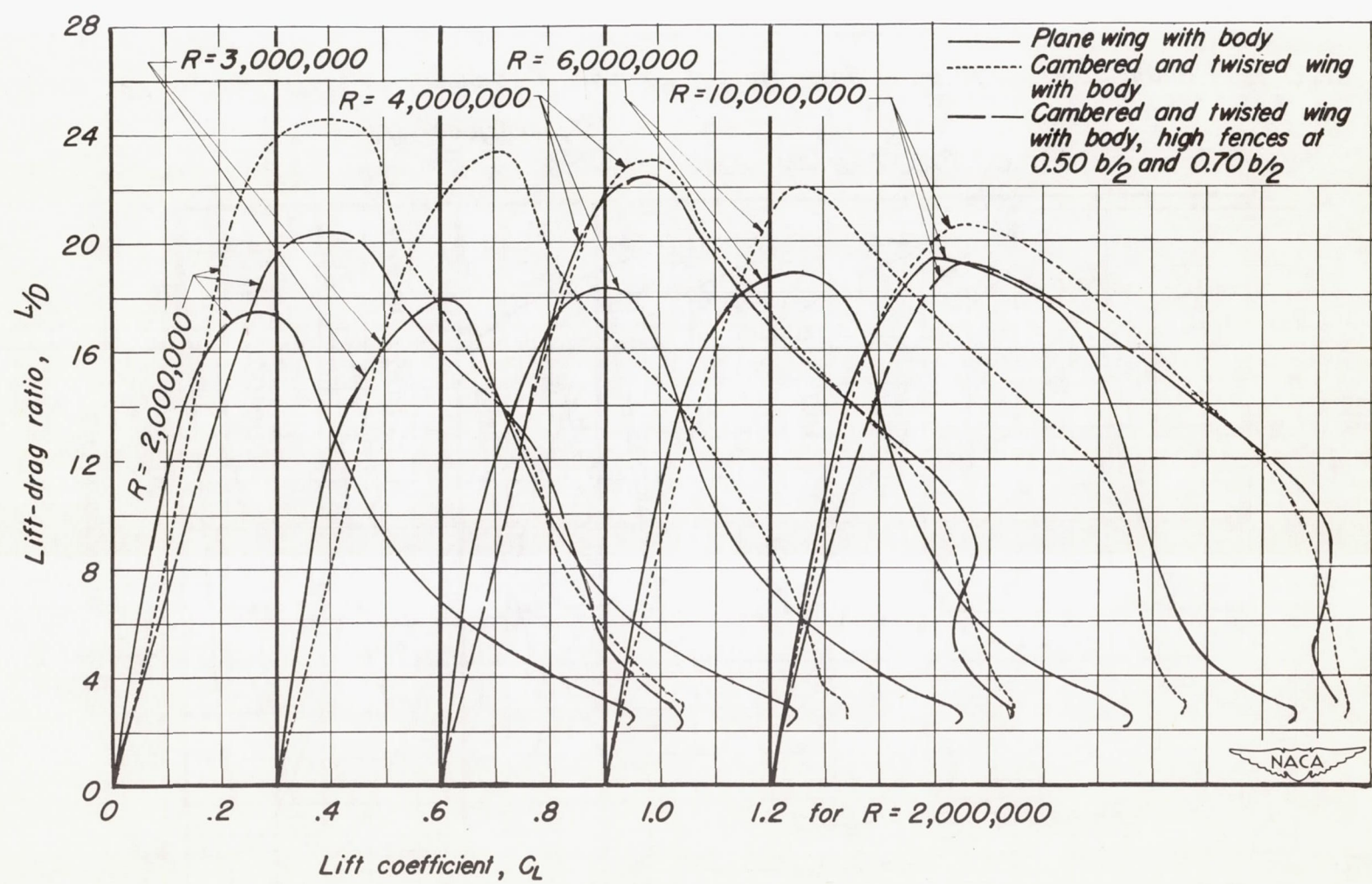
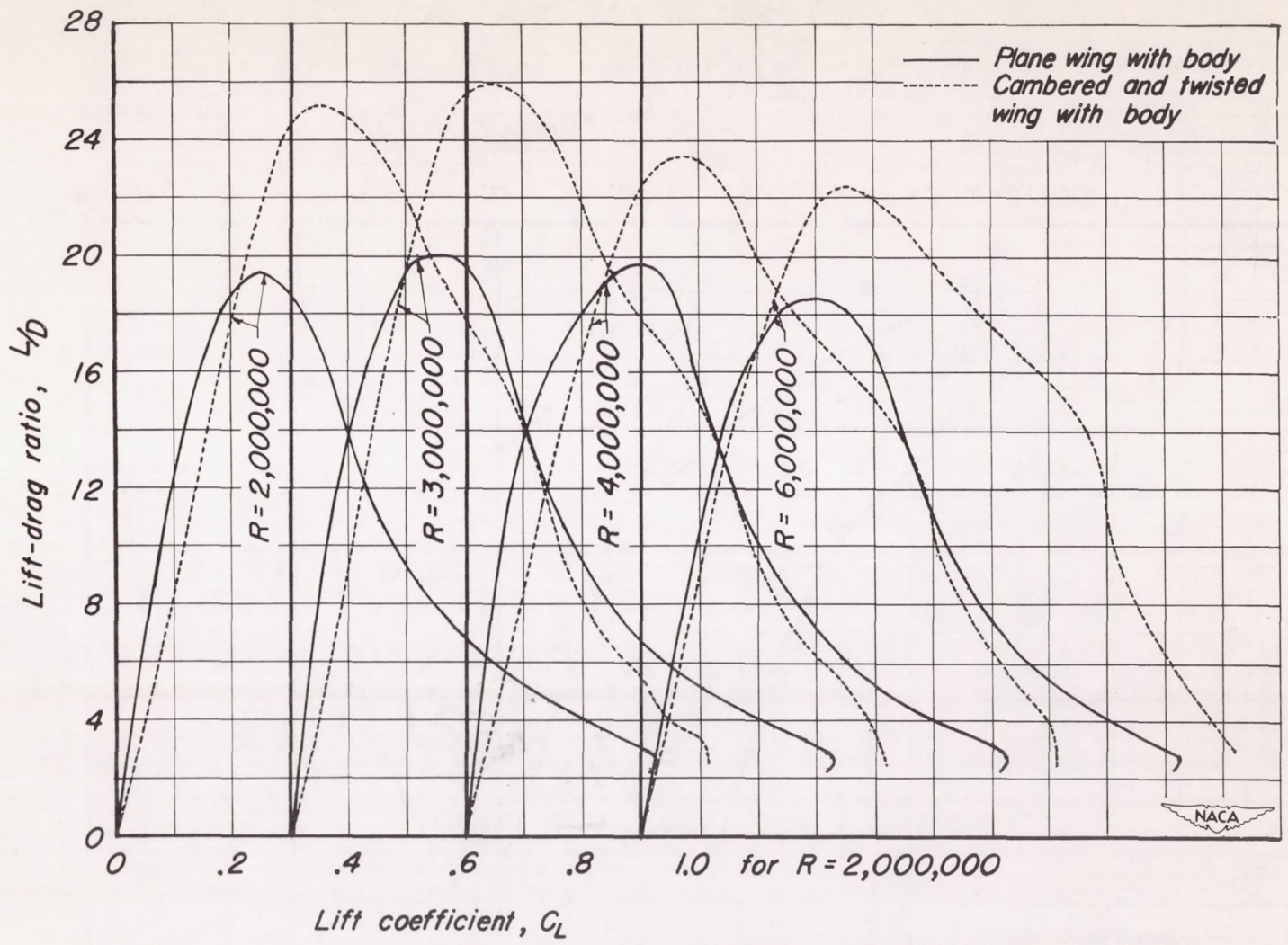


Figure 27. - The effect of Reynolds number on the lift-drag ratio of the wing alone. $M, 0.25$.



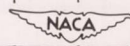
(a) $M, 0.25$

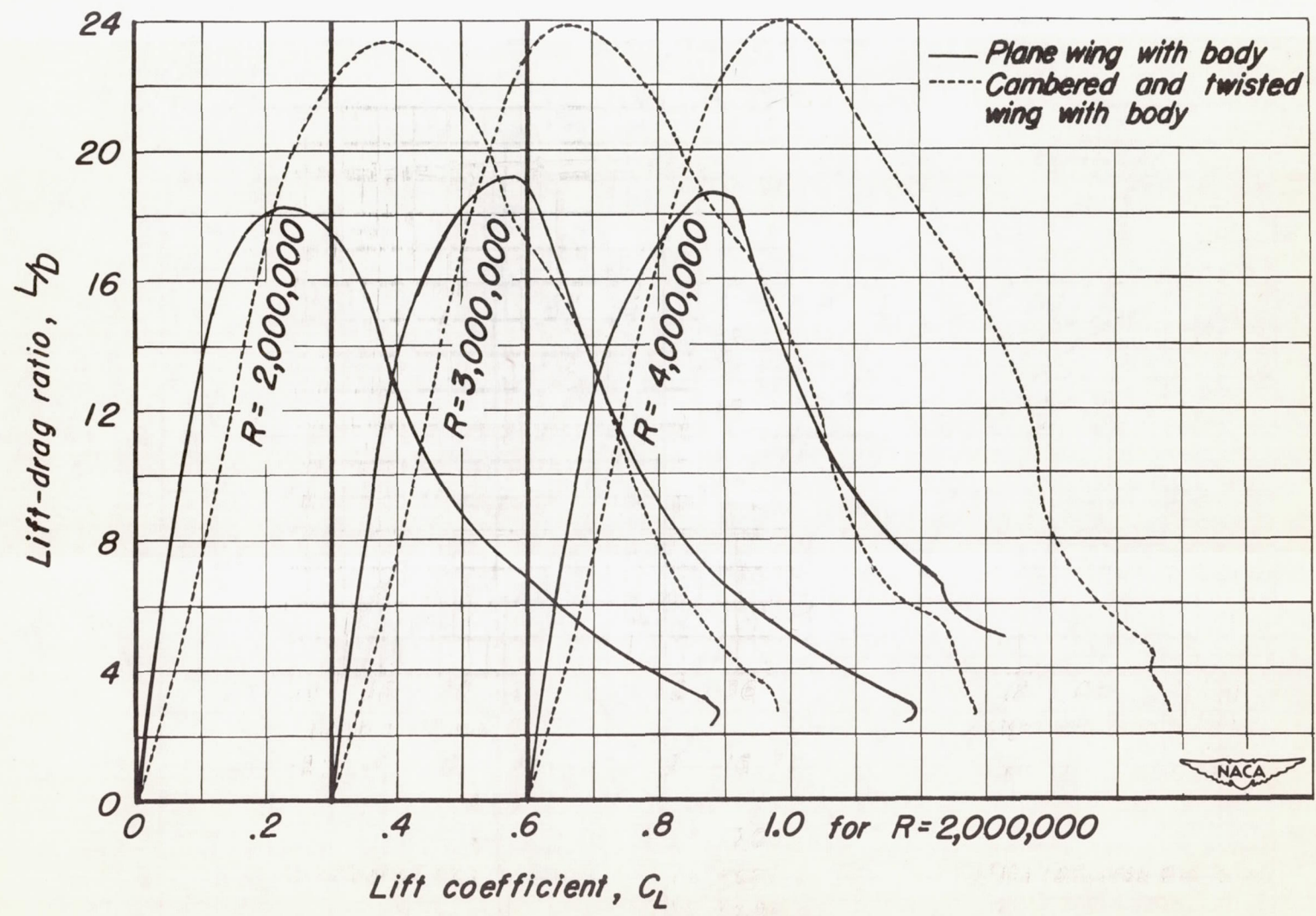
Figure 28.—The effect of Reynolds number on the lift-drag ratio of the wing with the body.



(b) $M, 0.40$

Figure 28. -Continued.





(c) $M, 0.60$

Figure 28. -Concluded.